

EFFECT OF AXIAL LOAD ON SHEAR BEHAVIOR OF SHORT
RC COLUMNS UNDER CYCLIC LATERAL DEFORMATIONS

By

H. Ramirez

and

J. O. Jirsa

Report on a Research Project

Sponsored by

National Science Foundation
Directorate for Applied Science and Research Applications
Division of Problem-Focused Research Applications
Grant No. ENV77-20816

Phil M. Ferguson Structural Engineering Laboratory
The University of Texas at Austin

June 1980

Any opinions, findings, conclusions, or recommendations expressed in this publication are those of the authors and do not necessarily reflect the views of the National Science Foundation.

A C K N O W L E D G M E N T S

The development of the bidirectional loading facility was supported by the Division of the Advanced Environmental Research Applied to National Needs Program under Grant No. ENV75-00192. With this support a floor-wall reaction system was constructed. A system for applying bidirectional lateral load using a servo-controlled hydraulic actuator was developed. The loading and data acquisition are computer-controlled.

Under Grant No. ENV75-00192, testing of short columns was initiated. Funding for a comprehensive test program on columns failing in shear was received (Grant No. ENV77-20816) from the National Science Foundation's Directorate for Applied Science and Research Applications, Division of Problem-Focused Research. The grant provides funding for extensive experimental work, data reduction and evaluation aimed towards establishing behavioral models, and development of design recommendations for frame structures subjected to bidirectional deformations.

The project staff has had the guidance and input of an Advisory panel consisting of the following:

Professor V. V. Bertero, University of California, Berkeley
Dr. W. G. Corley, Portland Cement Association, Skokie, Illinois
Mr. James Lefter, Veterans Administration, Washington, D.C.
Mr. C. W. Pinkham, S. B. Barnes & Associates, Los Angeles,
California
Mr. Loring A. Wyllie, Jr., H. J. Degenkolb & Associates,
San Francisco, California

The assistance of the Advisory Panel and the National Science Foundation Program Manager, Dr. John B. Scalzi, is gratefully acknowledged.

The project was conducted at the Phil M. Ferguson Structural Engineering Laboratory at the Balcones Research Center of The University of Texas at Austin. The Laboratory is under the direction of Dr. John E. Breen. Thanks are extended to Dr. Kyuichi Maruyama, who was a coworker on this project with the authors; George E. Moden, Dan Perez, David Marschall, laboratory technicians, and Michael Lumsden, draftsman, who assisted in the conduct of the work; and Kyle A. Woodward, who developed much of the software for the data reduction system. The authors wish to acknowledge the support of the other laboratory staff, Messrs. Gorham Hinckley, Joe Longwell, Larry Johnson, and David Stolle, who assisted in the construction of facilities and in the testing.

Portions of this report were part of a Ph.D. dissertation by Horacio Ramirez presented to the Graduate School of The University of Texas at Austin. The dissertation was supervised by James O. Jirsa.

A B S T R A C T

The influence of axial loads on the behavior of reinforced concrete short columns under cyclic bidirectional deformations was studied. The experimental program consisted of ten tests of short column specimens subjected to predetermined load sequences. All specimens had the same geometry and reinforcement. The specimen had a 12 in. (30 cm) square cross section with a shear span of 1.5 times the thickness of the cross section. The shape of the specimen was selected to simulate a short column framing into a stiff floor system.

The lateral loading was controlled by monitoring deformations. Two basic histories were selected: one with displacement variation in only one direction and the other with displacements applied alternately in orthogonal directions. Axial loads were held constant in some tests and varied in others. One level of constant compression and three levels of constant tension were considered. Two sequences simulated loads varying from tension to compression.

The main effect of axial compression was to increase shear strength and to accelerate the shear deterioration at higher levels of deformation as compared with the deterioration of a specimen without axial loads.

In tests with constant tension, the shear capacity and the stiffness were reduced but the shear deterioration was decreased as compared with tests with constant compression or with no axial load. The effect of tension alternating with compression was reflected as a reduction in shear and stiffness but only during that part of the loading history where tension was imposed.

In order to develop a design approach for columns failing in shear, a parameter was defined for identifying shear behavior.

Guidelines for satisfactory performance in terms of energy dissipation were established. The procedure developed appeared to reflect adequately the influence of the main variables as indicated by the limited test data available.

C O N T E N T S

Part		Page
1	INTRODUCTION	1
	1.1 General	1
	1.2 Background	2
	Ductility of Sections	2
	Basic Experimental Studies on Cyclic Loads	3
	Analytical and Experimental Studies Regarding Bidirectional Effects	4
	1.3 Energy Dissipation and Strength of Columns	6
	1.4 Purpose	8
2	EXPERIMENTAL PROGRAM	9
	2.1 Design of Experimental Program	9
	2.2 Limits of Horizontal Deflections	11
	2.3 Number of Cycles	12
	2.4 Load Variations	12
	2.5 Test Details	15
3	TEST SPECIMEN AND PROCEDURES	21
	3.1 Specimen Details	21
	3.2 Fabrication	25
	3.3 Materials	25
	3.4 Loading System	29
	3.5 Instrumentation	29
4	TEST RESULTS	33
	4.1 General	33
	4.2 Load-Deflection Curves	34
	4.3 Peak Value Tables	36
	4.4 Shear-Deterioration Diagrams	36
	4.5 Distribution of Strain in Ties	38
	4.6 Crack Patterns	38
	4.7 Effect of Different Material Properties	41
	Concrete	41
	Longitudinal Steel	43

Part		Page
	Second Order Effects--Compressive Axial Loads	43
	Second Order Effects--Tensile Axial Loads . .	47
5	CONSTANT COMPRESSION	51
	5.1 Introduction	51
	5.2 Description and Comparison of Test Results . .	51
	Load-Deflection Curves	51
	Envelopes of Load Deflection	55
	Shear Deterioration	60
	Strain in Transverse Reinforcement	60
	5.3 Study of the Behavior	66
	Mechanism of Failure	66
	Strength and Deformation Characteristics . . .	71
	Summary of the Influence of Constant Compression	75
6	CONSTANT TENSION	77
	6.1 Introduction	77
	6.2 Description and Comparison of Test Results . .	77
	Load-Deflection Curves	77
	Envelopes of Load Deflection	80
	Shear Deterioration	84
	Strain in Transverse Reinforcement	84
	Crack Patterns	90
	6.3 Study of the Behavior	97
	Mechanism of Failure	97
	Strength Characteristics	97
	Summary of the Influence of Constant Tension .	100
7	ALTERNATE TENSION AND COMPRESSION	101
	7.1 Introduction	101
	7.2 Load-Deflection Curves and Shear Deterioration	101
	7.3 Envelopes of Load Deflection	105
	7.4 Strain in Transverse Reinforcement	114
	7.5 Commentary	120
8	A DESIGN APPROACH FOR COLUMNS WITH DIFFERENT LEVELS OF AXIAL LOAD	125
	8.1 Introduction	125
	8.2 Basic Requirements for Columns with Constant Compression	126

Part	Page
8.3 A Proposed Design Criterion	129
Identification of Shear-controlled Behavior	130
Design Options	132
Deflection Limits	134
8.4 Bidirectional Effects	138
8.5 Evaluation of the Design Approach	138
120C-U	138
00-U	140
8.6 Columns with Constant Axial Tension	141
Bidirectional Effects	146
8.7 Evaluation of the Design Approach for Axial Tension	146
50T-U	147
100T-U	147
8.8 Columns with Alternating Tension and Compression	150
9 SUMMARY AND CONCLUSIONS	153
9.1 Summary of the Investigation	153
Test Specimen	153
Lateral Load History	153
Axial Load History	154
9.2 Test Results	154
Effect of Constant Axial Compression	154
Effect of Constant Axial Tension	154
Effect of Alternate Axial Load	155
9.3 Design Approach	155
9.4 Recommendations for Future Work	156
Axial Loads	156
Transverse Reinforcement	156
Shear Span	157
Behavioral Model	157
9.5 Conclusions	157
REFERENCES	159

T A B L E S

		Page
2.1	Test Schedule	17
3.1	Concrete Material Properties	26
4.1	Peak Values, Test 00-U	37
4.2	P- Δ Effect, Tests 120C-U and 120C-B	48
4.3	P- Δ Effect, Tests with Constant Tension	48
5.1	ACI Nominal Shear Strength	73
5.2	Maximum Peak Shear Compared with $2M_n/L$	73
6.1	Maximum Peak Shear Compared with $2M_n/L$ (Tension)	98
6.2	ACI Nominal Shear Strength (Tension)	98
8.1	Data from Ref. 29	137
8.2	Measured and Predicted Values of S_R	144

F I G U R E S

		Page
2.1	Specimens used by other investigators	10
2.2	Columns subjected to axial load variations	13
2.3	Building frame with overhang	13
2.4	Basic lateral deformation histories	16
2.5	Application sequence of axial loads, test ATC-U	18
2.6	Application sequence of axial loads, test ATC-B	20
3.1	Specimen nominal dimensions	22
3.2	Interaction diagram for the prototype	23
3.3	Reinforcing steel stress-strain curves	28
3.4	Test setup	30
4.1	Load-deflection curve, test 00-U	35
4.2	Shear deterioration, test 00-U	39
4.3	Strain distribution in tie bars, test 00-U	40
4.4	Progressive development of cracks, test 00-U	42
4.5	Interaction diagram--steel from first lot	44
4.6	Interaction diagram--steel from second lot	45
4.7	Free body diagram of specimen and equilibrium equations	46
5.1	Load-deflection curve, test 120C-U	52
5.2	Load-deflection curve, 120C-B - NS direction	53

	Page
5.3	Load-deflection curve, 120C-B - EW direction 54
5.4	Load-deflection curve, 00-B - NS direction 56
5.5	Load-deflection curve, 00-B - EW direction 56
5.6	Envelopes of load deflection, 00-U and 120C-U 57
5.7	Envelopes of load deflection, 120C-U and 120C-B 58
5.8	Envelopes of load deflection, 00-B and 120C-B 59
5.9	Shear deterioration, tests 00-U and 120C-U 61
5.10	Shear deterioration, tests 00-B and 120C-B 62
5.11	Strain distribution in ties, test 120C-U 63
5.12	Progressive strain in a tie, tests 00-U and 120C-U 64
5.13	Strain distribution in tie bars, test 120C-B 65
5.14	Progressive strain in a tie, tests 00-B and 120C-B 67
5.15	Crack patterns test 120C-U 68
5.16	Appearance of test specimens 00-B and 120C-B after completion of loading 69
5.17	Load-deflection curves for various a/d ratios 76
6.1	Load-deflection curve, test 50T-U 78
6.2	Load-deflection curve, test 100T-U 78
6.3	First cycles, test 100T-U 79
6.4	Load-deflection curve, test 200T-U 79
6.5	Load-deflection curve, test 50T-B 81
6.6	Envelopes of load deflection, tests with constant tension and history U 82
6.7	Envelopes of load deflection, tests 50T-U and 50T-B 83
6.8	Envelopes of load deflection, tests 50T-B, 00-B, and 120C-B 85

	Page	
6.9	Shear deterioration tests with constant tension and history U	86
6.10	Shear deterioration, tests 00-B and 50T-B	87
6.11	Strain distribution in tie bars, test 50T-U	88
6.12	Strain distribution in tie bars, tests 100T-U and 200T-U	89
6.13	Progressive strain in a tie, tests with constant tension and history U	91
6.14	Progressive strain in ties, tests 50T-U and 50T-B	92
6.15	Crack patterns, test 50T-U	93
6.16	Crack patterns, test 50T-B	94
6.17	Crack patterns, test 100T-U	95
6.18	Crack patterns, test 200T-U	96
7.1	Load-deflection curve, ATC-U	102
7.2	Load-deflection curve, ATC-U first cycles	103
7.3	Shear deterioration, tests ATC-U, 100T-U, and 120C-U	104
7.4	Load-deflection curve, ATC-B - NS direction	106
7.5	Load-deflection curve, ATC-B - EW direction	107
7.6	Shear deterioration, tests ATC-B, 50T-B, and 120C-B	108
7.7	Envelopes of load deflection, ATC-U, 100T-U, and 120C-U	110
7.8	Envelopes of load deflection, tests ATC-B, 50T-B, and 120C-B (NS direction)	111
7.9	Envelopes of load deflection, tests ATC-B, 50T-B, and 120C-B (EW direction)	112
7.10	Envelopes of load deflection, tests ATC-B, 50T-U, and 120C-U (NS direction)	113

	Page
7.11	Envelopes of load deflection, tests ATC-B and 120C-U 115
7.12	Strain distribution in ties, ATC-U 116
7.13	Strain distribution in ties, ATC-B 117
7.14	Progressive strain in two ties, ATC-U and 120C-U . 118
7.15	Progressive strain in a tie, ATC-B and 120C-B . . . 119
7.16	Idealization of inclined cracks 121
7.17	Appearance of Specimens ATC-U and 120C-U after testing 122
7.18	Appearance of Specimens ATC-B and 120C-B after testing 123
8.1	Shear behavior vs flexural behavior 128
8.2	Design of R/C columns under cyclic loads 133
8.3	Lateral deflection limit 135
8.4	Example of calculations, redesign of 120C-U 139
8.5	Reduction due to axial tension 143
8.6	Design of R/C columns under cyclic loads and constant axial tension 145
8.7	Example of calculations, redesign of 50T-U 148

CHAPTER 1

INTRODUCTION

1.1 General

During major earthquakes, structures are exposed to loadings in a random mode. Reinforced concrete columns may be subjected to a number of cycles of lateral load, with components in both principal directions, as well as cycles of axial load including axial tension. In the design of reinforced concrete structures it is generally assumed that lateral forces or deformations coincide with a principal axis of the structure or member. It may also be assumed that the axial load is constant on the members. However, this procedure may be unconservative when strong earth motions occur. Observed failures, after earthquakes, offer evidence of highly variable loads on columns.

Extensive research has been reported regarding the behavior of columns under unidirectional lateral loads (the direction of lateral load coinciding with one of the principal axes) and compressive axial loads. The limited studies that have been carried out show that bidirectional lateral motions have a marked influence on the behavior of structures, as compared with unidirectional motions. To date no test results have been reported regarding combinations of axial tension--constant or variable--and lateral forces. It is clear that there is a growing need for an evaluation of the importance of complex load histories on seismic behavior. Experimental data are needed to develop methods for including the effect of complex loading histories on the design and analysis of reinforced concrete framed structures.

The present study is one of a series of investigations regarding columns and beam-column joints being performed at The

University of Texas at Austin. The studies constitute a comprehensive experimental program aimed at evaluating the importance of bidirectional loading histories. In the study described herein, only columns were included and emphasis was given to evaluation of the effect of varying axial loads in combination with different lateral load histories. The specimen geometry and reinforcement were not varied. An important departure from all previous studies was the imposition of axial tension on selected specimens. Exterior columns in structures located in seismic zones may be subjected to bidirectional lateral loads and axial tension produced by overturning moments.

1.2 Background

To provide background from which general behavioral characteristics of reinforced concrete members can be established, previous investigations relating to bidirectional and unidirectional lateral cyclic loads on columns and the ductility of reinforced concrete sections are reviewed briefly.

Ductility of Sections. (a) Burns and Siess [1,2] investigated the behavior of beams and beam-column connections of reinforced concrete, under repeated and reversed loading. They concluded that with proper attention to details almost any degree of ductility required or desired can be developed for redistribution of moments.

(b) Park and Sampson [3] discussed ductility requirements for eccentrically loaded reinforced concrete column sections. Defining the ductility of a section using curvature, it was pointed out that the required content of transverse steel for ductility depends not only on the material strengths and longitudinal steel content but on the level of axial load as well. Changes in the present Code recommendations for transverse steel to include those variables were suggested.

(c) Gulkan and Sozen [4] discussed the role of stiffness and energy dissipation on the response of reinforced concrete structures to strong ground motions. Results of dynamic tests on reinforced concrete frames were used to illustrate the effects of changes in stiffness and energy dissipating capacity on dynamic response. A decrease in stiffness and an increase in the capacity to dissipate energy was observed as the structures were subjected to large displacements.

Basic Experimental Studies on Cyclic Loads. (a) Hirosawa, Ozaka and Wakabayashi [5], in reviewing studies conducted in Japan on the response of structures to seismic loads, listed the following trends to be considered in developing experimental programs.

- (1) Ductility factors obtained through response analysis of structures subjected to severe shocks are around 3 or 4 at most, if the strength and rigidity of a building are not excessively limited.
- (2) The number of peak accelerations corresponding to approximately 80 percent of the maximum have been reported to be around 10 times.
- (3) Member response under alternate cyclic loading generally becomes apparent within 10 cycles of loading.

A research plan conducted in a number of laboratories was organized [5]. The basic test specimen was a short column, a member which is vulnerable to brittle failure and to deterioration of strength and stiffness. It was observed that specimens with high shear stress tend to fail in a brittle manner, despite heavy web reinforcement, and that the ductility of the column could be classified according to the reduction of strength under a given number of cycles at specified deformation levels.

(b) Shimazu and Hirai [6] surveyed a number of static tests in which the strength degradation of reinforced concrete columns subjected to multi-cycle reversals of lateral load were considered.

Many factors were observed to affect the strength of reinforced concrete columns subjected to multi-cycle reversals of lateral load, including number of cycles, type of lateral loading, ratio of transverse reinforcement, shear span ratio, level of axial stress, and level of shear stress.

(c) Wight and Kanoh [7] reported tests on twelve column specimens subjected to loading reversals into the inelastic range. The principal variables were the axial load, the percentage of transverse reinforcement, and the required displacement ductility. It was concluded that the generally accepted formula for calculating the ultimate shear strength of reinforced concrete members--adding the contribution of both concrete and transverse steel--was not always valid for inelastic loading reversals. A failure mechanism was suggested in which two critical stages were recognized, the first corresponding to the total utilization of the concrete compressive strength and the second to the splitting and spalling of the shell concrete. Yielding of the stirrups occurring at a point between the two stages dictated the behavior of the specimen. From the results of the study, the authors stressed the importance of considering the expected number of inelastic cycles and the deformation in each cycle in the design of reinforced concrete members resisting seismic loading. The contribution of concrete to the shear capacity of the core should be reduced in all members subjected to shear reversals.

Analytical and Experimental Studies Regarding Bidirectional Effects. (a) Selna, Morrill, and Ersoy [8] studied the shear collapse of the Olive View Hospital Psychiatric Day Clinic which occurred during the 1971 San Fernando earthquake. The shear failure criterion was assumed as an elliptical surface, the axes representing the shear capacity in each direction based on the contribution of concrete and steel to shear strength. The importance of bidirectional

effects was examined. It was suggested that lateral reinforcement (size and spacing) in a tied column should relate to the maximum ductility factor, the number and magnitude of inelastic excursions, the variations of axial load, and the moment/shear ratio. The importance of bidirectional testing, in order to allow better representation of behavior, was stressed.

(b) Pecknold and Sozen [9] carried out inelastic dynamic response analyses of the Olive View Memorial Center for four different ground motions--the 1971 Pacoima Dam record adjusted to two different maximum accelerations, the El Central 1940 record, and an artificially generated earthquake. Some of the analyses included the effect of biaxial interaction under orthogonal horizontal components of ground motion. Substantially increased story drifts for two-dimensional interaction (compared with uniaxial motions) were observed. It was concluded that the results based on uniaxial motion might have been acceptable (inelastic story drifts less than 4 times column yield), while those based on biaxial motion would have caused concern.

(c) Karlsson, Aoyama, and Sozen [10] studied spirally reinforced columns subjected to idealized earthquake loading and developed hysteresis curves which could be included in a dynamic analysis. Comparisons with measured response were found to be accurate. Spiral reinforcement did not reach yield and excellent column performance could be attributed to the spiral confinement.

(d) Aktan and Pecknold [11] showed analytically that stiffness, moment, and energy dissipating capacities of reinforced concrete members under cyclic biaxial bending can be significantly reduced in comparison to those under uniaxial bending. The studies showed that bidirectional deformation response was from 20 to 200 percent greater than unidirectional responses.

(e) Okada, Seki, and Asai [13] tested six reinforced concrete columns under bidirectional horizontal cyclic loading. The variable was the pattern of the horizontal displacement trace in the plane of the column section--linear, elliptical, and circular traces were used. Significant strength deterioration and loss of ductility due to bidirectional effects were observed. It was concluded that bidirectional effects of behavior should be considered in the development of rational seismic design methods.

1.3 Energy Dissipation and Strength of Columns

In reinforced concrete design an important consideration which can be added to the requirements of strength and serviceability is ductility or the ability to absorb energy. This consideration is of utmost importance in seismic design. In order to survive a severe earthquake, a structure must be capable of absorbing and dissipating energy by postelastic deformations. By permitting inelastic behavior, the lateral loads specified in codes may be reduced from those generated in a structure subjected to severe ground motion when elastic behavior is assumed [14].

Severe damage and collapse of reinforced concrete framed structures during major earthquakes led to a recognition of the need for more investigations of columns failing in shear [15,16,17]. Design recommendations (ACI 318-71 Building Code Requirements [18]), which are intended to provide ductility in columns, may not adequately take into account the level of axial load on the member. A number of investigators [3,32] have examined the influence of axial load in establishing energy absorbing characteristics.

The influence of axial loads (tension or compression) on the shear strength of elements under monotonic loads is well documented. Specific design requirements are given in the ACI Code [18] which are based on the report of the Joint ASCE-ACI Task Committee 426 on Shear and Diagonal Tension [38]. The recommendations for columns in the report of Committee 426 are summarized as follows.

In columns subjected to moments causing flexural yielding at the ends, shear failures tend to resemble those in axially loaded beams. For this type of failure the ACI Code Section 11.4.3 seems adequate. For columns with small M/V_d ratios, shear failure may occur prior to flexural yielding. Such members generally are designed using ACI Code Eqs. (11.6) and (11.7).

For members in compression,

$$v_c = 2(1 + 0.0005 N_u/A_g)\sqrt{f'_c} \quad (11.6)$$

and v_c shall not exceed:

$$v_c = 3.5 \sqrt{f'_c} \sqrt{1 + 0.002 N_u/A_g} \quad (11.7)$$

where v_c is the nominal permissible shear stress carried by the concrete, N_u is the design axial compressive force, and A_g is the gross area of the cross section.

For members subjected to significant axial tension, the ACI Code gives the Eq. (11.8), $v_c = 2(1 + 0.002 N_u/A_g)\sqrt{f'_c}$, where N_u is negative for tension.

The contribution of shear reinforcement perpendicular to the longitudinal axis is computed according to Eq. (11.13) of the ACI Code, in which the effectiveness of the shear reinforcement is assumed not to be altered with axial load. For columns under tensile axial loads, the use of inclined shear reinforcement is encouraged in order to prevent shearing displacements along horizontal cracks.

Changes in stiffness and energy dissipation capacity under cyclic loading determine the response of reinforced concrete frames to strong ground motions. Hysteretic behavior must be determined experimentally with repeated loading tests. While both stiffness and energy dissipation can be related to ductility, ductility

does not define the hysteretic behavior of reinforced concrete structures.

Thus it is evident that there is a growing need for an evaluation of the importance of complex load histories, including bidirectional lateral loads and varying axial loads, on seismic behavior. A review of both analytical and experimental studies regarding the behavior of reinforced concrete structures under two-dimensional lateral motions indicates that many of the parameters influencing behavior have been identified. For structures failing in a flexural mode, the existing knowledge is sufficient to adequately model the response. While flexural deformations are preferable in any structure subjected to large earthquake ground motions, it is not always possible to proportion the members to ensure such behavior. To date there has been little work done to realistically model shear response due mainly to the lack of data; however, such a model is needed in order to simulate behavior in two-dimensional analyses.

1.4 Purpose

The need for an evaluation of the importance of bidirectional lateral loading histories, and variable axial loads on the response of columns failing in shear has been documented in the brief review of other investigations reported in the literature.

In a previous series of tests [27] the specimen geometry was held constant, no axial load was imposed and the only variable was the lateral history. The purpose of the study reported herein is to extend the previous work and to examine experimentally the influence of axial loads on short columns under cyclic lateral deformations. Two basic lateral deformation histories were used in combination with different levels of axial tension and compression as well as alternate application of both.

CHAPTER 2

EXPERIMENTAL PROGRAM

2.1 Design of Experimental Program

Because the main objective was to investigate the effect of complex load histories, the specimen geometry was held constant. The column section was square because a symmetrical section permitted easier comparisons of the influence of various loading histories. The reinforcing steel was selected to represent a column designed in accordance with current practice. The shear span was selected with the aim of producing a column controlled by shear rather than by flexural response.

The test specimen was a 2/3-scale section of an 18 in. square prototype column with eight #9 bars and 1-1/2 in. cover. A 2/3-scale model provided a very convenient 12 in. column, eight #6 bars, and 1 in. cover. The 2/3 scale permitted a reduction in the applied loads without scale effects becoming important.

With a column length of 36 in., the shear span-to-column thickness ratio was 1.5. With a ratio of 1.5, shear failures were likely to occur.

In Fig. 2.1, some of the specimens used in past studies of the effect of repeated loading on members are schematically represented. Type (a) has been used to study beams (flexure) rather than columns. Types (a), (b), and (c) are adequate for unidirectional lateral loads; bidirectional lateral loads cannot be applied easily. Types (b), (d), and (e) can be subjected to anti-symmetrical lateral loading as induced by earthquake motions.

The specimen used in this study is similar to Type (d), because it represents a column in a building with stiff floor systems. In previous studies Type (d) was used with unidirectional

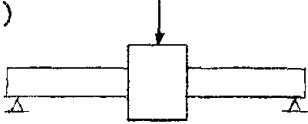
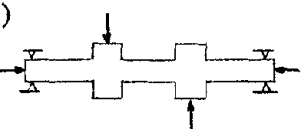
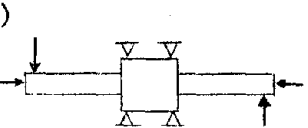
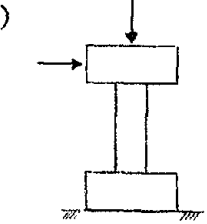
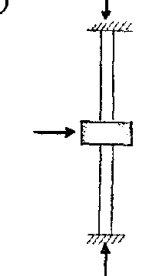
Type	Reference	Loading (lateral)
a) 	Burns and Siess (1) (2)	unidirectional
b) 	Shimazu and Hirai (6)	unidirectional anti-symmetrical
c) 	Wight and Kanoh (7) Karlson, Aoyama and Sozen (10)	unidirectional
d) 	Hiroswawa, Oazki and Wakabayashi (5)	unidirectional anti-symmetrical
e) 	Okada, Seki and Asai (13)	bidirectional anti-symmetrical

Fig. 2.1 Specimens used by other investigators

lateral loading but there are no technical impediments for using it with bidirectional lateral loading. Another important consideration was that the specimen is more suitable for the application of tensile and/or compressive axial loads than the other types of specimens examined.

2.2 Limits of Horizontal Deflections

There is a tendency to classify the ductility of a column according to the reduction of strength under a given number of cycles at a specified deformation. Umemura, Hirose, and Endo [21] concluded that, during seismic disturbances horizontal deflections of 3 to 4 times the deflection-producing yield in the main bars, Δ_y , may be observed. On the other hand, reported results [5,7] show that cyclic loadings to deflection limits of about 4 times the yield deflection, Δ_y , provide an indication of the type of behavior to be expected. If Δ_y is defined as the deflection at which yield strain is initiated in the longitudinal bars, the deflection will depend on loading and on support conditions. In order to allow for comparisons and for consistency with the previous studies, the value of Δ_y in this study was selected as the horizontal deflection (in a specimen without any axial load) at which yield strain was observed in the longitudinal reinforcement. The value observed was about 0.2 in. and is used as the reference deflection in all tests, regardless of the loading conditions. Because the reference deflection does not necessarily correspond to the initiation of yield for other load conditions (different lateral load histories and/or application of axial loads) it will be referred to as initial rather than yield deflection, and represented as Δ_i . Peak deflections of 1, 2, 3, and 4 times the initial deflection were imposed at each stage and repeated for a selected number of cycles.

2.3 Number of Cycles

The number of load repetitions is important in determining the behavior of a member. The number of cycles imposed during a test must correlate with the number produced during an actual earthquake if the data are to be meaningful for design purposes. Previous studies [5,21] show that during a seismic event, deformations of about 3 to 4 times the yield deformation can be repeated from 5 to 10 times. A review of tests carried out in Japan [5,6] shows that the behavioral characteristics were apparent in less than 10 cycles of load at a given deflection level.

Tests conducted [22] on groups of two identical specimens under the same lateral loading but with 3 cycles at each deflection level in one and 10 cycles in the other showed similar behavior in each group. This suggests that behavior was more influenced by the deflection level than by the number of cycles. On the other hand, in another study [23] the characteristics defining shear failure on columns were detected within the first 3 cycles at a critical displacement ductility.

It was decided that 3 cycles at each deflection level would be sufficient for the purposes of this investigation, i.e., at each deflection level (1, 2, 3, or 4 times the initial deflection) three cycles were imposed.

2.4 Load Variations

Earthquakes induce not only lateral loads but axial loads as well on the columns of a reinforced concrete framed structure. The level of the axial load depends on the column position in the general layout of the structure and on the characteristics of the earth movement. For instance, a column located in the central part of a rectangular building is likely to maintain a constant level of axial load produced primarily by dead load, except when vertical seismic accelerations occur. On the other hand, circled columns on the schematic plan view of the structure in Fig. 2.2 may be subjected

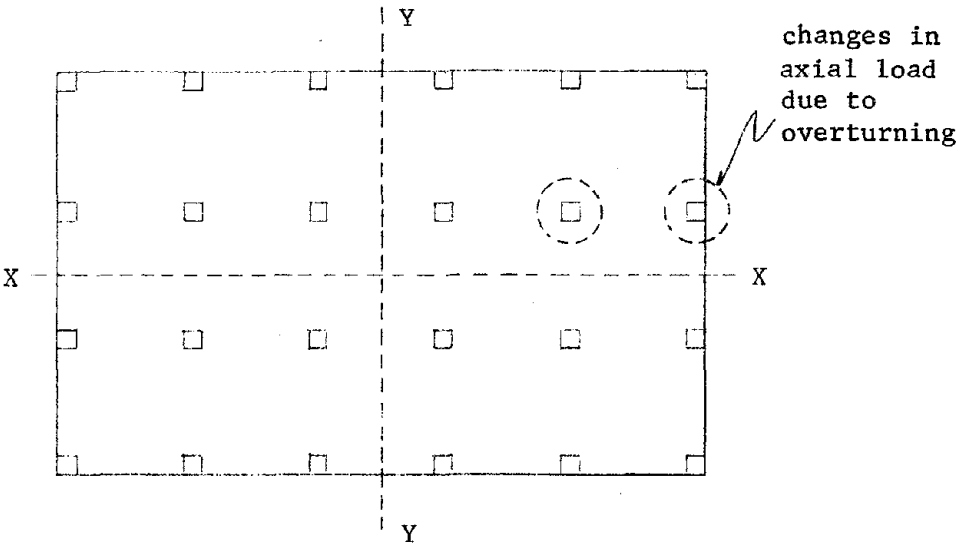


Fig. 2.2 Columns subjected to axial load variations

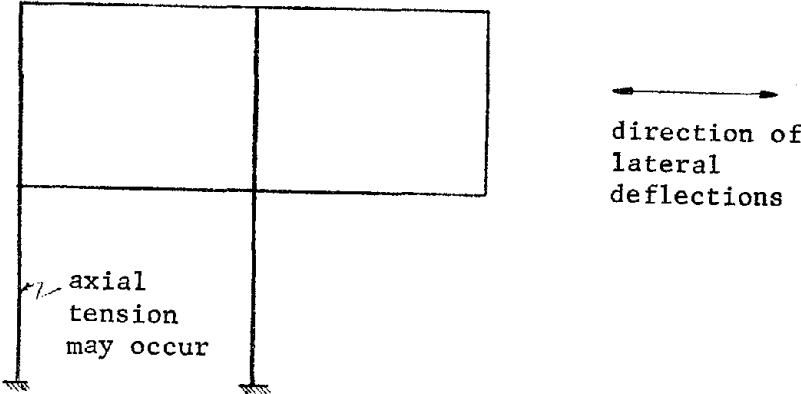


Fig. 2.3 Building frame with overhang

to varying axial load, including tension for overturning in the long direction and more constant levels of axial load for overturning in the short direction.

Exterior columns of buildings with overhangs may also be subjected to varied axial loads. Figure 2.3 represents the frame of a building with an overhang in which the lower left side column may be subjected to tension during some stages of the lateral movement induced by an earthquake. The overturning effect producing tension in exterior columns in slender buildings may also be present in other types of structures. This is the case of buildings with nonstructural filler walls, which for design purposes are not considered as part of the lateral force resisting system. The addition of the filler walls transforms the structure from a complex flexible system into a relatively simple stiff system. As a result of the stiffness increase, an increase in base shear and overturning moment occurs, producing varying axial loads--including tension--on exterior columns [20].

Tension forces in column can also be produced and/or increased when the vertical component of the seismic acceleration is important. The role of vertical seismic acceleration in seismic design can be significant [24].

Thus, during earthquakes a wide range of varying axial forces, including tension in exterior columns of reinforced concrete framed buildings, can occur due to one or a combination of several factors including:

- (a) Cantilever behavior (overturning effect)
- (b) Overhanging parts
- (c) Vertical seismic accelerations

Because no data have been reported regarding cyclic lateral loads in combination with axial tension, it was decided to include three levels of axial tension and only one of compression. The

upper limit for tension axial force is represented by the force required to produce yield in the vertical reinforcing bars. Regardless of the fact that tensile yield may not be realistic, it was considered because it represents a limiting point for reference. The other two levels of tension were one-fourth and one-half of the tensile yield force. The level for axial compression was chosen to represent the effects of gravity dead loads on a structure. In some tests the axial load was kept constant and in others varied from tension to compression.

2.5 Test Details

Two basic lateral deformation histories were selected. In one, history U, increasing deformation was applied in one direction, while zero deformation was held in the other direction--unidirectional loading. In the other, history B, deformation was applied alternately in both directions at each peak deflection level--bidirectional loading.

In Fig. 2.4, a representation of the two basic lateral deformation histories is shown. Lateral deformation histories were selected to study the effect of axial loads at different levels and modes of application ranging from compression to tension on shear behavior. Although other experimental studies [13,27] have shown that patterns of horizontal displacement with components in two orthogonal directions (square and elliptical) are more severe than unidirectional or bidirectional alternate traces, more complex lateral deformation histories were not considered because data were unavailable regarding cyclic lateral loads and axial tension. The intention was to develop basic data on which decisions regarding lateral and axial load histories for future experimental work could be founded.

The complete test schedule adopted is shown in Table 2.1. Tests 1 to 5 form a group in which the influence of axial load

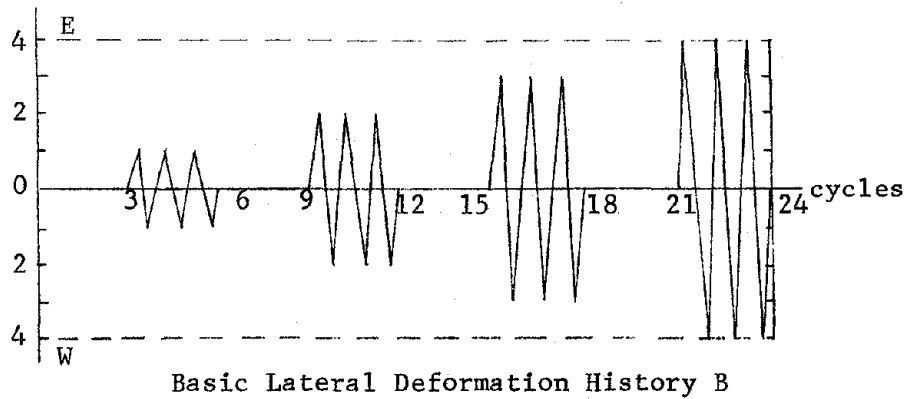
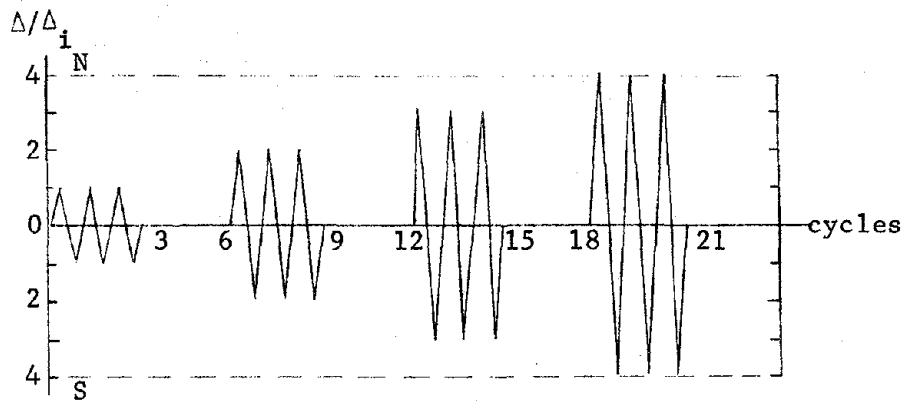
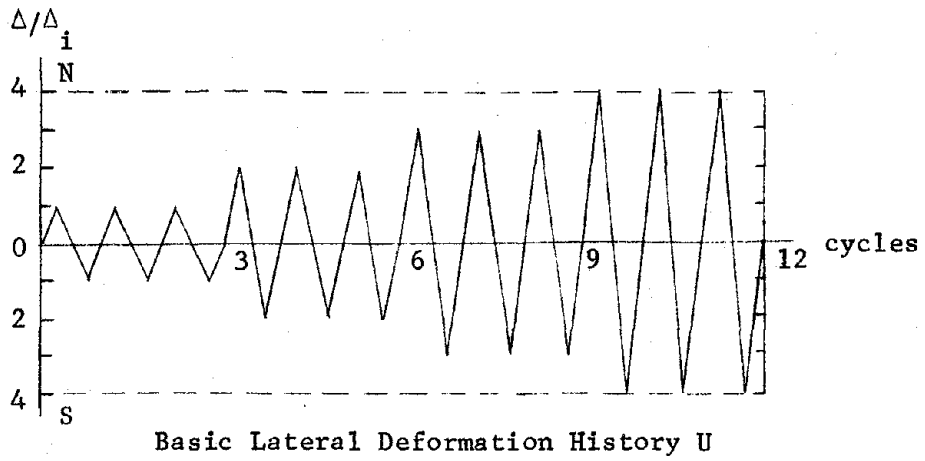


Fig. 2.4 Basic lateral deformation histories

TABLE 2.1 TEST SCHEDULE

No.	Mark	Lateral History	Axial Load		
			Mode	Level(kips)	Stress*
1	120C-U	U	Constant Compression	120	$f_c = 1.2 \text{ Ksi}$
2	00-U	U	No axial load	0	0
3	50T-U	U	Constant Tension	50	$f_s = f_y / 4$
4	100T-U	U	Constant Tension	100	$f_s = f_y / 2$
5	200T-U	U	Constant Tension	200	$f_s = f_y$
6	ATC-U	U	Alternate	100 tens. 120 comp.	$f_s = f_y / 2$ $f_c = 1.2 \text{ Ksi}$
7	120C-B	B	Constant Compression	120	$f_c = 1.2 \text{ Ksi}$
8	00-B	B	No axial load	0	0
9	50T-B	B	Constant Tension	50	$f_s = f_y / 4$
10	ATC-B	B	Alternate	50 tens. 120 comp.	$f_s = f_y / 4$ $f_c = 1.2 \text{ Ksi}$

* Compressive stress taken on core area

Mark nomenclature:

First symbol - The axial load mode (and the level when applicable) C for compression, T for tension, and ATC for alternate.

Second symbol- The lateral deformation history
U for unidirectional and B for bidirectional.

level on the shear behavior under unidirectional loading was studied. In a more limited way, tests 7 to 9 form a similar group for the bidirectional loading.

Test ATC-U was designed to simulate the loads induced by an earthquake on an exterior column of a reinforced concrete building, in which tension alternating with compression occurs in the first stage of the shock where afterwards only compression is present. This case may arise in a reinforced concrete framed building with stiff but low-strength filler walls. The sequence of application of axial force in relation to the lateral displacement used in test ATC-U is shown in Fig. 2.5.

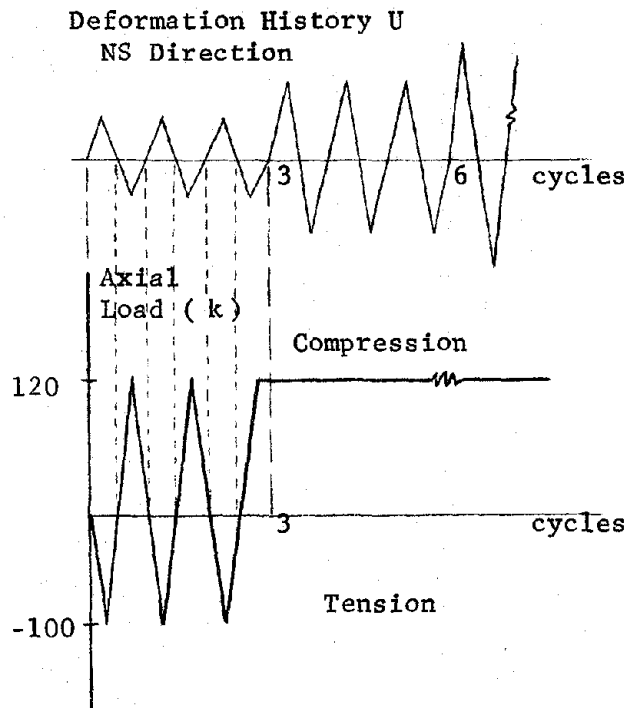


Fig. 2.5 Application sequence of axial loads, test ATC-U

Test ATC-B was designed to simulate the loads induced by an earthquake on an exterior column of a slender reinforced concrete building in which tension alternating with compression occurs for deformations in one direction and only compression for deformations in the other direction. This is the case illustrated in Fig. 2.2. The sequence of application of axial force in relation to the lateral displacement used in test ATC-B is shown in Fig. 2.6.

The two main objectives considered in designing the test program can be summarized as follows:

- (a) To study the effect of the constant axial load level for unidirectional and bidirectional displacement traces.
- (b) To study the effect of varying axial loads compared with constant axial load for both unidirectional and bidirectional lateral displacement traces.

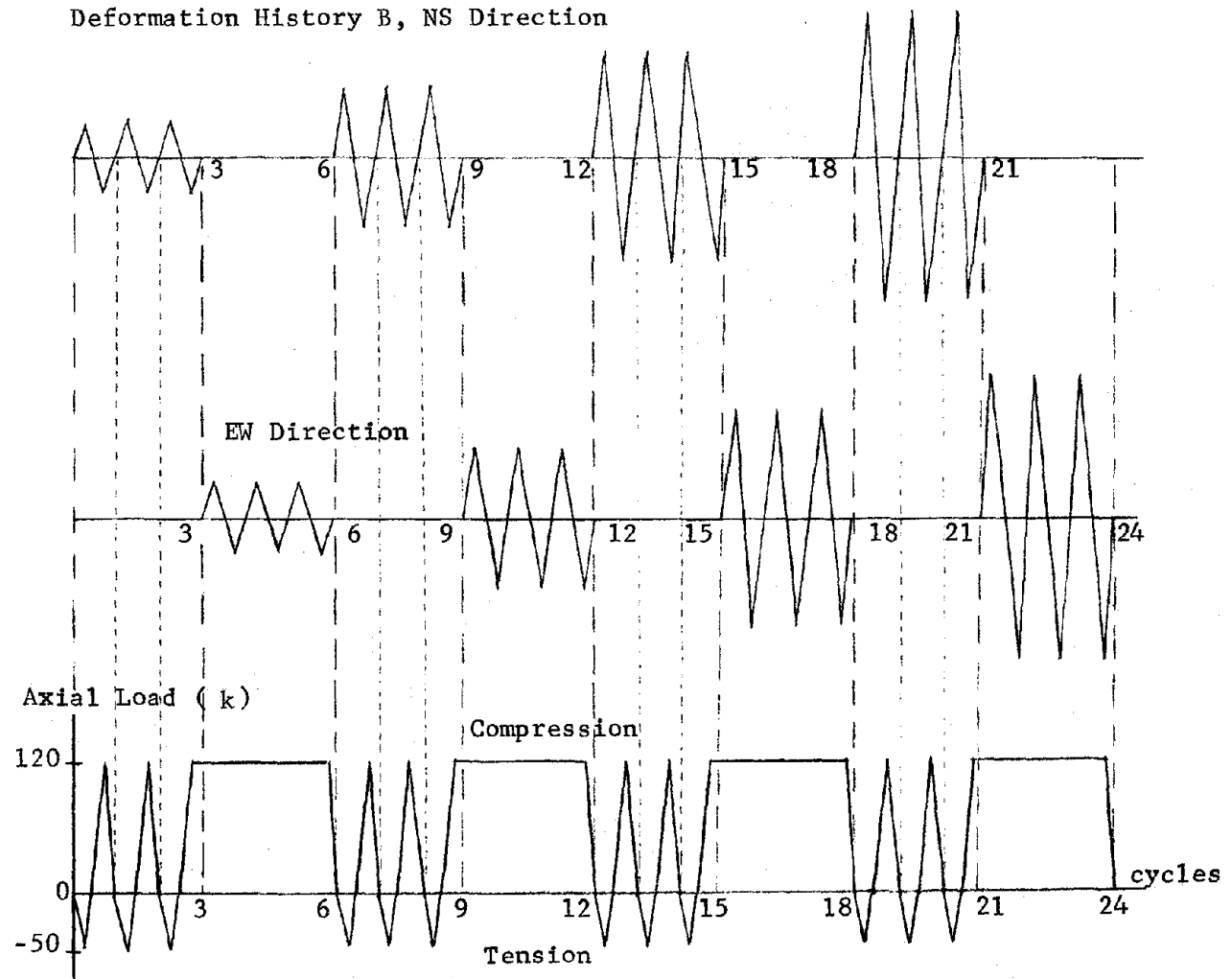


Fig. 2.6 Application sequence of axial loads, test ATC-B

C H A P T E R 3

TEST SPECIMEN AND PROCEDURES

3.1 Specimen Details

The specimen dimensions and reinforcement are shown in Fig. 3.1. The test specimen cross section is a 2/3 scale of the prototype section (dimensions shown in parentheses).

The spacing of the #2 closed stirrups was determined with the objective of producing a specimen failing in shear. Using current state-of-the-art design techniques, the performance of the column might not be satisfactory under the imposed loads but the column would represent typical practice in column design in seismic areas. In accordance with the above criteria, two limiting points for the spacing of ties can be calculated. One is the spacing required to provide shear strength corresponding to maximum moment at the ends of the column and no axial load. The second corresponds to the condition at minimum eccentricity.

Ignoring second order effects, the shear V for a given moment M is given by $V = M/a$ where a is the shear span. As discussed in Chapter 2, a shear span of 18 in. was selected to produce specimens governed by shear behavior. Using a shear span of 18 in. in connection with the interaction diagram shown in Fig. 3.2, the tie spacings using Eqs. (11.3), (11.6), and (11.13) of the ACI Code [18] are as follows:

Spacing for maximum moment under zero axial load:

2.2 in. - prototype
1.5 in. - specimen

Spacing for minimum eccentricity (point A on the interaction diagram):

18 in. - prototype
12 in. - specimen

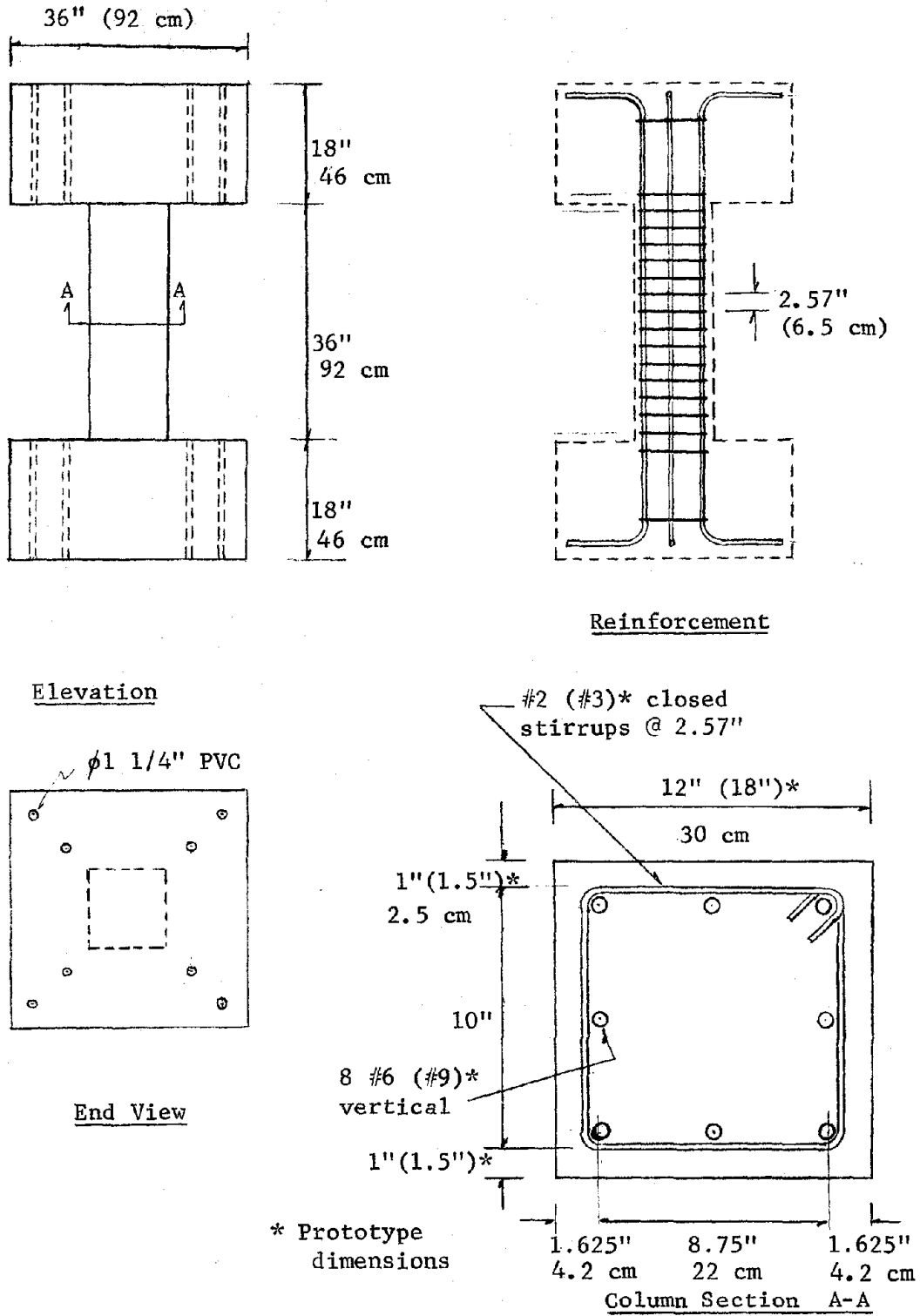


Fig. 3.1 Specimen nominal dimensions

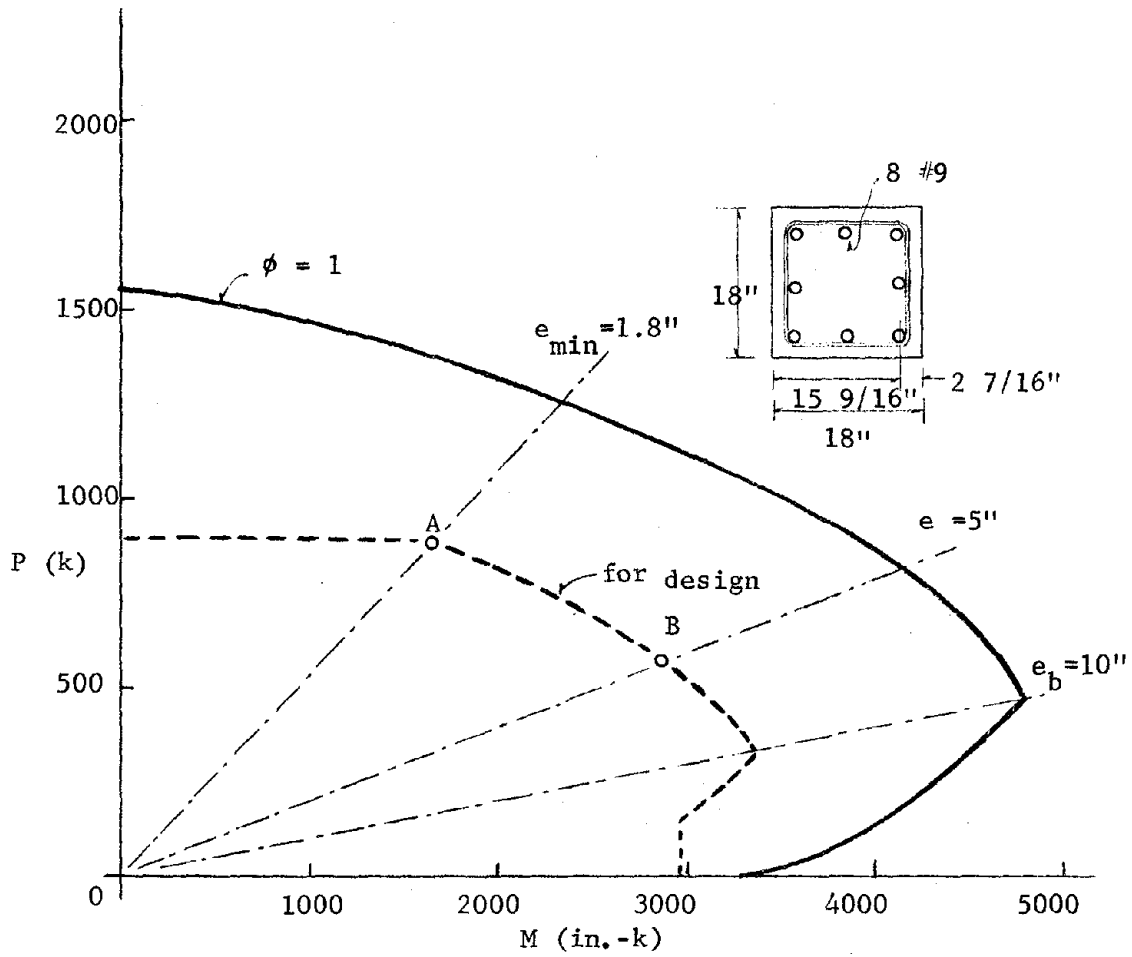


Fig. 3.2 Interaction diagram for the prototype

The spacing used, 2.57 in. (6.5 cm), is between the two limits and the shear strength provided will correspond to point B on the interaction diagram. Point B is a reasonable value for a column subjected to axial forces produced primarily by gravity dead load coupled with lateral seismic loads.

The main column bars were designed with 90° hooks in order to provide adequate development length. Following the ACI Code [18], the required development length (in tension) is $l_d = 18$ in. (46 cm). With an end block thickness of 18 in., a bond failure may occur if straight bars are used. Since anchorage failure was to be avoided, the bars were bent as shown in Fig. 3.1. According to Section 12.8 of the ACI Code [18], the hook can develop a tensile stress of 32 ksi (220 MPa). In order to develop the full nominal yield stress at the critical section between the column and the end block, a straight lead length of 11 in. (28 cm) is required (Section 12.5, ACI Code [18]). A recent study [25] indicated that hooks develop higher stresses than predicted in ACI 318. According to that study, the equation applicable in this particular case is

$$f_h = 700(1 - 0.3d_b) f'_c$$

where f_h is the stress developed by an ACI standard hook. Using this criterion, the stress developed by the hook is 38 ksi (270 MPa) and the straight lead length required will be 9.5 in. (38 cm). The same study indicated that if spalling is prevented in the tail zone of the hook the constant in the above equation can be increased to 980. Considering the restrictions provided by the components of the test frame, no spalling is expected and the stress developed will be 53 ksi (360 MPa) with a required lead of 5.5 in. (14 cm). The required lead will probably lie between 5.5 and 9.5 in. The actual straight lead provided was 13 in. (32 cm).

3.2 Fabrication

In order to simultaneously cast two specimens, forms were built to permit casting the entire specimen, including end blocks, in one operation. Details of the formwork are given in Refs. 27 and 39. Details of the supplementary reinforcement in the end blocks are given in Ref. 39. The required cover for the column portion as well as the vertical position of the steel cage relative to the form was controlled by means of metal chairs. PVC pipe was placed in the form to provide ducts for fixing the specimen to the loading frame. The concrete was cast through the upper end of the formwork which was left open for that purpose. The concrete was vibrated continuously during casting using two small internal vibrators. Vibrators were inserted through temporary openings in the lower end block. The openings were closed after vibration of the lower portion was completed.

At completion of the casting operation, the concrete surface was screeded and finished with a steel trowel. After casting, plastic sheets were placed over the forms and the control cylinders. Forms were removed two or three days after casting and the specimens were stored indoors for future testing.

3.3 Materials

(a) Concrete. Concrete was manufactured by a local ready-mix plant according to the following specifications:

Mix proportions:

Water	312 lb/cu yd
Cement	520 lb/cu yd
Fine aggregate	1340 lb/cu yd
Coarse aggregate	1770 lb/cu yd
Airsene (water reducing admixture)	25 oz
Required slump	4 to 6 in.
Required strength at 28 days - f'_c	= 4000 to 5000 psi (28-35 MPa)

The concrete was delivered with a water content below the one specified and was adjusted when the concrete arrived at the Laboratory. Water was added until the desired slump was reached. Two specimens were cast simultaneously. Six standard 6 in. × 12 in. control cylinders were cast with each specimen. The control cylinders were cured under the same conditions as the specimens. In Table 3.1 the date of casting and testing, average cylinder strength, slump, and age of the concrete at testing for each of the ten specimens are listed.

TABLE 3.1 CONCRETE MATERIAL PROPERTIES

Test Mark	Date			Slump (in)	Cylinder test	
	Casting	Testing	Cylinder test		Average strength(psi)	Age (days)
00-U	12-2-77	1-17-78	1-18-78	5	5,000	47
00-B	1-25-78	2-23-78	2-24-78	6	6,000	30
120C-B	1-25-78	3-2-78	3-3-78	6	5,950	37
50T-U	2-16-78	3-16-78	3-17-78	8	5,100	29
100T-U	3-10-78	4-13-78	4-14-78	6	5,600	35
200T-U	3-10-78	4-20-78	4-21-78	6	5,800	42
120C-U	4-26-78	5-25-78	5-26-78	5	4,450	30
ATC-U	4-26-78	6-8-78	6-9-78	5	4,700	44
50T-B	5-16-78	6-15-78	6-16-78	7	4,650	31
ATC-B	5-16-78	6-22-78	6-22-78	7	5,000	37

(b) Reinforcing Steel. Three sizes of A615-68 bars were used as reinforcement for the column specimens. A706 steel was considered because the properties were more closely controlled; however, a check with suppliers indicated that it could not be obtained in small lots in the sizes needed.

The main steel for the column specimens came from two different shipments from the same mill. The steel used for shear reinforcement came from a single shipment. The #2 deformed bars were 6 mm bars fabricated in Sweden and obtained through the Portland Cement Association Laboratories. Several tests were performed on coupons cut from some of the bars. In some of the tests two strain gages diametrically opposed were attached to the coupons in order to obtain accurate values of the modulus of elasticity. In some of the tests an extensometer was attached to the coupons in order to obtain complete stress-strain curves.

A total of 18 coupon tests was conducted on the #2 and #6 bars. No coupon tests were performed on the #3 bars because they were used as secondary reinforcement only in the end block and did not influence the strength or the general behavior of the column section.

Figure 3.3 shows the stress-strain curves for the reinforcement. Both lots of #6 bars had similar modulus of elasticity but the yield strength and postelastic behavior were different. The second lot had a higher yield than the first and the stiffness in the strain hardening region was higher. Ultimate for the second lot was higher than the first but occurred at a lower strain. Six specimens (00-U, 00-B, 120C-B, 50T-U, 100T-U, and 200T-U) were fabricated with #6 bars from the first lot and four (120C-U, ATC-U, 50T-B, and ATC-B) with bars from the second lot.

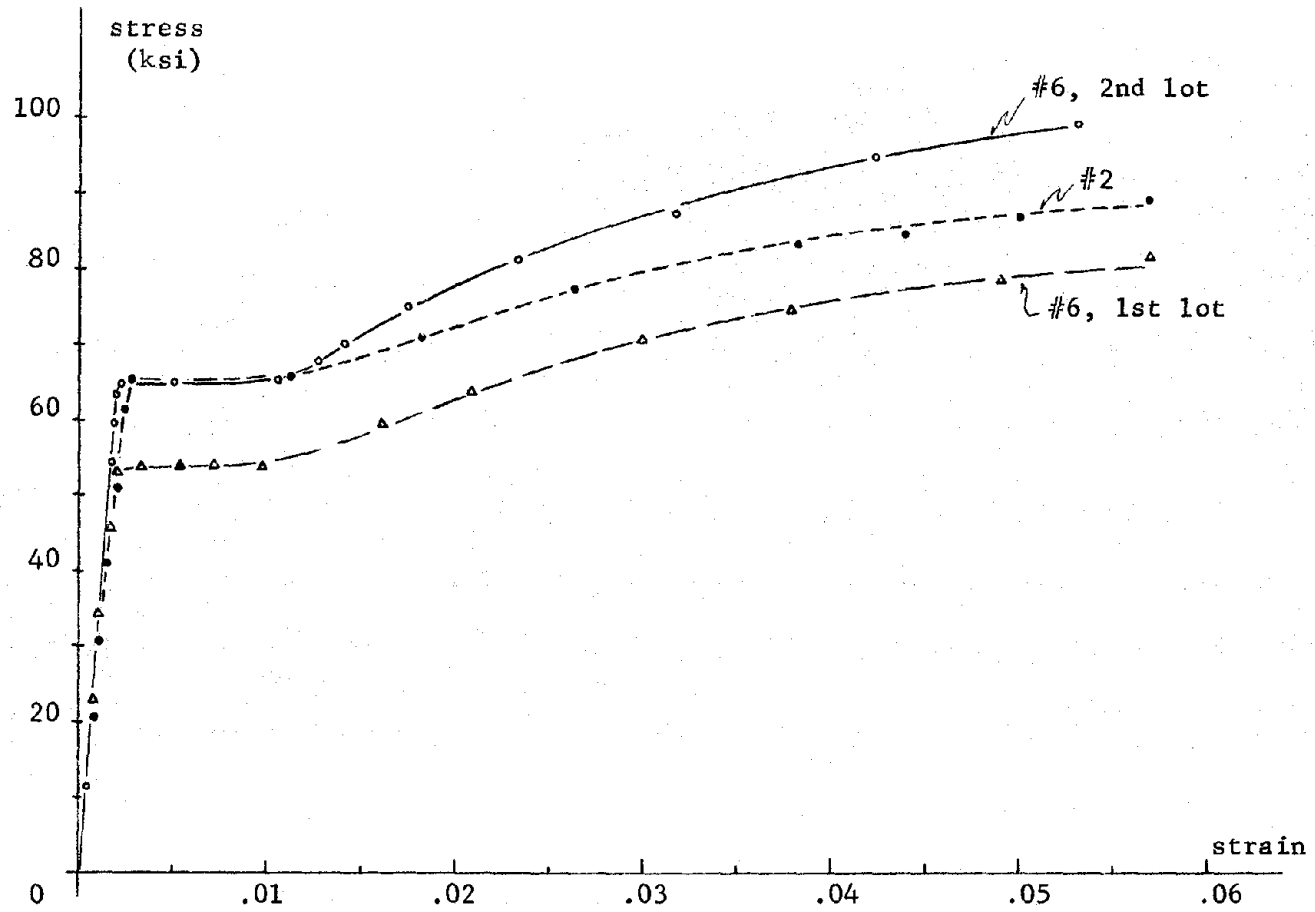


Fig. 3.3 Reinforcing steel stress-strain curves

3.4 Loading System

The loading system consisted of a structural loading frame, two lateral load actuators, one axial load actuator, and three hydraulic positioning systems to control the specimen end rotations. It was designed to utilize the existing facilities and equipment including the strong floor-wall system, the closed-loop hydraulic loading system, and the digital data acquisition system. Figure 3.4 shows the test setup. The loading and data acquisition system is described in detail in Refs. 39 and 40.

Lateral loading components were deformation-controlled while the axial load component was load-controlled. The servo-controllers could be manually or computer-controlled. Six tests were performed using the manual mode and the rest were monitored by the computer.

3.5 Instrumentation

During a test, the lateral loads corresponding to the lateral displacements imposed, the axial load, and the resulting forces in the paired positioning systems, were recorded using the data acquisition system. The displacements at the top end of the column specimens were measured in all three directions. Two systems for measurement of displacements were used during the course of the experimental program. The first system consisted of special supports to hold the transducers. The supports were connected to the lower end block of the specimen and it was assumed that the rotation of the end block was negligible so that relative deformations were being monitored. After several tests were run, dial gages were connected to the lower end of the specimen in subsequent tests and it was observed that the bottom end block rotated during testing. Therefore, a second support system was developed. A frame was constructed which rested directly on the structural floor and was not connected to the specimen. Twelve transducers were

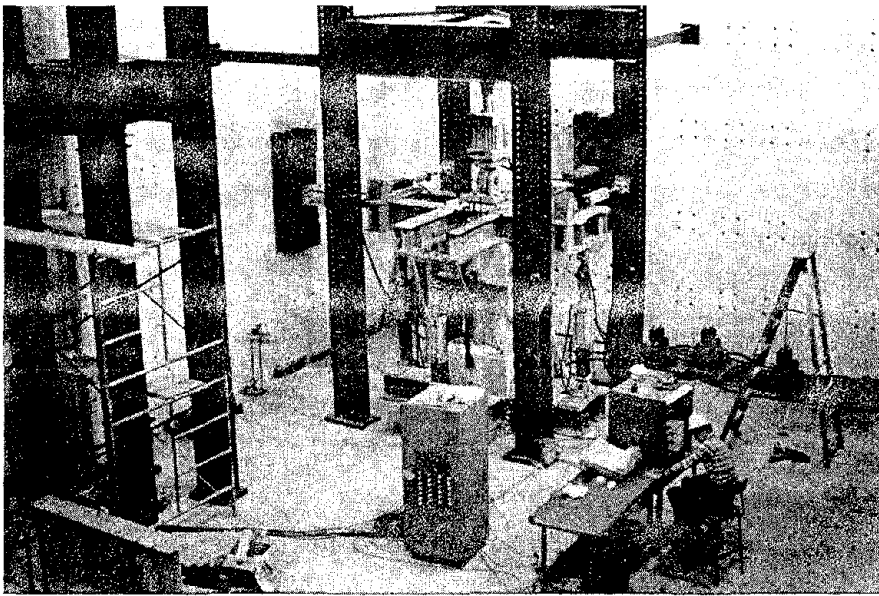


Fig. 3.4 Test setup

supported by this frame: eight transducers to measure rotations and displacements of the upper end, and four to measure the rotation of the lower. With this instrumentation total rotations and/or displacements were measured.

Strains in the transverse and longitudinal reinforcement were measured using paperbacked wire strain gages. Gaged stirrups were distributed along the length of the column portion. The number of strain gages used in the early tests was judged to be excessive, mainly because the longitudinal bars yielded early in the test and the gages were not operating. Thus, for the remainder of the tests the number of strain gages was reduced. Only two corner longitudinal bars were gaged. Six stirrups were gaged per specimen: two gages on opposite legs for unidirectional lateral histories, and four strain gages (one on each leg) for bidirectional lateral histories.

XXXXXXXXXX XXXX

C H A P T E R 4

TEST RESULTS

4.1 General

The objective in analyzing the data was to study the influence of axial loads with respect to the two lateral deflection histories. Three modes of application of axial loads were studied: constant compression (Chapter 5), constant tension (Chapter 6), and alternate tension and compression (Chapter 7). The analysis was based on comparisons of tests with and without axial load (00-U and 00-B) for the study of the effect of constant compression and constant tension, and with tests with similar levels of axial loads (constant tension or compression) for the study of alternating axial loads.

For each group of tests, basic data will be described first. Next, a more elaborate analysis of the data will be presented to obtain comparative behavioral trends. Finally, the results will be utilized to develop design approaches. In each of the three chapters (5, 6, and 7) the first step is based on the basic information explained in this chapter and presented here for test 00-U.

The basic data (voltage readings) were analyzed using a data reduction package for readings stored in the computer and on tape. The availability of a plotting software program made the task more efficient. The data were rearranged to produce plots of load deflection and shear deterioration, tables of peak forces, and distributions of strain in transverse reinforcement. The basic data were reduced for all ten tests to visualize general trends to

facilitate further analysis. The main objective of this chapter is to describe the presentation of the data using the results of test 00-U as an example.

4.2 Load-Deflection Curves

The hysteretic behavior of the specimens under the imposed cyclic deformations and axial loads is best represented by load-deflection curves. Unidirectional tests are represented by one curve while bidirectional tests require two, one for each orthogonal direction. Load-deflection curves plotted on a uniform scale permit visual comparisons of the hysteretic behavior of the specimens. Of particular interest is the stiffness (slope), peak values of lateral loads and deflections, shape of the hysteretic loops, and shear deterioration. The slope of the load-deflection curve at any point represents the stiffness of the element. The change in stiffness is caused by cracking and local spalling of the concrete as well as slip of the bar relative to the concrete.

For direct comparisons, envelopes of peak values were used. The envelopes unite peak values in the load-deflection curve in the first, second, or third cycles. Envelopes were used to obtain comparative hysteretic characteristics between different tests and to observe the changes in shear with cycling at a deflection level.

Except for test 00-U, all the curves were obtained using the plotting software which permitted plotting the complete test or selected parts. The positive direction of the axes represents loads and deflections in the N direction for unidirectional tests and in the N and E directions, respectively, for bidirectional loading. The load-deflection curve for test 00-U is shown in Fig. 4.1. To clarify the definition of the peak envelopes, curves for the first and third peaks are shown in Fig. 4.1. The monotonic curve obtained by Maruyama (Ref. 27) is also shown for reference.

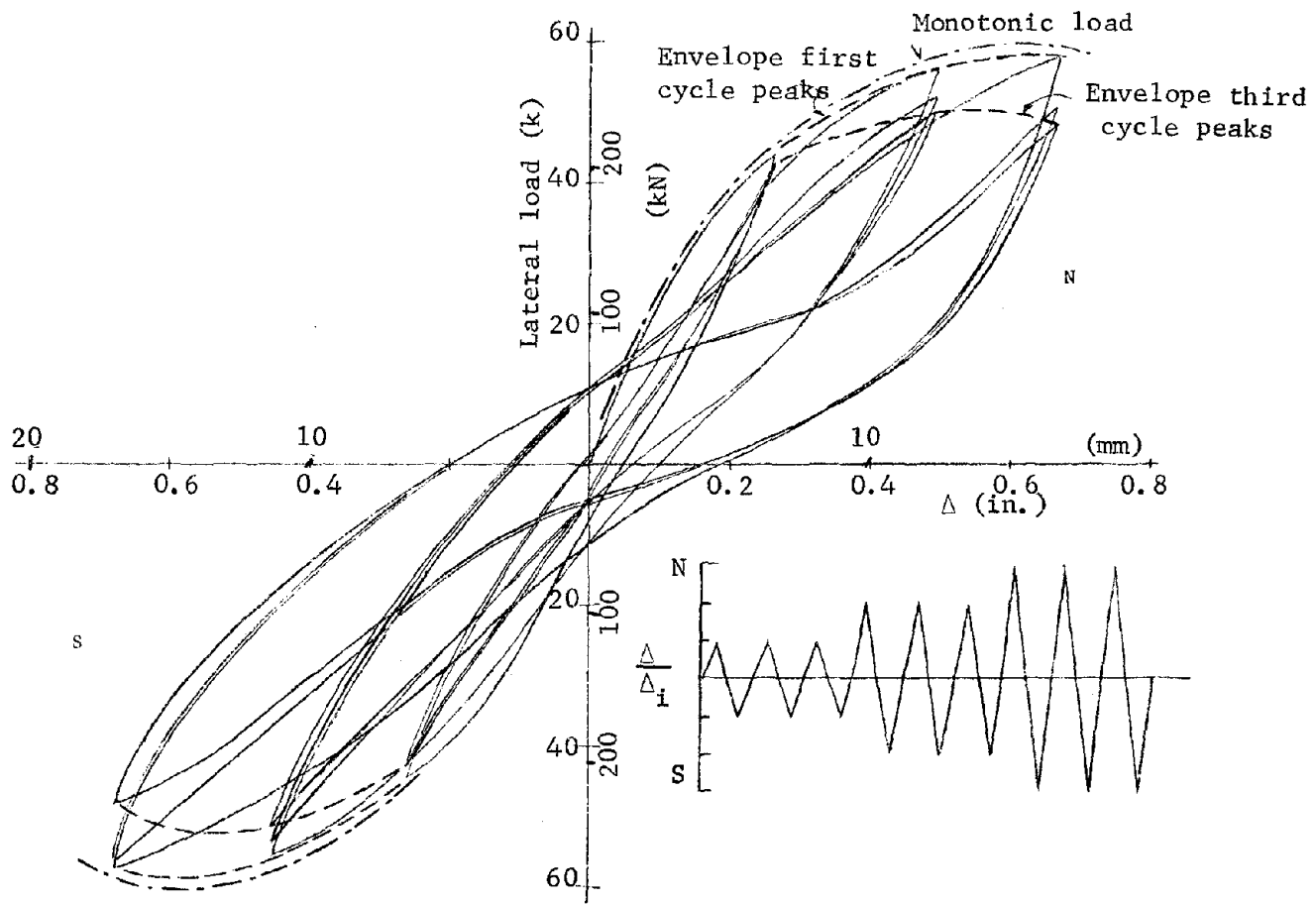


Fig. 4.1 Load-deflection curve, test 00-U

It was observed that first peaks at 00-U were very near the monotonic case as was also observed in Refs. 14 and 26. Because of the similarity between the envelope of the peaks in cycles to different deflection levels and the monotonic curve, the envelope can be utilized to make comparisons between tests. Therefore, it was decided that monotonic tests at each axial load level were not necessary and could be omitted in order to study a wider range of axial load variations.

A pinching effect on the hysteresis loops was observed for all levels of deformation. "Pinching" is defined as the tendency of the stiffness to decrease appreciably when the element is unloaded. The loss of stiffness at the neutral position results in low energy dissipation.

4.3 Peak Value Tables

Peak values of axial load, applied lateral load or shear, normalized shear stress, and corrected deflections were tabulated for all the tests. Table 4.1 shows values for Specimen 00-U. Normalized shear stresses were calculated dividing the total applied peak load in pounds by the core area, assumed as 100 in.^2 throughout testing, and the square root of the concrete strength. The core area was used in order to define shear stresses under large lateral deflections because the contribution of the concrete shell is low once extensive cracking and spalling has occurred. The tabulated shear forces and normalized stresses were utilized to construct envelopes of load-deflection relationships as well as shear-deterioration diagrams.

4.4 Shear-Deterioration Diagrams

To document the shear deterioration which occurred in each test, peak normalized shear stresses were plotted against load cycle. The lateral deflection history and axial load pattern are

TABLE 4.1 PEAK VALUES, TEST 00-U

cycles at	N	V	$V/A_c \sqrt{F'_c}$	Δ
Δ_i	0.0	44	6.2	0.254
	0.0	-45	-6.4	-0.251
	0.0	43	6.1	0.258
	0.0	-43	-6.1	-0.255
	0.0	43	6.1	0.255
	0.0	-43	-6.1	-0.256
$2 \Delta_i$	0.0	56	7.9	0.489
	0.0	-56	-7.9	-0.456
	0.0	52	7.4	0.492
	0.0	-54	-7.6	-0.468
	0.0	50	7.1	0.496
	0.0	-51	-7.2	-0.458
$3 \Delta_i$	0.0	58	8.2	0.686
	0.0	-57	-8.1	-0.670
	0.0	51	7.2	0.675
	0.0	-56	-7.9	-0.691
	0.0	48	6.8	0.670
	0.0	-48	-6.8	-0.671

are included for better visualization of the relationship between shear deterioration and load history.

The shear deterioration diagram for test 00-U is shown in Fig. 4.2. The shear deterioration diagrams graphically show the reduction in peak shear with cycling at a given deflection level, as well as the relative magnitude of the reduction at different deflection levels. The slope of the line connecting peak values at given deflection levels represents the shear deterioration from one cycle to the next at a given deflection level.

4.5 Distribution of Strain in Ties

Values of strain in the ties can be represented in many ways. The complete history of strains for a tie with respect to the lateral deformation history does not give useful information because strains exceed yield early in the history in many tests. Therefore, it was decided to plot peak values of strain for each level of lateral deformation. The goal was to obtain envelopes of strain in the ties for each peak and each cycle. Using these plots, it is possible to compare strain distributions for different applications of axial load and to develop the mechanism of failure as well as the role of the ties in the failure mechanism.

Distribution of peak strain in the ties for first and last peaks are shown in Fig. 4.3. Intermediate peaks (second cycle) are not shown. Each level of deformation is represented and the value of strain at yield is clearly marked.

4.6 Crack Patterns

From the photographs taken after three cycles at each deflection level, a diagram of the progressive development of cracks was obtained. These diagrams represent evidence of progressive damage to the specimen due to the applied loads. The main use of the diagrams in the analysis of the test results was as

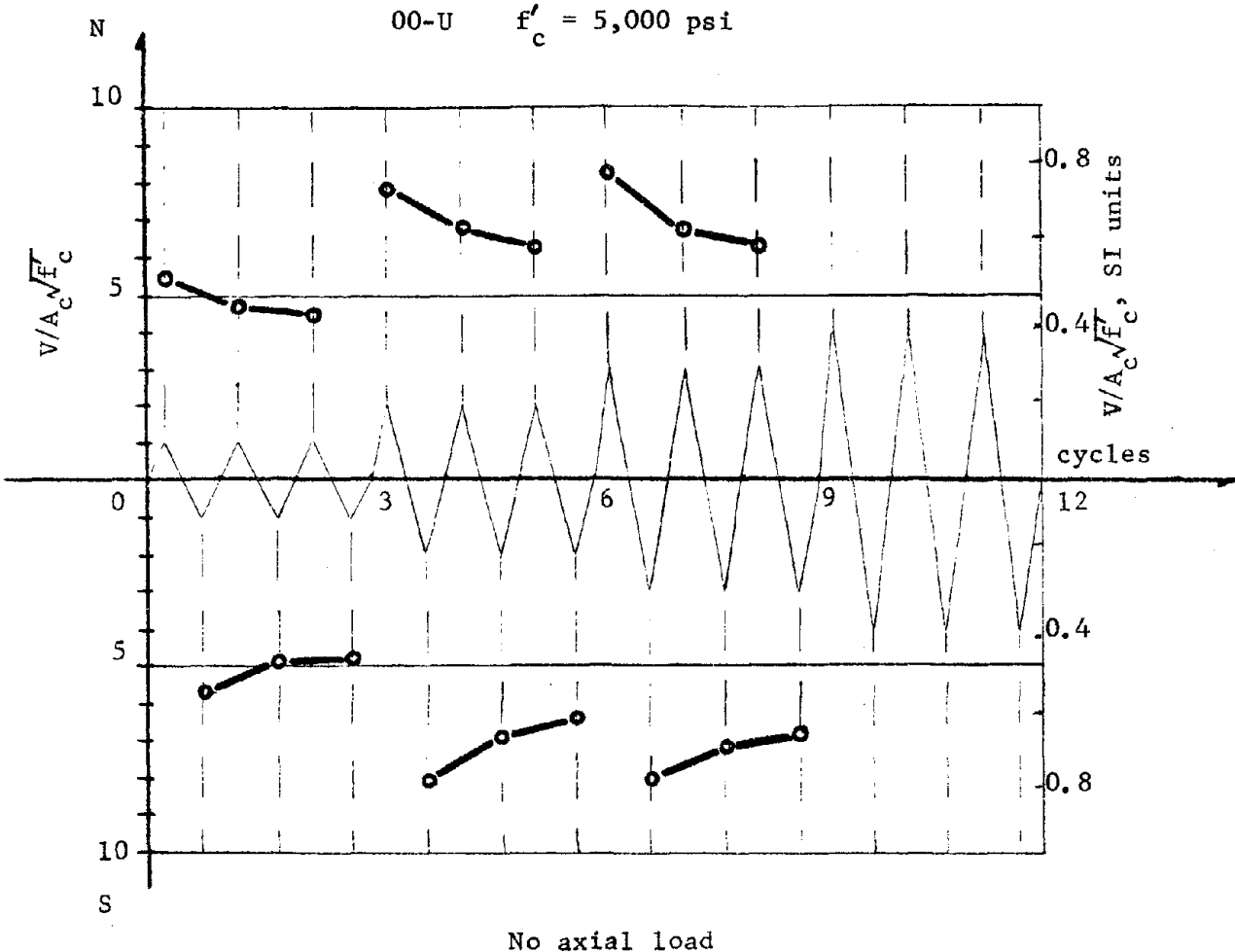
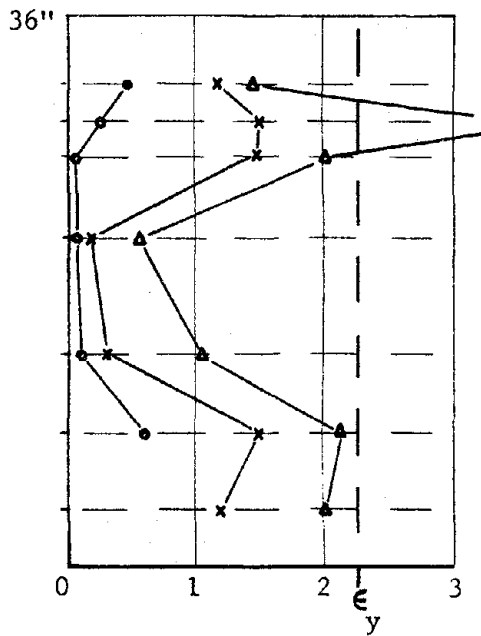
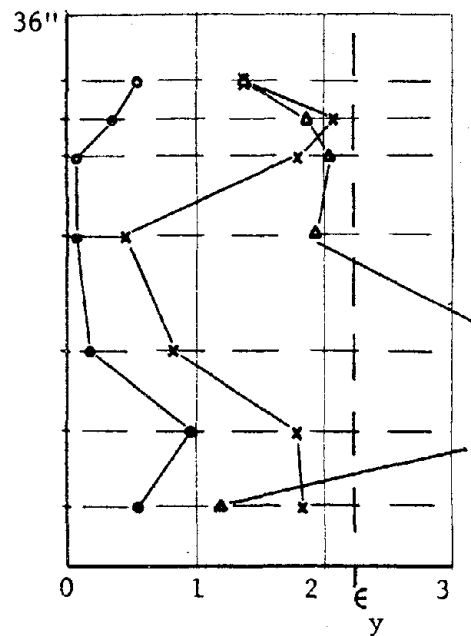


Fig. 4.2 Shear deterioration, test 00-U



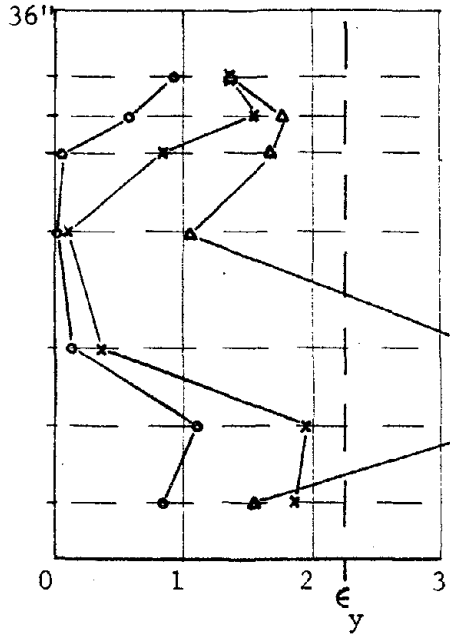
1ST Peak 1ST Cycle
(North)



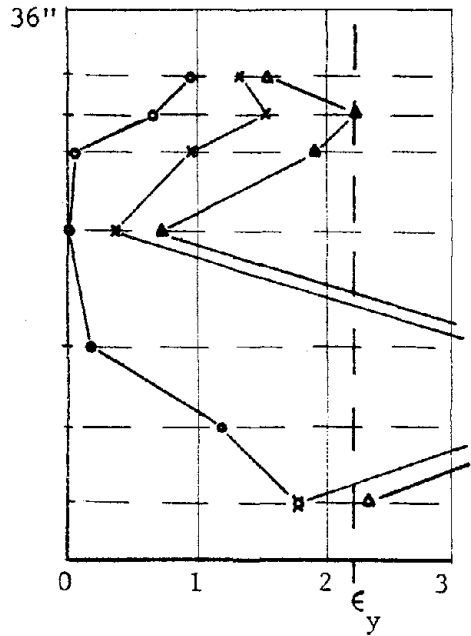
1ST Peak 3RD Cycle
(North)

○—○ Δ_i
 ×—× $2\Delta_i$
 △—△ $3\Delta_i$

($\times 10^{-3}$)



2ND Peak 1ST Cycle
(South)



2ND Peak 3RD Cycle
(South)

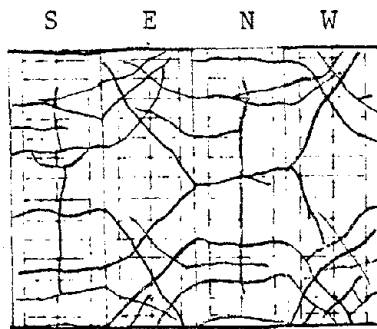
Fig. 4.3 Strain distribution in tie bars, test 00-U

complementary information to support observations made from other data. The crack pattern at each deflection level for test 00-U is shown in Fig. 4.4. At the end of three cycles at the Δ_i level several continuous inclined cracks in both directions were present on faces parallel to the direction of loading (E and W) indicating shear distress. On the other faces horizontal cracks were due mainly to flexure. Some vertical cracks were observed indicating splitting of the concrete shell due to large strains in the central longitudinal bar. At the $2\Delta_i$ level new cracks were present in appreciable numbers, while previous inclined cracks opened. From the $2\Delta_i$ level to the $3\Delta_i$, no new cracks were formed except small noncontinuous cracks. Some previous inclined cracks were quite wide and were accompanied by some spalling. In Fig. 4.4, a photograph showing final appearance of Specimen 00-U is included.

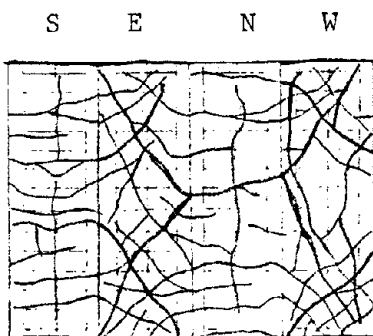
4.7 Effect of Different Material Properties

The variables related to geometry and material properties were not considered in the planning of the experimental program. The intention was to fabricate specimens with minimal variations in geometry and material strengths. However, because the steel was purchased at different times and the concrete was supplied by a local ready-mix plant, there was a variation in material properties which was sufficient to require a careful examination of the possible implications of such variations on the behavior before further analysis of the data was carried out.

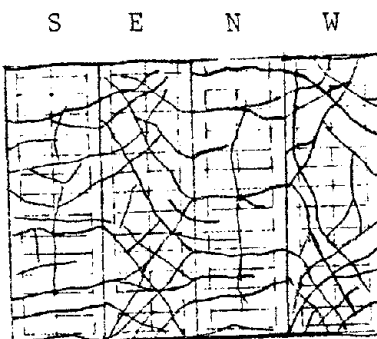
Concrete. The concrete mix was designed to give a strength of 5000 psi (34 MPa); the mean strength from all specimens was 5225 psi (36 MPa) with a standard deviation of about 500 psi (3.4 MPa). However, the main purpose in this work was to analyze qualitatively the influence of axial loads on the behavior based on comparisons among test results. An attempt to eliminate the influence of different concrete strengths was made by dividing the



After 3 cycles at Δ_i



After 3 cycles at $2\Delta_i$



After 3 cycles at $3\Delta_i$



Final appearance of specimen

Fig. 4.4 Progressive development of cracks, test 00-U

measured applied shears by the square root of the strength, assuming that the shear strength is dictated by the tensile strength of the concrete. This assumption may not be true for large deflection levels because the shear strength is dictated by aggregate interlock and confinement of the ties, and comparisons based on total applied shear may be better.

The effect of different concrete strengths is not relevant if flexure is considered for the range of axial loads utilized. Figures 4.5 and 4.6 present interaction diagrams for the column section considering concrete strengths in the range of those observed and the strength of the two lots of longitudinal steel, respectively. In Figs. 4.5 and 4.6 the concrete and longitudinal steel strengths corresponding with each specimen are included. The interaction diagrams show almost no difference due to concrete strength for low compressive axial load or tension. The difference with axial loads of 120 kips compression is still negligible.

Longitudinal Steel. The influence of the strength of the longitudinal steel on the shear strength of the specimen is assumed to be negligible. The spacing of ties is close enough to prevent local buckling of the longitudinal steel.

If flexure is considered, the tensile strength of the main steel has a direct influence. Because the phenomenon studied is a combination of shear and flexure, the possible influence of different longitudinal steel strengths will be examined when comparison among tests are made.

Second Order Effects--Compressive Axial Loads. Figure 4.7 shows the free body diagram of a column specimen under the applied loads and also shows the related equilibrium equations. The application of lateral deformations through the loading frame causes the axial load to be inclined. Second order effects are induced which increase the applied shear with respect to that measured.

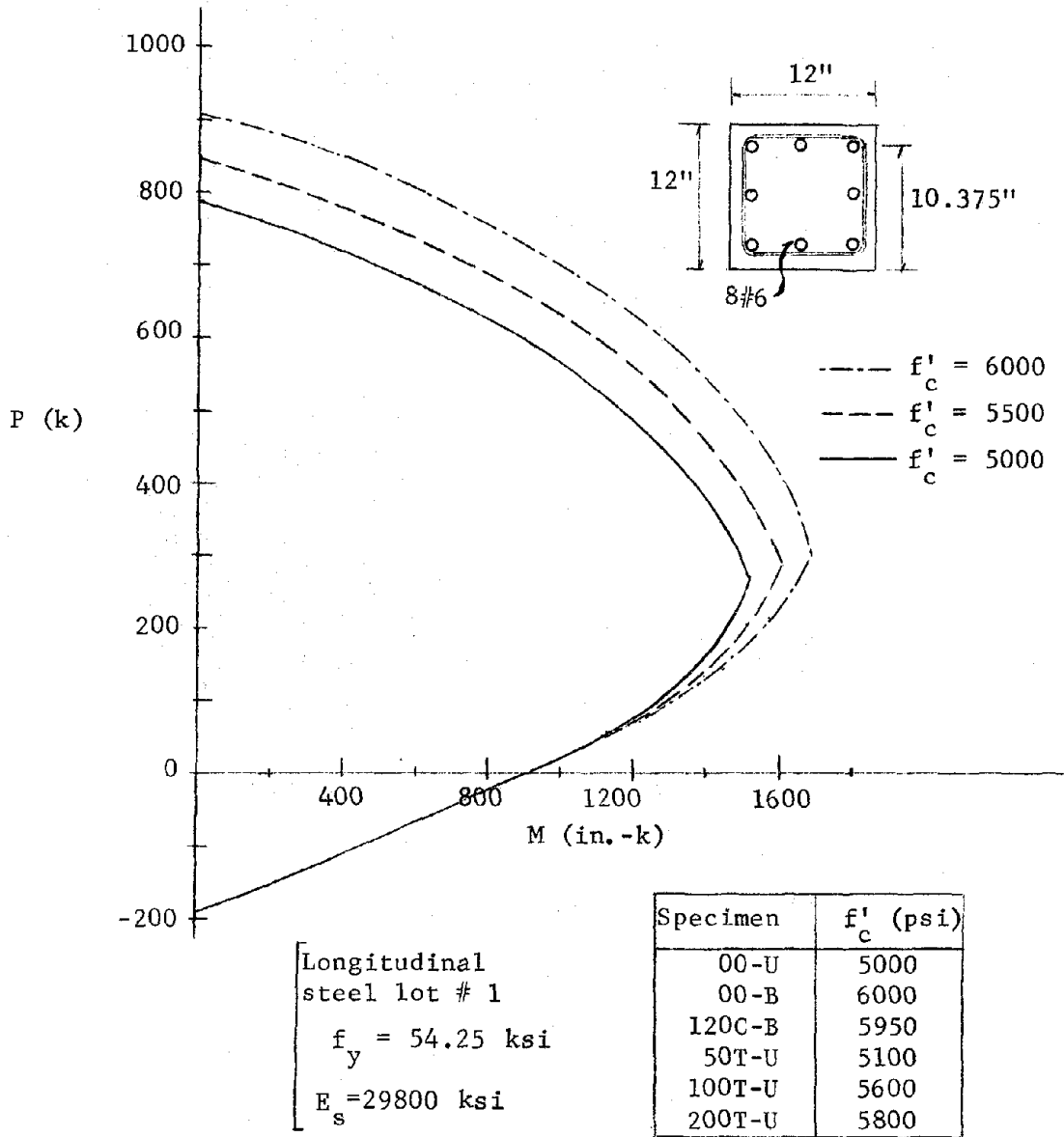


Fig. 4.5 Interaction diagrams--steel from first lot

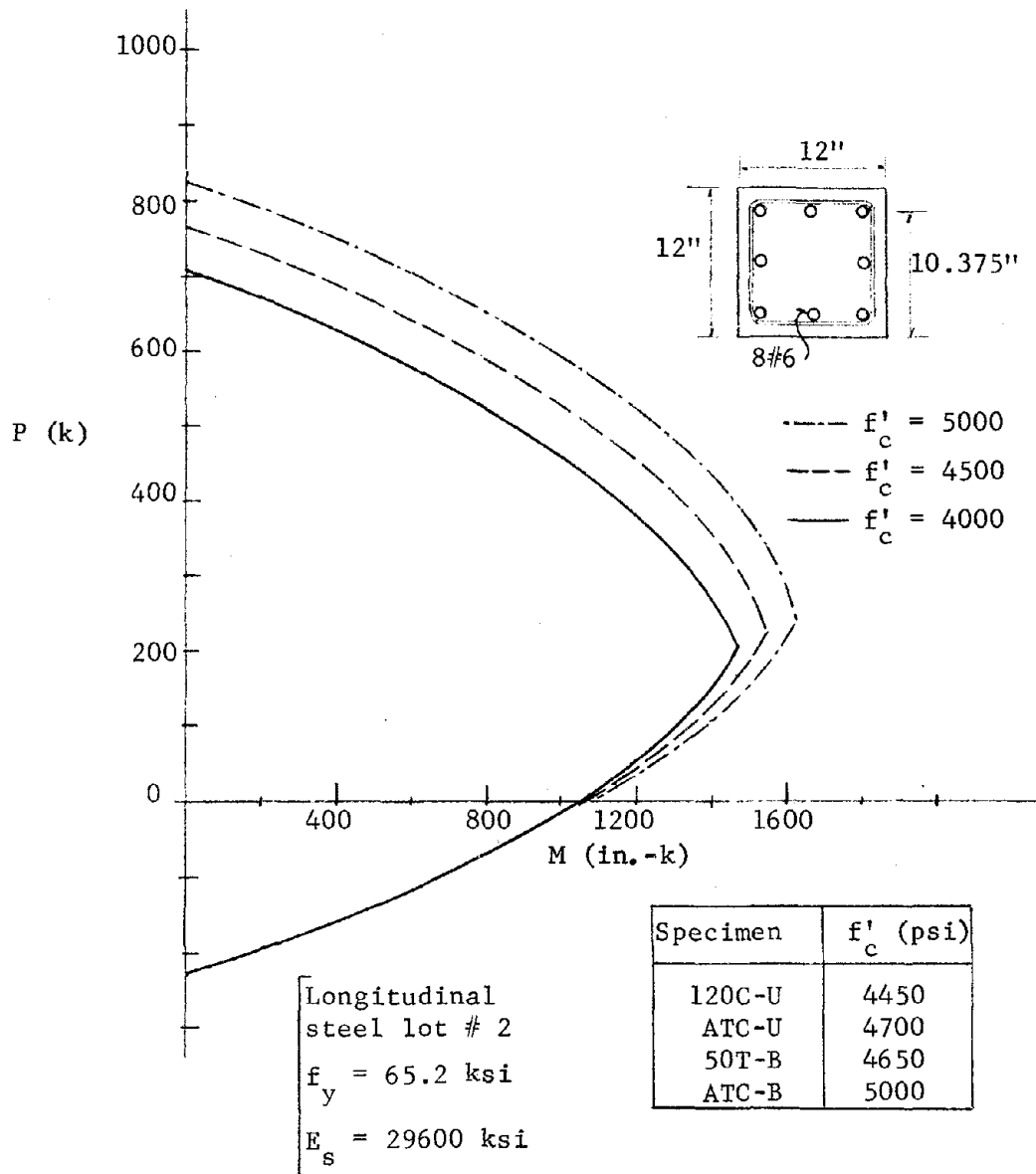
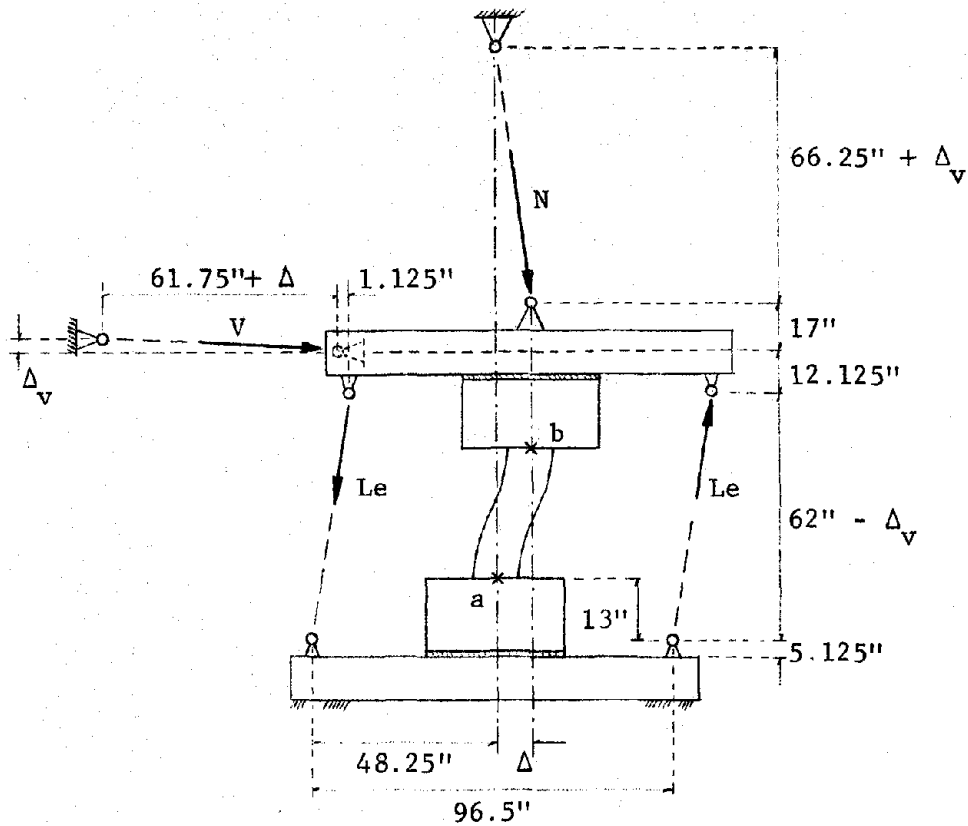


Fig. 4.6 Interaction diagrams--steel from second lot



Equilibrium Equations:

$$V_a = \frac{61.75 + \Delta}{\sqrt{(61.75 + \Delta)^2 + \Delta_v^2}} V + \frac{\Delta}{\sqrt{(66.25 + \Delta_v)^2 + \Delta^2}} N$$

$$N_a = \frac{\Delta_v}{\sqrt{(61.75 + \Delta)^2 + \Delta_v^2}} V + \frac{66.25 + \Delta_v}{\sqrt{(66.25 + \Delta_v)^2 + \Delta^2}} N$$

$$M_a = \frac{(61.75 + \Delta)(61.125 - \Delta_v) - \Delta_v(49.375 - \Delta)}{\sqrt{(61.75 + \Delta)^2 + \Delta_v^2}} V + \frac{\Delta(78.125 - \Delta_v) + (66.25 + \Delta_v)\Delta}{\sqrt{(66.25 + \Delta_v)^2 + \Delta^2}} N - \frac{(62 - \Delta_v)96.5}{\sqrt{(62 - \Delta_v)^2 + \Delta^2}} Le$$

Fig. 4.7 Free body diagram of the specimen and equilibrium equations

The applied shear is given by the first equilibrium equation shown in Fig. 4.7. Considering that Δ_v and Δ are small compared with the dimensions of the loading frame, the following simplification can be made:

$$V_a = V + \frac{N\Delta}{66.25} \quad \text{or} \quad V_a = (1 + e_v/100)V$$

where V is measured shear and $e_v = 1.51 N\Delta/V$ represents the percent error in assuming the measured shear is equal to the total applied shear force. The simplifications assumed in the formula for V_a are satisfactory because the errors computed without the simplifications are very near those computed with the simplifications. For instance, for 120C-U at $4\Delta_i$, $e_v = 6.0$ without the simplifications, and $e_v = 5.9$ with the simplifications.

Table 4.2 presents the computed maximum and minimum percent of error for each deflection level of test data for 120C-U and 120C-B. The errors are not significant in the unidirectional test, but they are high at the $4\Delta_i$ level for the bidirectional test. However, at that level, shears are very low and the error in the lateral shear is less than 2 kips in the worst case. No modifications in shear due to second order effects were made because at high shear levels the error was small and at large deformations the shear was small and the correction did not change comparisons between tests.

Second Order Effects--Tensile Axial Loads. With the axial load in tension, the actual shear applied to the column section is less than measured. Using the free body in Fig. 4.7 (T instead of N) and using the same simplification adopted in the case of compressive axial loads, the applied shear can be expressed as:

$$V_a = V - \frac{T\Delta}{66.25} \quad \text{or} \quad V_a = (1 - e_v/100)V$$

where $e_v = 1.51 T\Delta/V$ is the percent of error.

TABLE 4.2 P- Δ EFFECT, TESTS 120C-U AND 120C-B

Δ/Δ_i	Percent of error e_v					
	120C-U		120C-B NS		120C-B EW	
	min	max	min	max	min	max
1	0.7	0.8	0.7	0.8	0.6	0.7
2	1.2	1.3	1.0	1.2	1.1	1.3
3	1.8	2.8	1.7	3.0	2.7	5.6
4	3.2	5.9	5.1	11.4	9.3	27.5

$$e_v = 1.51 N\Delta/V$$

$$V_a = (1 + e_v/100) V$$

TABLE 4.3 P- Δ EFFECT, TESTS WITH CONSTANT TENSION

Δ/Δ_i	Percent of error e_v									
	50T-U		100T-U		200T-U		50T-B NS		50T-B EW	
	min	max	min	max	min	max	min	max	min	max
1	0.5	0.7	1.2	1.6	8.7	12.2	0.5	0.6	0.5	0.5
2	0.7	0.9	2.0	2.9	11.7	13.8	0.6	0.7	0.7	0.7
3	1.0	1.3	2.8	4.1	13.7	15.1	0.8	0.9	0.9	1.0
4	1.4	1.8	3.6	5.1	14.3	17.1	1.2	1.8	1.6	2.4

$$e_v = 1.51 T\Delta/V$$

$$V_a = (1 - e_v/100) V$$

In Table 4.3, the maximum and minimum percent of error at each deflection level for tests with constant tension are presented. For levels of tension of 50k and 100k, the errors are not significant. Differences of less than 1k are involved for tests with 50k tension and less than 1.5k for the test with 100k tension. For the test with 200k tension the errors are high; however, shear forces in this test are very low. Thus, the measured shears are not appreciably different from the total applied shears. For instance, for this test corrected peak values at first cycles in the north direction are 4.4, 8.7, 12.1, and 15.4 kips, while the measured peak values were 5, 10, 14, and 17 kips.

THE UNIVERSITY OF CHICAGO
LIBRARY

CHAPTER 5

CONSTANT COMPRESSION

5.1 Introduction

In this chapter the influence of constant compression is analyzed. Results from tests with constant compression (120C-U, 120C-B) and zero axial load (00-U, 00-B) under both lateral deflection histories are compared. From the comparisons made, behavioral trends are obtained and design considerations are discussed.

5.2 Description and Comparison of Test Results

Load-Deflection Curves. Figure 5.1 shows the load-deflection curve for test 120C-U. The envelope of first peaks of test 00-U is also shown for comparison (first peaks of 00-U approximate the monotonic curve). The applied shear to attain a certain displacement is greater in 120C-U than in the case with no axial load (00-U) for Δ_i and $2\Delta_i$ levels. For higher levels of deformation, however, shear decay proceeded more rapidly in Specimen 120C-U than in 00-U. Under compressive load, the increase in shear strength at low deflection levels is accompanied by an increase in stiffness but at high deflection levels there is a decrease in both shear strength and stiffness. Pinching of the hysteretic loops is accentuated more with axial load than with no axial load.

The load-deflection curves for test 120C-B are shown in Fig. 5.2 (NS direction) and Fig. 5.3 (EW direction). The envelope of first peaks of test 120C-U is also shown for reference. The difference in strength can be attributed to differences in concrete strength. The behavior up to the $2\Delta_i$ level in both directions is

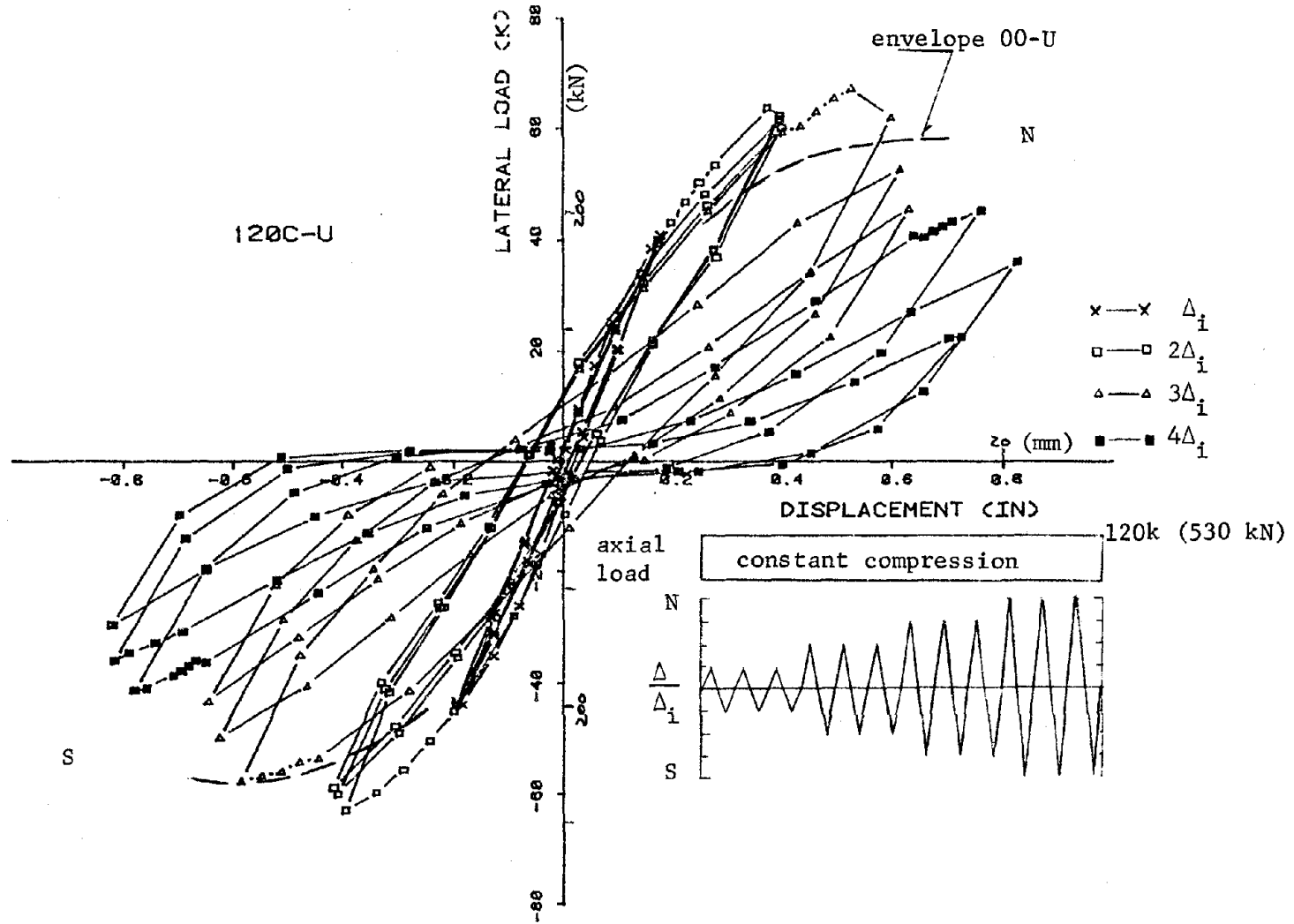


Fig. 5.1 Load-deflection curve, test 120C-U

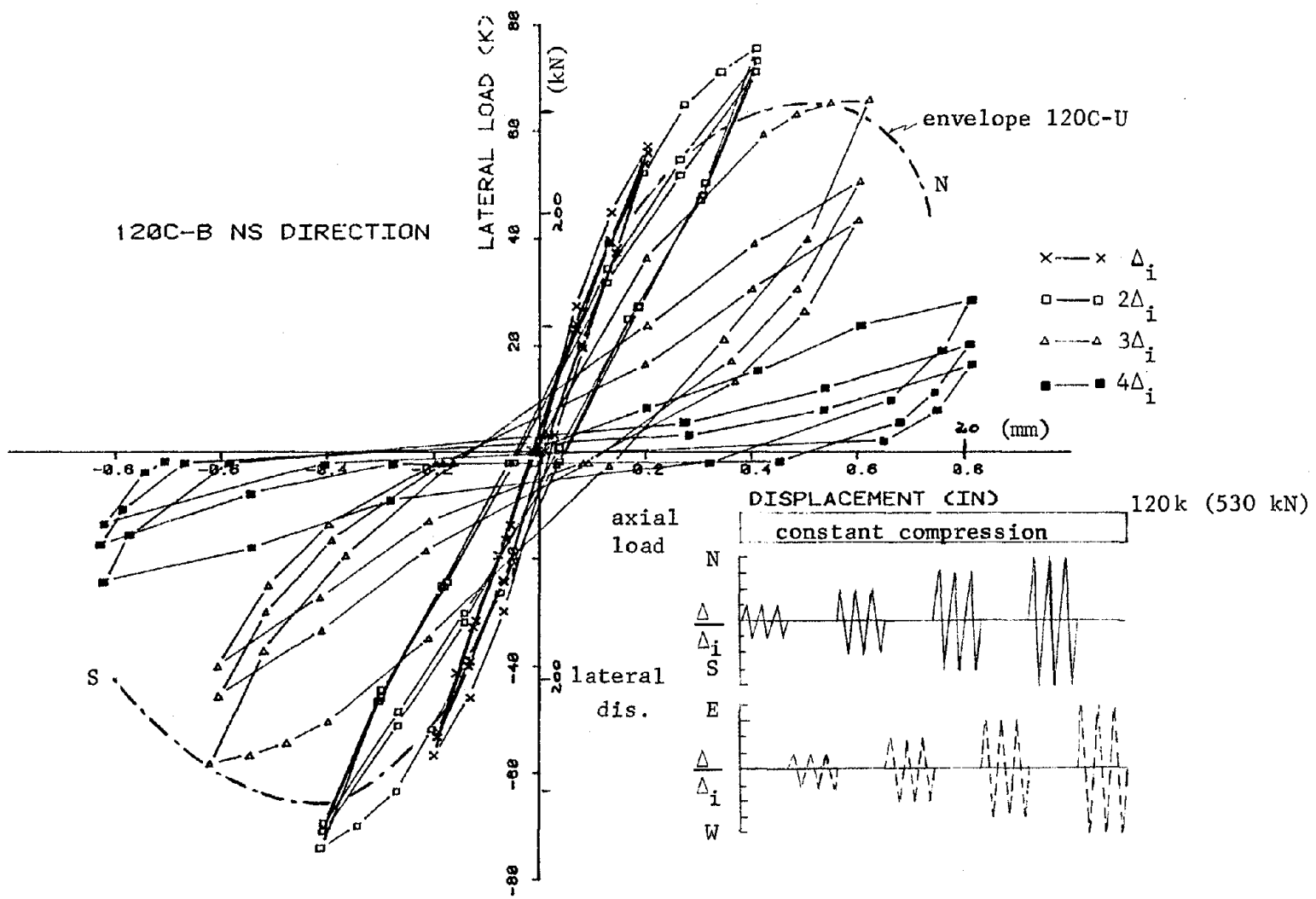


Fig. 5.2 Load-deflection curve, 120C-B - NS direction

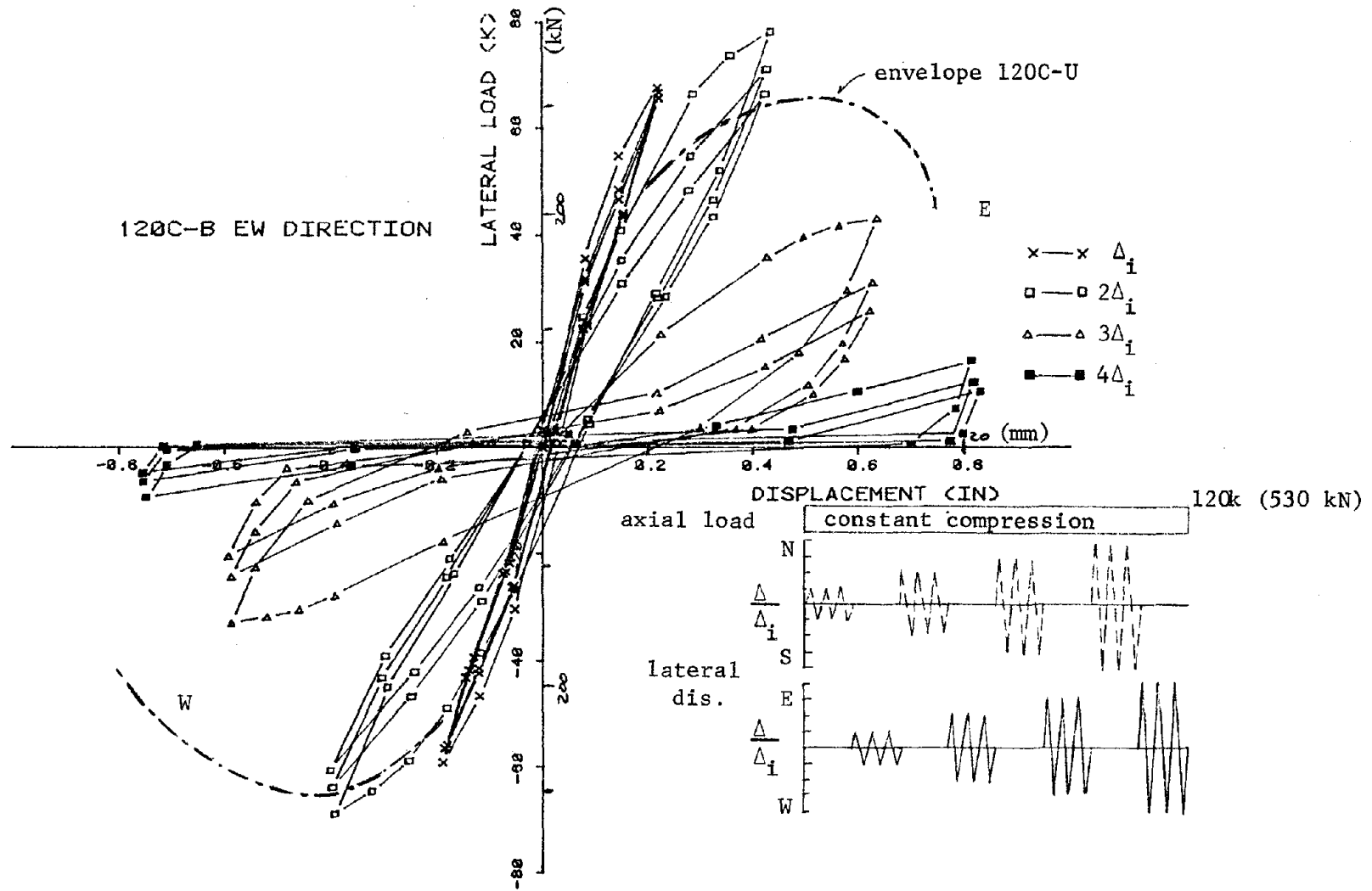


Fig. 5.3 Load-deflection curve, 120C-B - EW direction

similar. Again, for higher levels of deformation, shear decay and stiffness reduction is noticeable. For 120C-B, in the NS direction the shear decay was more rapid than observed in 120C-U and in the EW direction of 120C-B. The load-deflection curves for test 00-B are shown in Figs. 5.4 and 5.5. The envelope for first peaks for test 00-U is also shown. The adverse effect of alternate application of lateral deformations is evident.

Envelopes of Load Deflection. Envelopes of load-deflection relationships can be utilized to make more explicit comparisons. Figure 5.6 shows a comparison of the peak normalized shear (described in Section 4.2) envelopes for the first and third peaks of tests 00-U and 120C-U. The increase in shear strength for 120C-U compared to 00-U is about 30 percent. Considering monotonic loads, the increase in strength due to axial compression according to Eqs. (11.4) and (11.17) of the ACI Code [28] would be about 16 percent using gross area and about 20 percent using core area.

Figure 5.7 shows a comparison of the envelopes of the unidirectional and bidirectional tests with the same level of axial compression. Curves for the NS and EW direction of loading for test 120C-B are compared with unidirectional (NS) curves from 120C-U. Envelopes of the peaks only through the first direction of loading, i.e., N or E, are presented. Considering the NS direction of both tests, nearly identical behavior is observed in both cases. Considering the EW direction in 120C-B, for higher levels of deformation the shear decay proceeds at a rapid rate. The difference between first and last peaks is about the same in both areas, which indicates that the increase in shear degradation can be attributed to the effect of deformations in the orthogonal direction rather than to the number of cycles at any deflection level. Figure 5.8 shows a comparison of the envelopes of the peaks to the N and E for tests 00-B and 120C-B. Although the presence of lateral deformations in

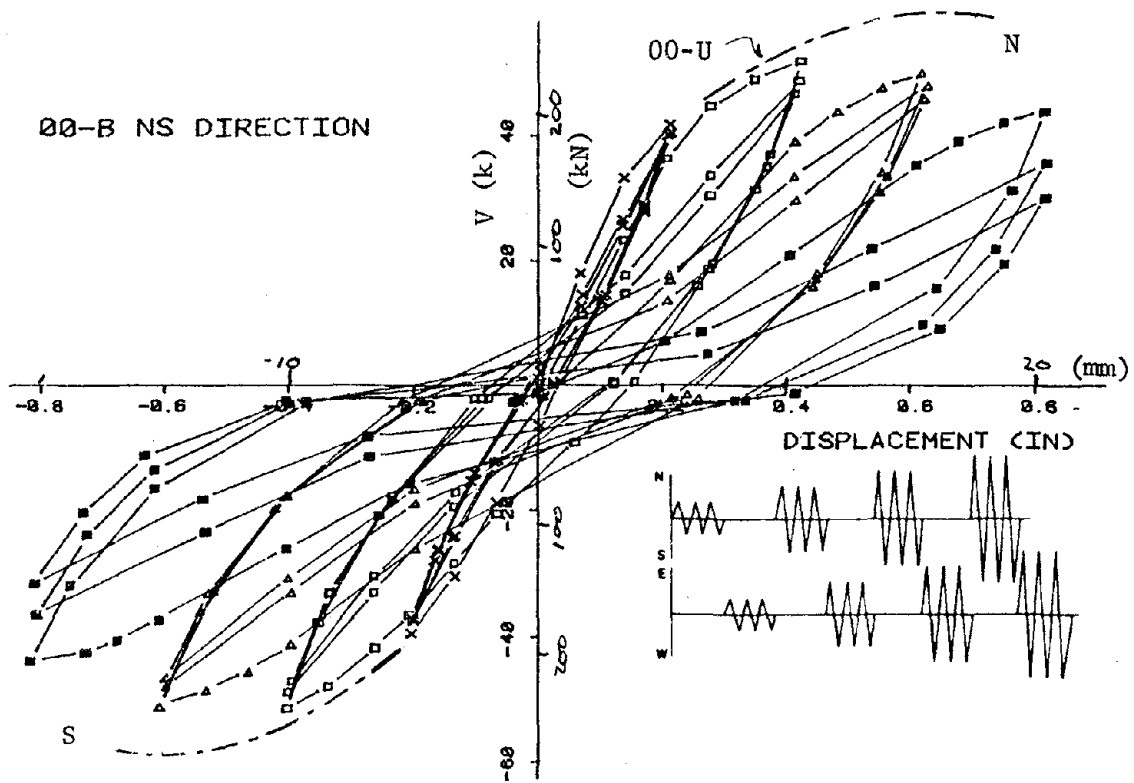


Fig. 5.4 Load-deflection curve, 00-B - NS direction

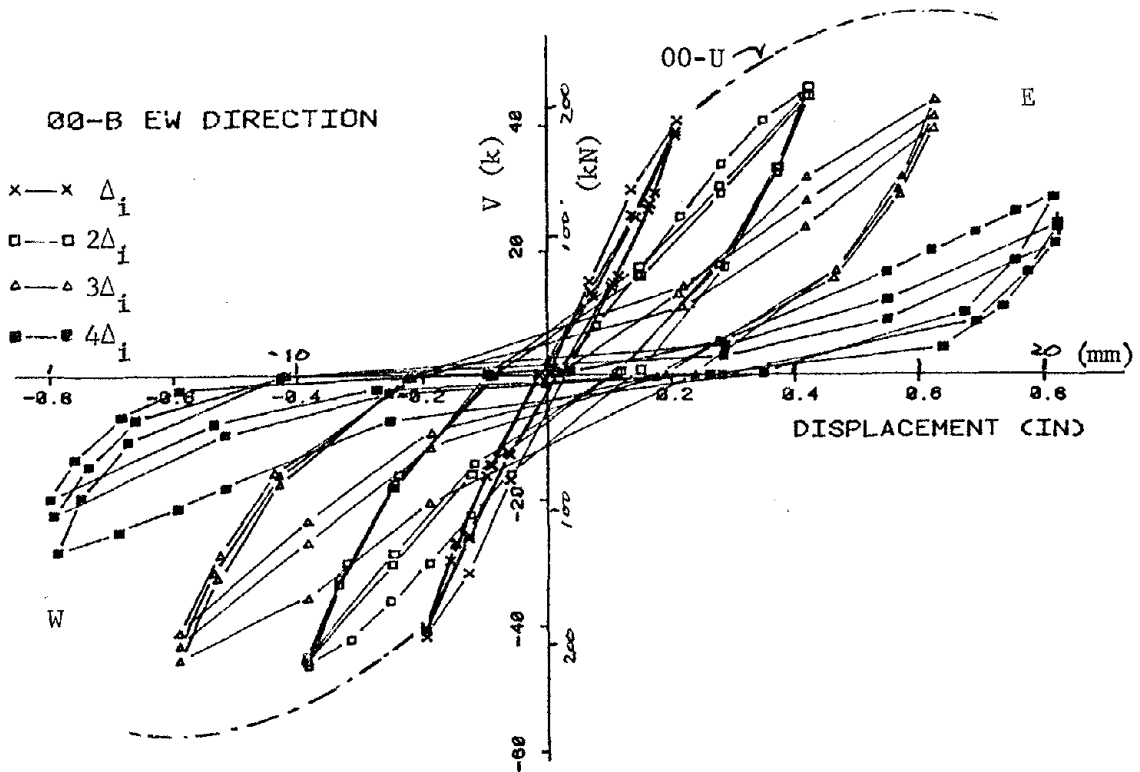


Fig. 5.5 Load-deflection curve, 00-B - EW direction

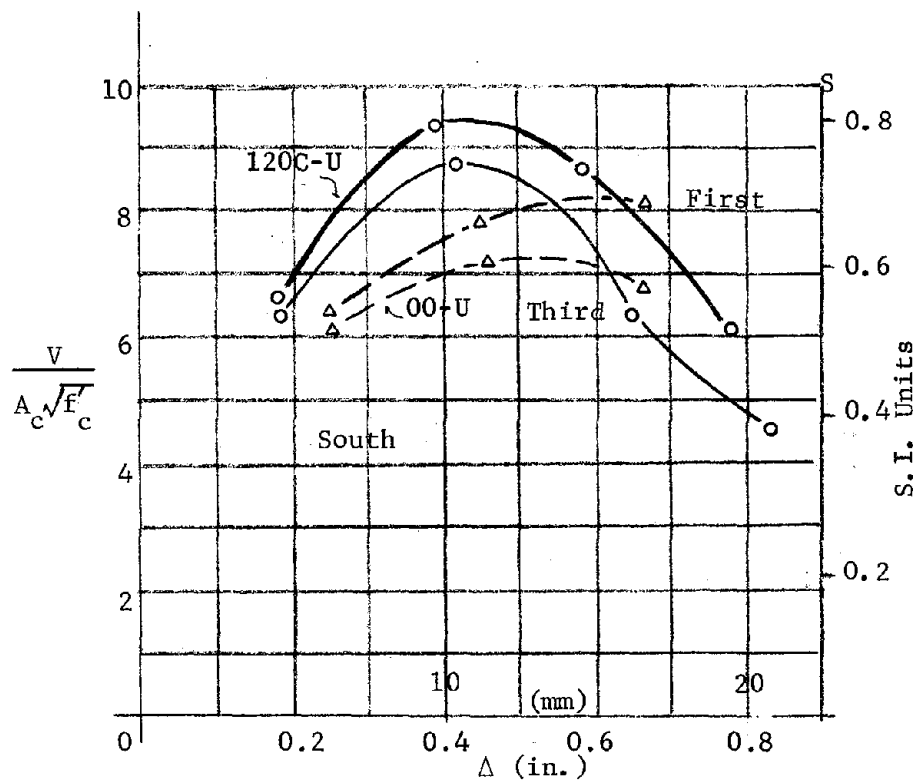
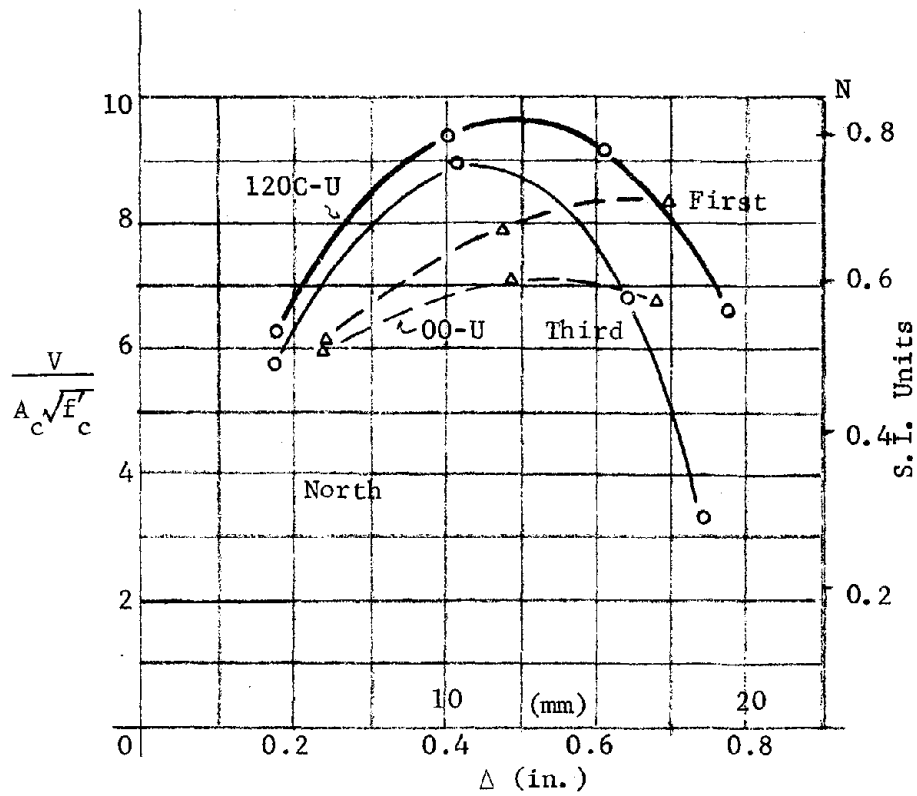


Fig. 5.6 Envelopes of load deflection, 00-U and 120C-U

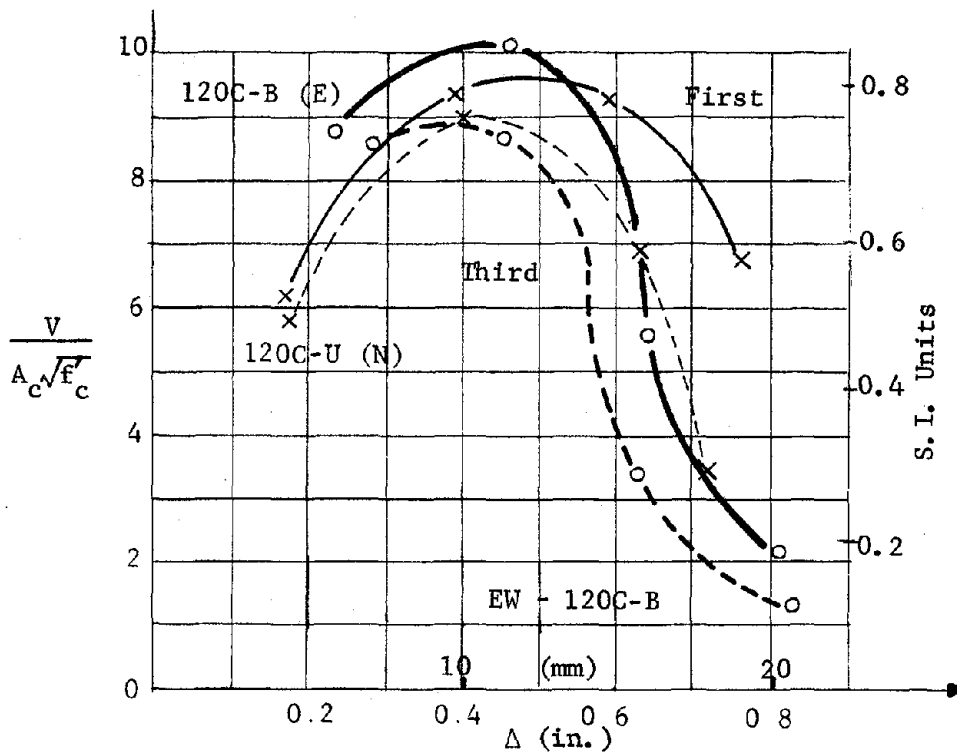
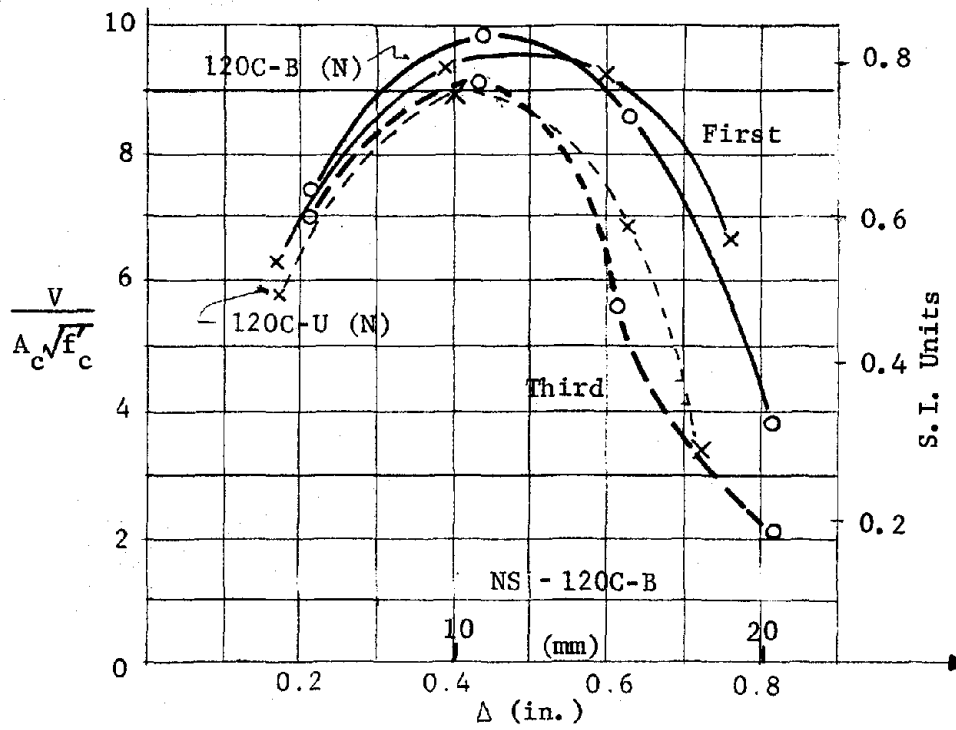


Fig. 5.7 Envelopes of load deflection, 120C-U and 120C-B

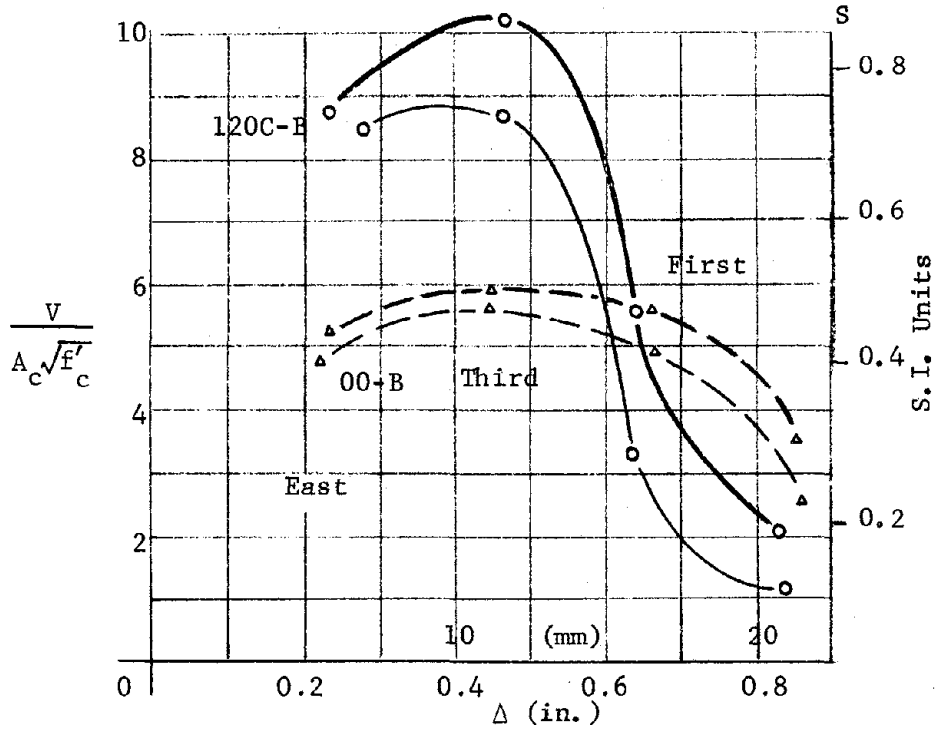
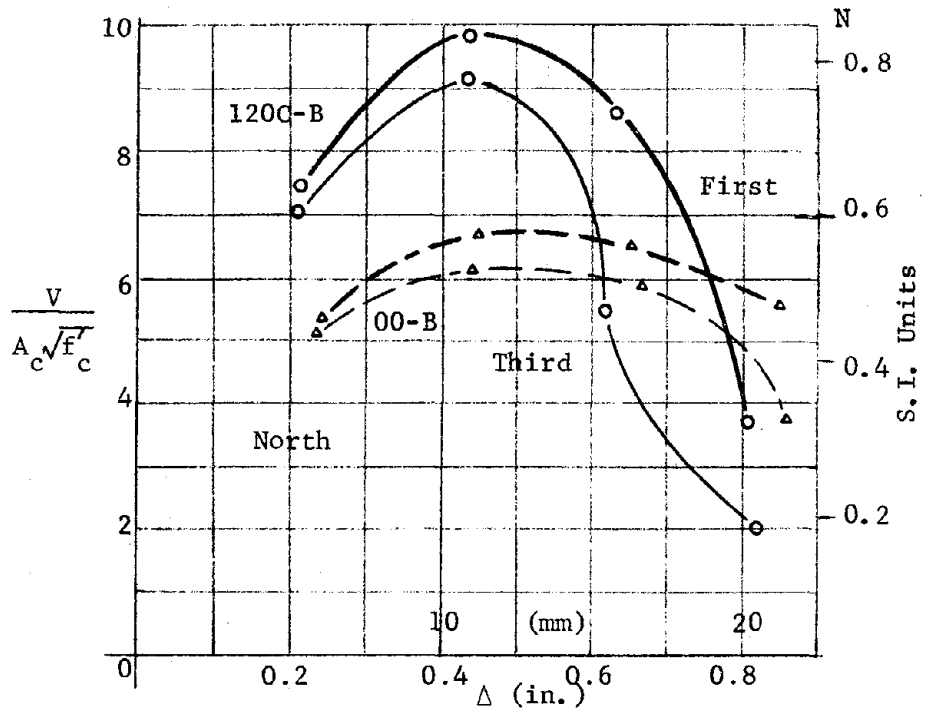


Fig. 5.8 Envelopes of load deflection, 00-B and 120C-B

the orthogonal direction produces shear decay when no axial load is present, it is not as severe as with axial compression.

Shear Deterioration. Figure 5.9 documents the shear deterioration which occurred in tests 120C-U and 00-U. For deformation levels higher than $2\Delta_i$, there was a larger difference between first and last peaks for test 120C-U than was observed in 00-U. Due to shear deterioration, shear values for 120C-U tend to approach those of 00-U as the level of deformation increases.

The shear deterioration observed in tests 120C-B and 00-B is presented in Fig. 5.10. The severe shear decay after the $2\Delta_i$ level in test 120C-B is clearly shown, especially in the EW direction. The largest shear decay from cycle to cycle occurred at the $2\Delta_i$ level in both directions for 120C-B.

With unidirectional or bidirectional lateral deflection history, the trends of the test with compression as compared with the test without axial load are similar, i.e., the shear on a member under compression is larger than on a specimen under no axial load for levels up to $2\Delta_i$. For larger deformations, rapid shear deterioration is observed. With no axial load, a nearly constant level of peak shear forces was observed.

Strain in Transverse Reinforcement. Figure 5.11 shows the observed average strain in the ties for test 120C-U. For comparison, some values of strain from test 00-U are included. In test 120C-U most of the ties were yielding at the $3\Delta_i$ level, while in test 00-U (Fig. 4.3) most of the ties were below yield at the $2\Delta_i$ and $3\Delta_i$ levels. Figure 5.12 shows a comparison of the progressive strain in a tie for tests 00-U and 120C-U. In 00-U, the tie remains below yield, while a similar tie in test 120C-U reaches yield at the $2\Delta_i$ level.

Figure 5.13 shows average strain in the ties for first peaks in the first and third cycles (all levels of deformation) for both directions of loading in test 120C-B. As in 120C-U,

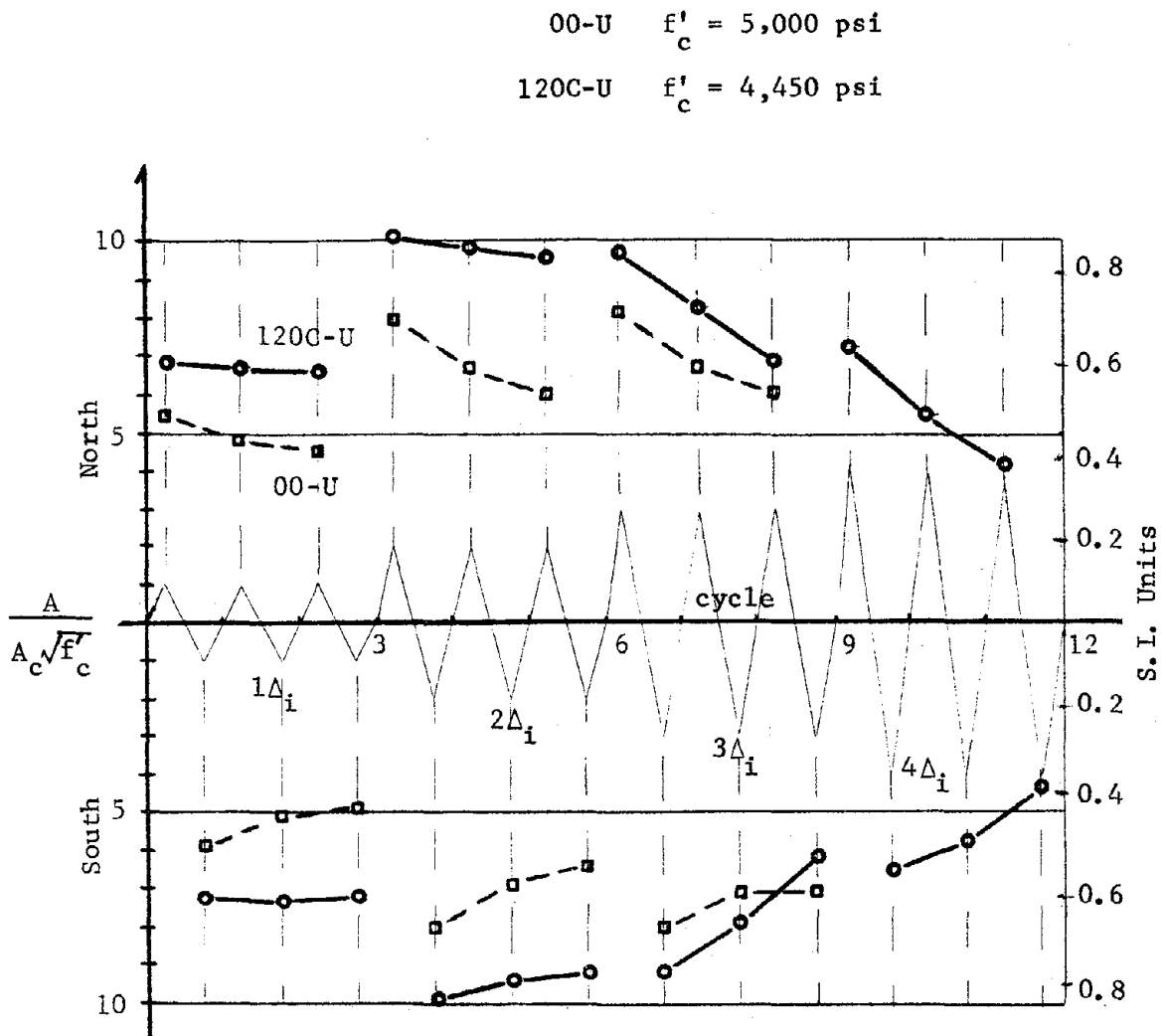


Fig. 5.9 Shear deterioration, tests 00-U and 120C-U

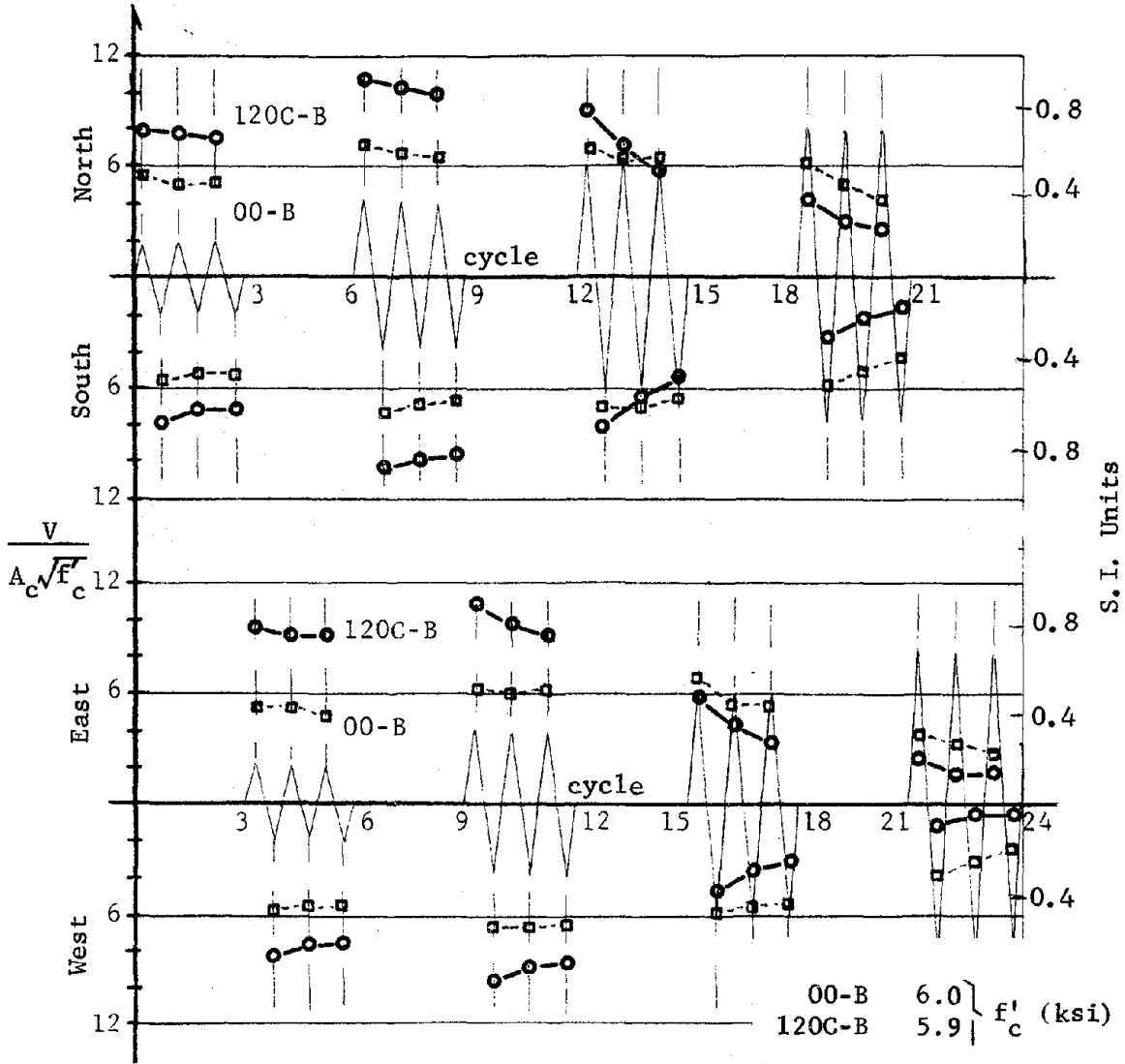
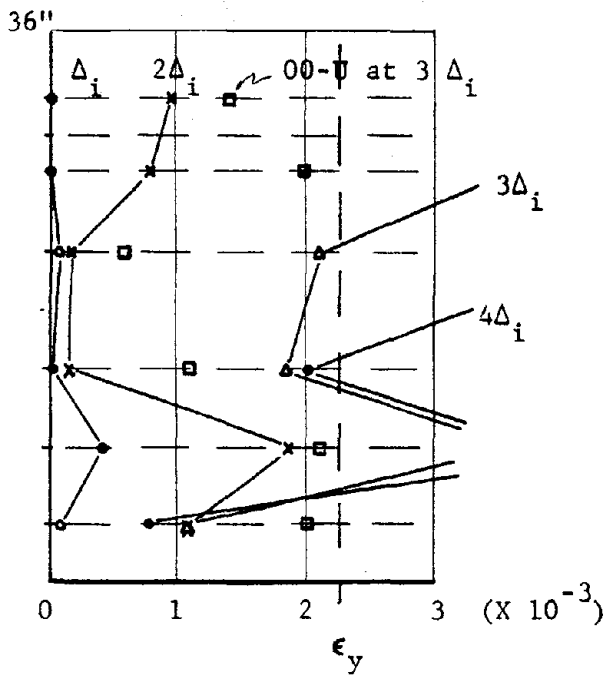
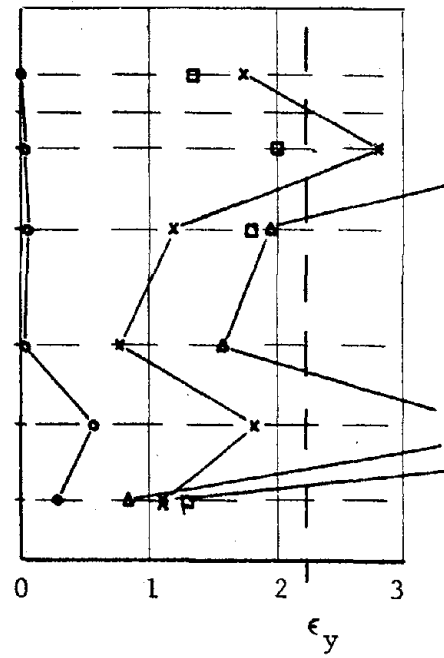


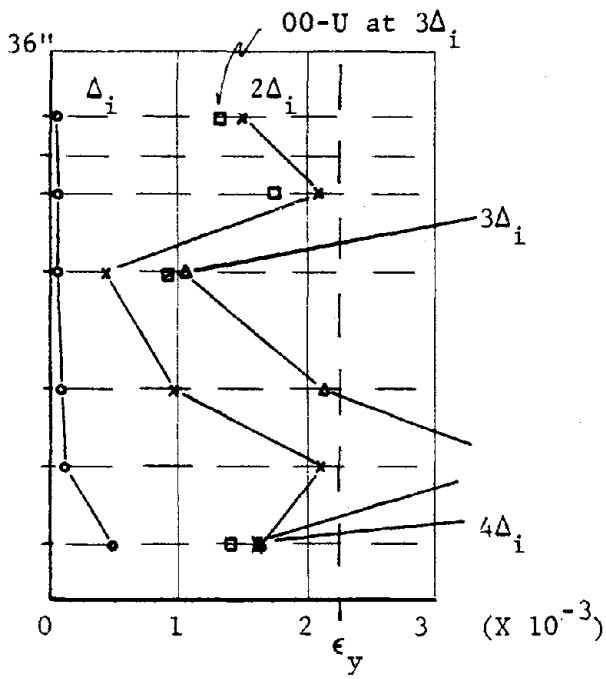
Fig. 5.10 Shear deterioration, tests 00-B and 120C-B



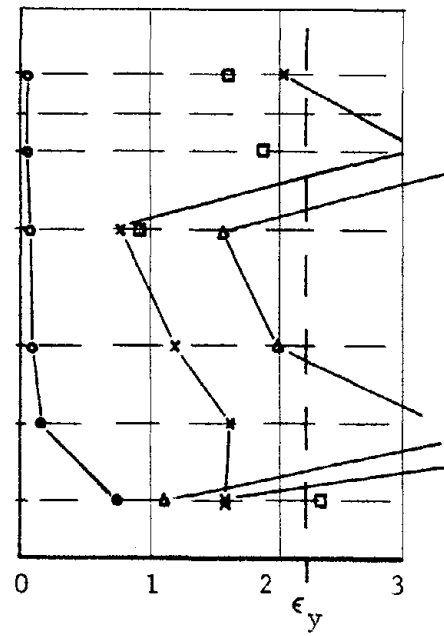
1st peaks 1st cycles
(North)



1st peaks 3rd cycles
(North)



2nd peaks 1st cycles
(South)



2nd peaks 3rd cycles
(South)

Fig. 5.11 Strain distribution in ties, test 120C-U

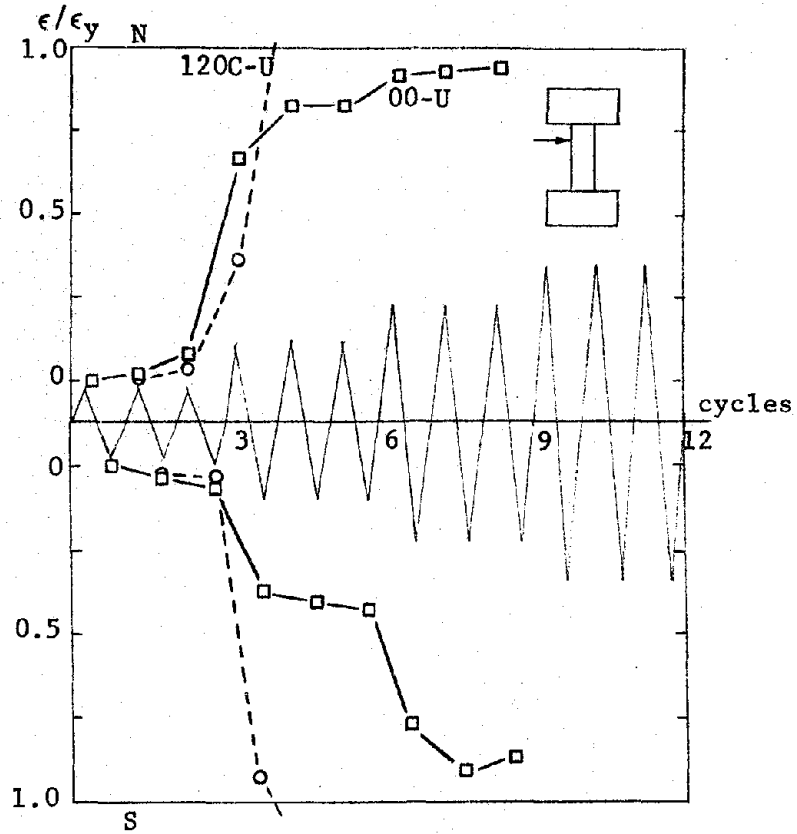
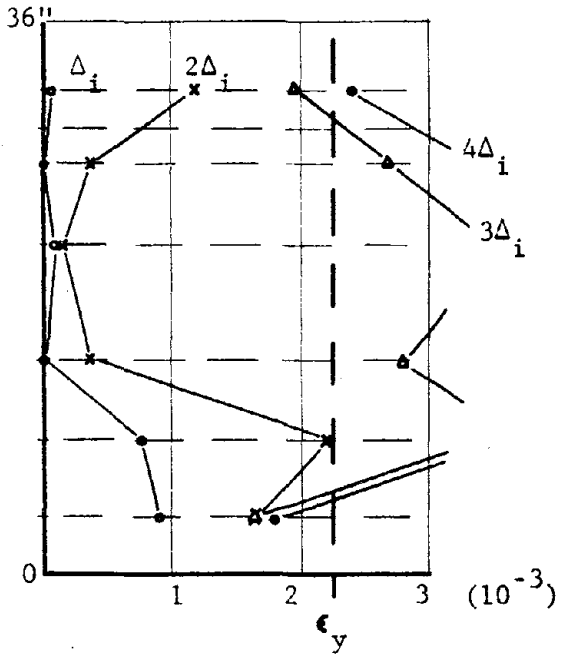
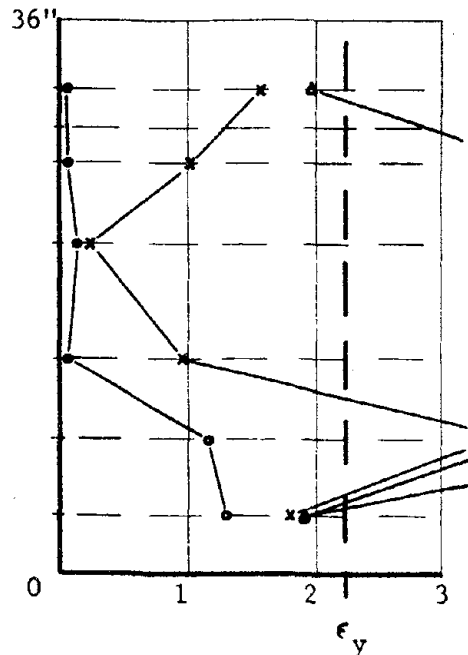


Fig. 5.12 Progressive strain in a tie, tests 00-U and 120C-U

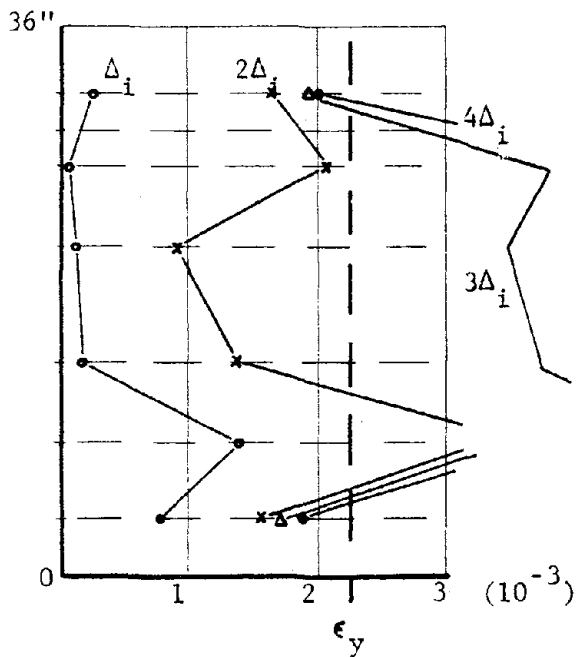


1st peak 1st cycle

N Direction

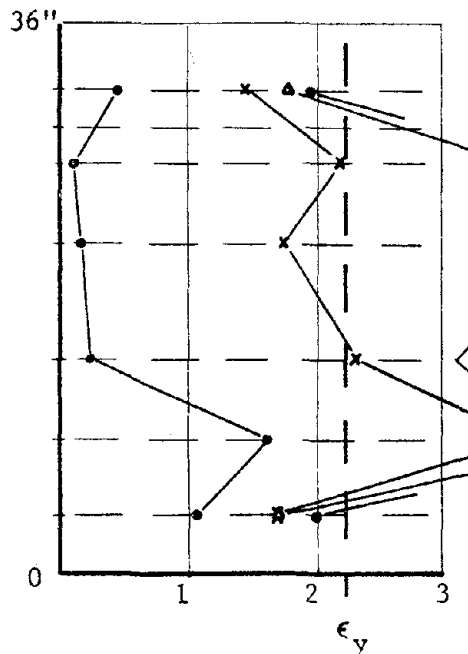


1st peak 3rd cycle



1st peak 1st cycle

E Direction



1st peak 3rd cycle

Fig. 5.13 Strain distribution in tie bars, test 120C-B

yielding of the ties occurred when the level of deformation was increased from $2\Delta_i$ to $3\Delta_i$. Figure 5.14 shows the comparison of the progressive strain in a tie for tests 00-B and 120C-B in both directions of loading. As in Fig. 5.12, ties reached yield faster when compression was present for both directions of loading.

Crack Patterns. Figure 5.15 shows the crack patterns observed at the end of the application of three cycles of loading at each deflection level for 120C-U. Comparing with the crack patterns for test 00-U presented in Fig. 4.4, it is apparent that the test without axial load shows about the same damage at 2 and $3\Delta_i$ levels, while 120C-U shows an increase in damage for each deflection level. This is likely a reflection of the reduced effectiveness (due to yielding) of the ties in shear when axial compression is present. In a similar way, test 120C-B exhibited more external damage than test 00-B, as can be seen in Fig. 5.16 which shows the appearance of the test specimens after completion of loading.

5.3 Study of the Behavior

Mechanism of Failure. The mechanism of failure appeared to be governed by three main factors: crushing of the concrete shell; yielding of the transverse reinforcement; and amount of damage, due to inclined cracks, to the concrete core. The factors were influenced by the pattern of lateral displacements and by the axial load. Inclined cracking was observed for deformations less than Δ_i . Following inclined cracking, the transverse reinforcement contributed a portion of the shear strength of the element. With an increase in deformation, the inclined cracks increased in number and width. At the end of the cycles at Δ_i , the contribution of the ties was appreciable for the case without axial load (Fig. 4.3). For the case with axial load (Fig. 5.11), the compressive stresses produced an increase in the concrete contribution and the web

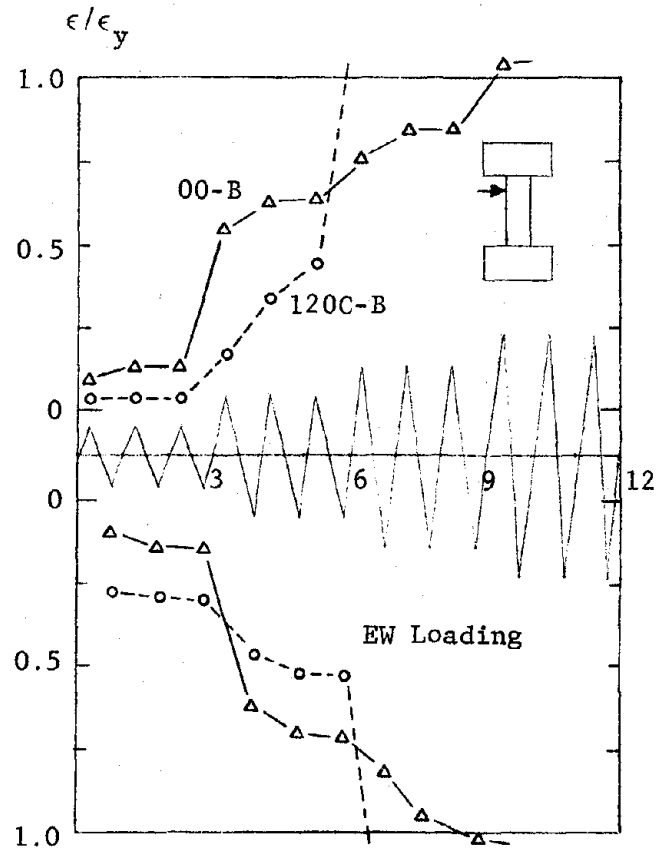
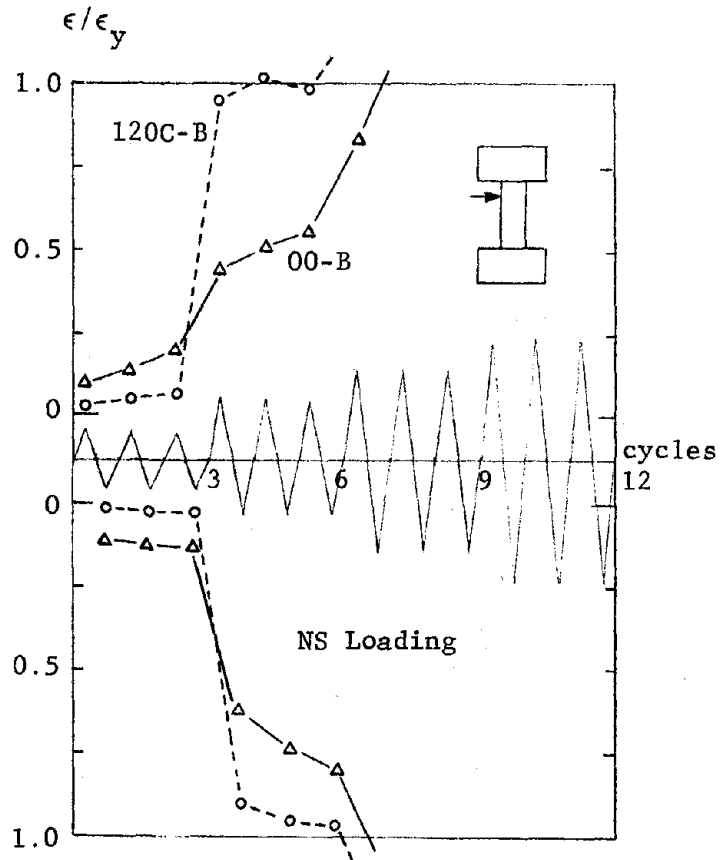
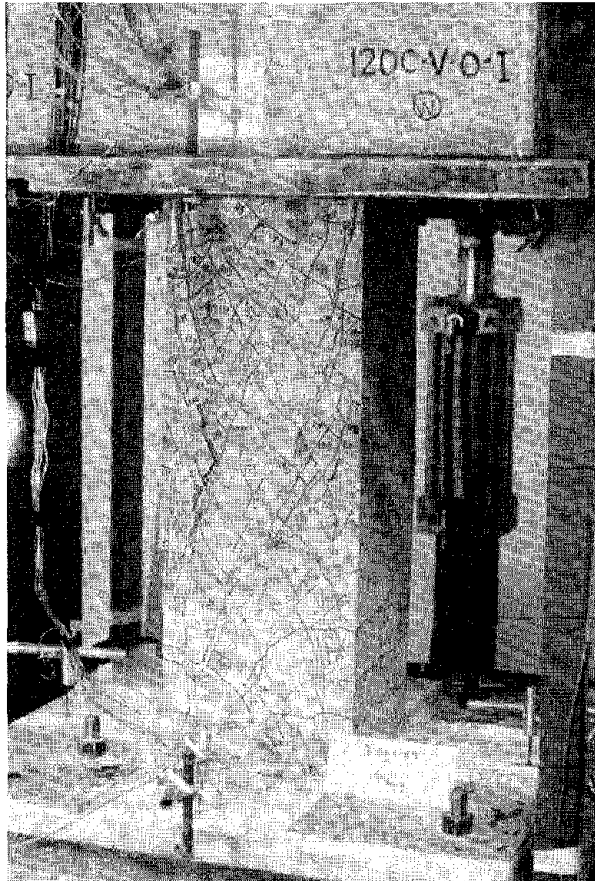


Fig. 5.14 Progressive strain in a tie, tests 00-B and 120C-B



Appearance of specimen after completion of loading

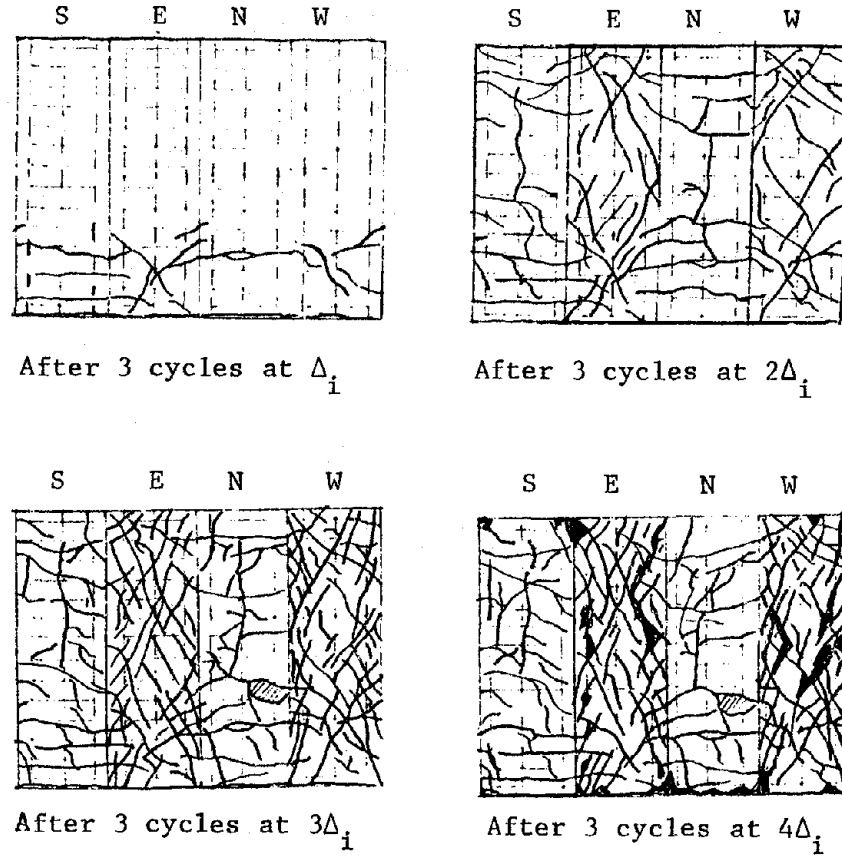
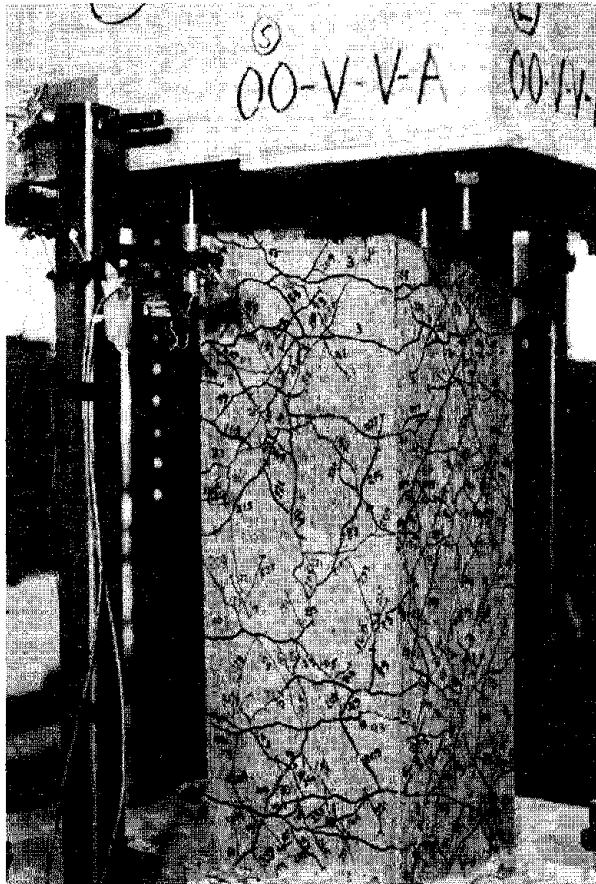


Fig. 5.15 Crack patterns, test 120C-U



00-B



120C-B

Fig. 5.16 Appearance of test specimens 00-B and 120C-B after completion of loading

reinforcement was not required to carry shear. The maximum strain in the ties in test 120C-U at the Δ_i level was 0.0008 while in test 00-U the maximum strain at the same deflection level was 0.0018. In the case with compression, the contribution of the ties was retarded until large deformations were imposed (Fig. 5.11). For larger levels of deformation, the strain in the ties increased at different rates for 00-U and 120C-U (Fig. 5.12) and the strain was continuously increasing as the lateral deformation increased. However, the cyclic behavior shows that the increase in strain did not correspond to an increase in shear once the shear decay started. Thus, the way in which the ties contributed to the strength changed during the test: for low levels of deformation the tie contribution may be assumed as in the truss analogy; for larger deformations the ties appeared to act primarily as confining reinforcement, i.e., the concrete core was resisting the shear but only because it was confined by the ties. Although the change in the role of the ties was gradual, there seemed to be a critical point where the change was more significant. The critical point can be identified in the envelope curves (Figs. 5.6 and 5.8), when a drastic reduction in the slope of the envelope curves was observed from one deformation level to the next. After that point the behavior depends on the ability of the ties to provide confinement and on the amount of damage to the core, both of which depend on the load history.

After the critical point, at the Δ_i level for 00-U and somewhere between Δ_i and $2\Delta_i$ for 120C-U, the shell was damaged (Figs. 4.4 and 5.15) and its contribution to shear capacity may be assumed low. Therefore, the shear must be resisted by the concrete core and the behavior was governed by the confinement provided by the ties. With confinement, forces in the concrete core can be developed through aggregate interlock occurring between the faces of inclined cracks. For 00-U, the critical point was reached with little damage to the core and with strain in the tie bars below

yield. Therefore, the shear strength increased after that point and shear deterioration was delayed until the $3\Delta_i$ level was reached. On the contrary, for 120C-U the critical point was reached when the specimen was severely cracked and with the ties already at yield. With the ties yielded, no reserve was available for carrying shear or for providing confinement. Evidence of the extreme lateral forces on the ties in test 120C-B was the barrel shape observed for the specimen after cycles at the $4\Delta_i$ level, which indicate the "softening" of the complete steel cage. The effect of lateral deformations in the orthogonal direction was reflected mainly after the critical point in the form of more rapid shear decay. Before the critical point the influence of perpendicular deformations was not significant. In tests without axial load the confinement from the ties was effective because it permitted the stabilization of the shear strength. In the tests with compression the ties were not effective because the shear strength deteriorated very rapidly. Thus, the amount of transverse reinforcement required to attain stabilized cyclic behavior depended on the axial load level and in general on the load history.

Strength and Deformation Characteristics. (a) Shear Strength.

If the prototype element discussed in Chapter 2 is to form a part of a special ductile frame meeting the requirements of Appendix A of the ACI Code [28], the amount of shear reinforcement provided is not sufficient. According to Appendix A, if the axial load is greater than $0.4P_b$, transverse reinforcement must be provided to confine the core. The required percentage of transverse steel to confine the core in the prototype is 1.47 percent based on core dimensions and #3 ties (#2 for the test specimen). Using Appendix A, the percentage of transverse reinforcement to resist shear produced under the formation of plastic hinges at both ends of the element is about 0.8 percent for zero axial load, about 1.2 percent for 120k compressive load. With #3 hoops at 4 in. in the prototype, $\rho_w = 0.4$ percent (#2 at 2.57 in. in the test specimen). Neither of

the requirements of ACI 318, Appendix A are met. The observed behavior of the specimens was better than might have been expected, based on the difference between required and provided transverse reinforcement. Table 5.1 shows computed values (total and normalized) of the concrete and transverse steel contributions to shear, using Eqs. (11.4) and (11.17) of the ACI Code and core dimensions. In Specimen 120C-U, peak values of shear were equal to or greater than the calculated strength, $V_n = V_s + V_c$, up to the $3\Delta_i$ deflection level. If it is conservatively assumed that all shear is resisted by the web reinforcement, $V_n = V_s$, then most of the peak values throughout the load history lie above the value for V_n .

Under the application of lateral deformations in both directions, Specimen 120C-B only withstood cycles at the $2\Delta_i$ level with shear strength greater than $V_n = V_c + V_s$ (Fig. 5.8 or 5.10). If the shear capacity is taken as $V_n = V_s$, after $3\Delta_i$ in the NS direction and $2\Delta_i$ in the EW direction the shear carried by the specimen falls below V_n .

(b) Flexural Strength. The computed moments at the bottom of the column corresponding to yield in the main bars were 730 in.-k for 00-U and 886 in.-k for 120C-U using the free body in Fig. 4.7. In both cases the moments at observed first yielding were less than the theoretical nominal yield moments of 750 and 1360 in.-k. However, shear and moment increased after reaching first yield in the reinforcement. At $2\Delta_i$ the moments at the bottom end were 865 in.-k for 00-U and 1350 in.-k for 120C-U. Because the moments were not equal at the top and bottom ends (top end moments were 1080 in.-k for 00-U and 990 in.-k for 120C-U), the shear required to produce plastic hinges will be compared with measured values. Table 5.2 shows normalized (with respect to $\sqrt{f'_c}$ and A_c) values of the shear required to produce plastic hinges computed as two times the ultimate nominal moment (from interaction diagrams, Figs. 4.5 and 4.6), divided by the length of the column and observed maximum values.

TABLE 5.1 ACI NOMINAL SHEAR STRENGTH

Test	V_s (k)	$V_s / \sqrt{f'_c A_c}$	V_c (k)	$V_c / \sqrt{f'_c A_c}$	V_n (k)	$V_n / \sqrt{f'_c A_c}$	Meas. peak shear	
							V (k)	$V / \sqrt{f'_c A_c}$
00-U	26.3	3.7	14.1	2.0	40.4	5.7	56	7.9
00-B	26.3	3.4	15.5	2.0	41.8	5.4	52	6.7
120C-U	26.3	3.9	21.3	3.2	47.6	7.1	63	9.4
120C-B	26.3	3.4	24.7	3.2	51.0	6.6	78	10.1

$$V_s = A_v f_{sy} d / s$$

$$V_c = 2(1 + N/2000A_c) \sqrt{f'_c} A_c$$

$$V_n = V_s + V_c$$

TABLE 5.2 MAXIMUM PEAK SHEAR COMPARED WITH $2M_n/L$

Test	Meas. peak shear		$V_f = 2M_n/L$	
	V (k)	$V / \sqrt{f'_c A_c}$	V_f (k)	$V_f / \sqrt{f'_c A_c}$
00-U	56	7.9	50	7.1
00-B	NS	52	50	6.5
	EW	46	50	6.5
120C-U	63	9.4	77	11.5
120C-B	NS	76	78	10.1
	EW	78	78	10.1

It is clear that the quantity of transverse reinforcement in 120C-U was inadequate to prevent failure by shear with cycling; however, it was sufficient to permit the development of a maximum shear which was over 80 percent of the shear corresponding to the formation of plastic hinges at the ends of the column. For test 120C-B, the measured peak shear was almost equal to the shear required to form plastic hinges.

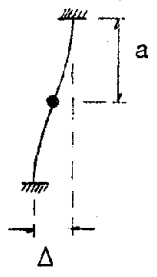
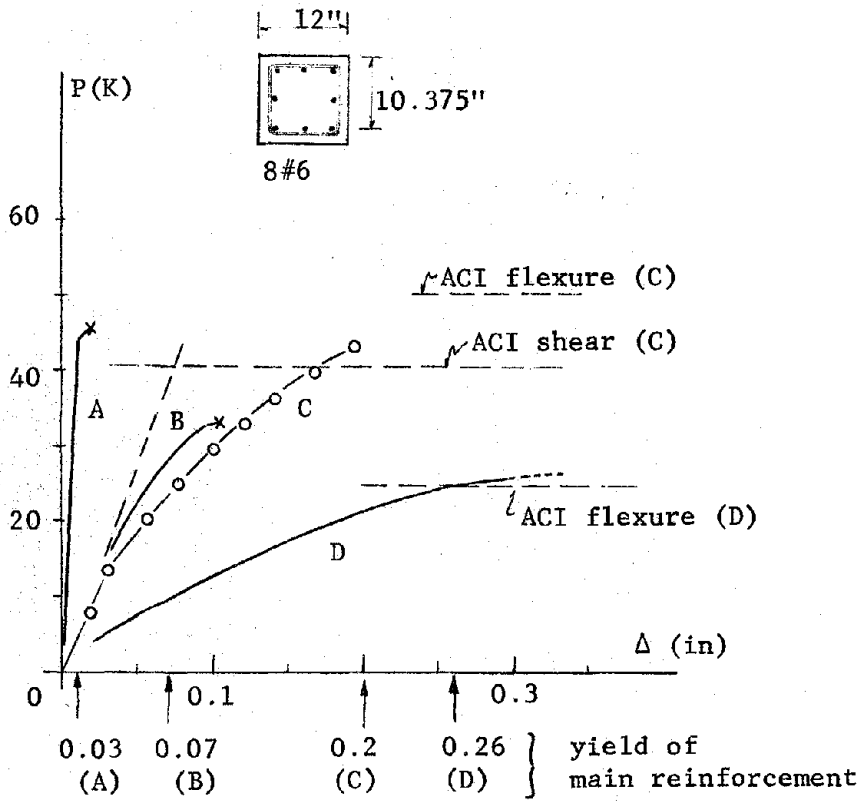
(c) Load Deformation. At first yield in tests 00-U and 120C-U, some shear distress was observed in the form of inclined cracks. Although shear distress was observed early in the load history, the element reached flexural strength following the development of large deflections because of the transverse reinforcement. Using the following calculations, the failure sequence can be explained. If Specimen 120C-U is assumed to fail in flexure, $M_u = 1380$ in.-k. If shear controls failure, the maximum shear should be about $V_u = V_c + V_s = 48k$ (from Table 5.1). In order to attain both modes of failure simultaneously, the length of the column should be $2M_u/V_u = 57$ in., which is larger than the actual column height. This means that failure is governed by shear. The maximum predicted shear (48k) was reached at about $2\Delta_1$ (0.4 in.) during testing.

As the load increases, the contribution of the web reinforcement to shear resistance increases as soon as diagonal cracks are formed. Strains in the ties imply that the diagonal cracks are opening and lateral deflections increasing. Yamada [29] observed better agreement between observed and measured deformations with very short columns (a/d near 1). In a very short column ($a/d \approx 1$), the shear strength will be reached at a very low lateral displacement and the behavior will be almost rigid elastic. In a short column with $a/d \approx 2$ and $\rho_w = 0$, the shear strength will be less than for $a/d \approx 1$ because of the increase in shear span. The stiffness will decrease also and there will be some inelastic

deformation after cracking. In a short column with $a/d \approx 2$ but with $\rho_w = 0.4$ (as in 00-U), the stirrups will carry shear after cracking is reached and the associated inelastic deflections will result in response resembling a long column. In Fig. 5.17, a schematic representation of the cases discussed is shown. To provide a basis for comparison, the response of 00-U is plotted (curve C) and calculations of deflections and strengths for the other cases discussed were made assuming the same specimen cross section and different column heights as follows: 24 in. for the very short column and 72 in. for the long column. It is clear that lateral displacements of short columns are functions of a/d , ρ_w , and level of axial load, and nonlinear deformations need to be taken into account.

Summary of the Influence of Constant Compression. The presence of constant compression influenced the behavior when compared with similar tests without axial load. Compression was observed to accelerate shear deterioration at higher levels of deformation.

Web reinforcement was effective in improving deformation capacity. Based on observed behavior, the effectiveness of the web reinforcement decreased with the presence of compressive axial load, the number of cycles imposed, and the application of deformations in the orthogonal direction. Thus, for the same history of lateral deformations, a column subjected to compressive axial load should have more web reinforcement than a similar one without axial load to achieve similar capacity.



- A - $a/d = 1.2$ (assumed)
- B - $a/d = 1.8$ $\rho_w = 0$ (assumed)
- C - $a/d = 1.8$ $\rho_w = 0.4\%$ (observed) - 00-U
- D - $a/d = 3.6$ $\rho_w = 0.2\%$ (assumed)

Fig. 5.17 Load-deflection curves for various a/d ratios

CHAPTER 6

CONSTANT TENSION

6.1 Introduction

In this chapter the influence of constant tension is analyzed. Results from tests with constant tension (50T-U, 50T-B, 100T-U, and 200T-U) and zero axial load (00-U and 00-B) are compared for both lateral deformation histories. Behavioral trends considering the effect of different levels of tension, as well as the overall effect of tensile axial loads in comparison with compressive axial loads are discussed.

6.2 Description and Comparison of Test Results

Load-Deflection Curves. Load-deflection curves for tests 50T-U and 100T-U are presented in Figs. 6.1 and 6.2. For clarity, the first cycles of 100T-U are shown in Fig. 6.3. Load-deflection curves for first cycles of test 200T-U are shown in Fig. 6.4; second and third cycles were similar to first cycles and are not shown.

An examination of the load-deflection curves for the three levels of tension and unidirectional lateral deflection history, shows a reduction in applied shear and stiffness for low level of deformation as compared with 120C-U (Fig. 5.1); however, little shear deterioration was observed at higher levels of deformation. The behavior with constant tension was reversed in relation to the behavior with constant compression. Axial compression caused a noticeable increase in shear strength and initial stiffness as compared with no axial load and severe shear deterioration was present for higher levels of deformation. Constant tension caused a

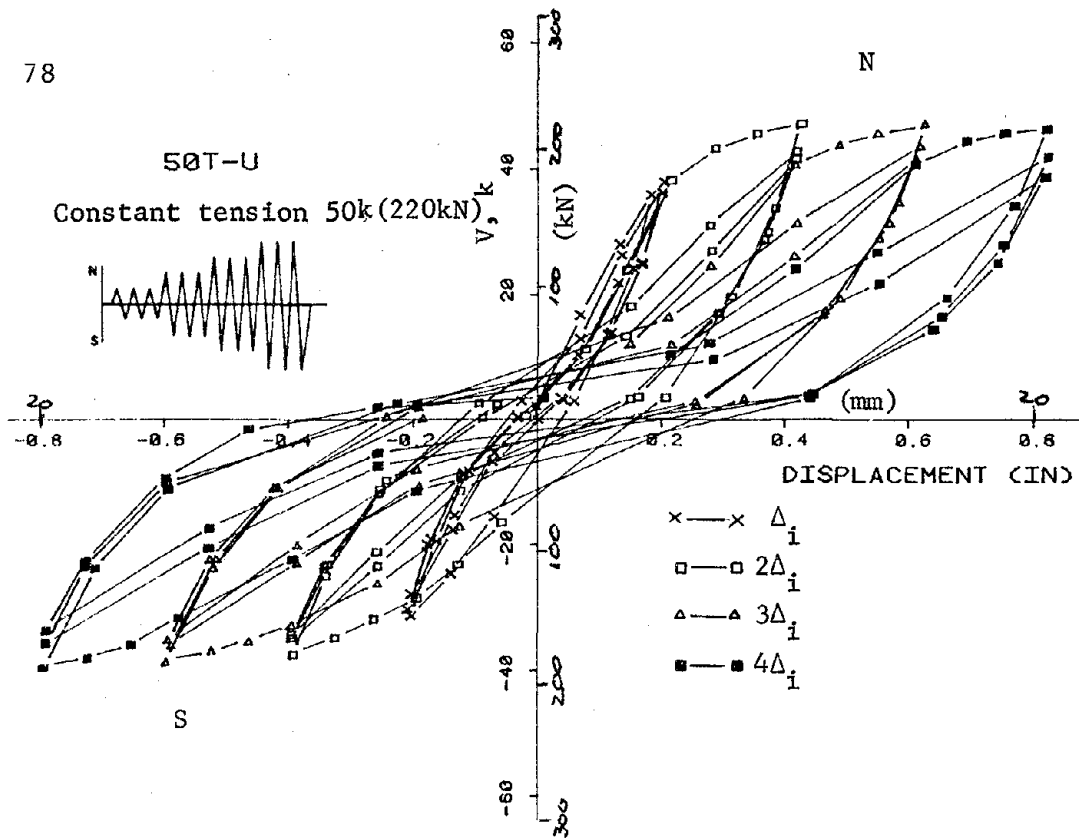


Fig. 6.1 Load-deflection curve, test 50T-U

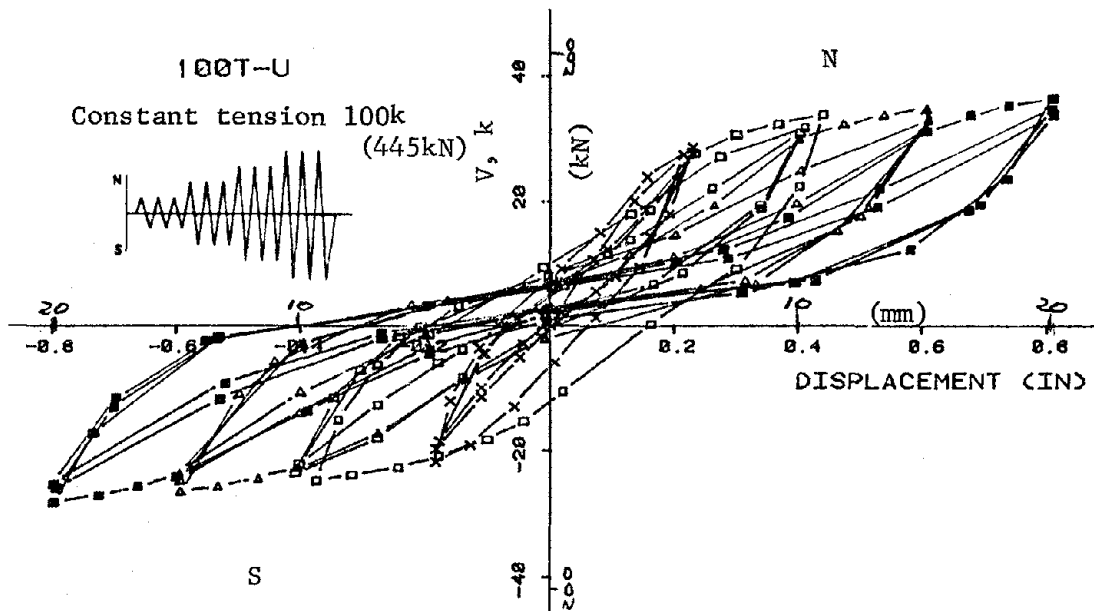


Fig. 6.2 Load-deflection curve, test 100T-U

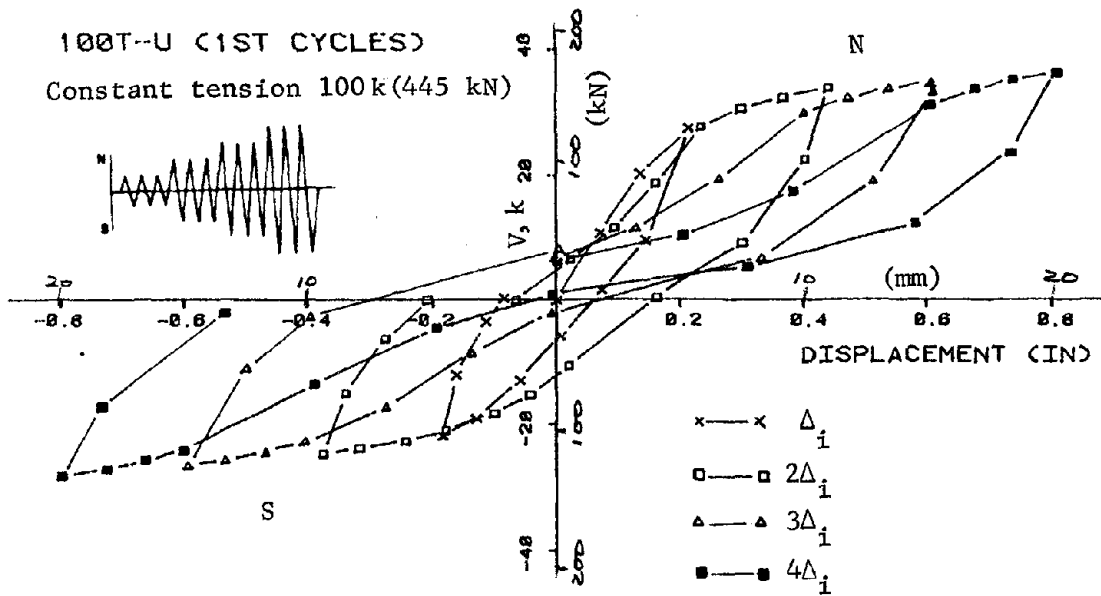


Fig. 6.3 First cycles, test 100T-U

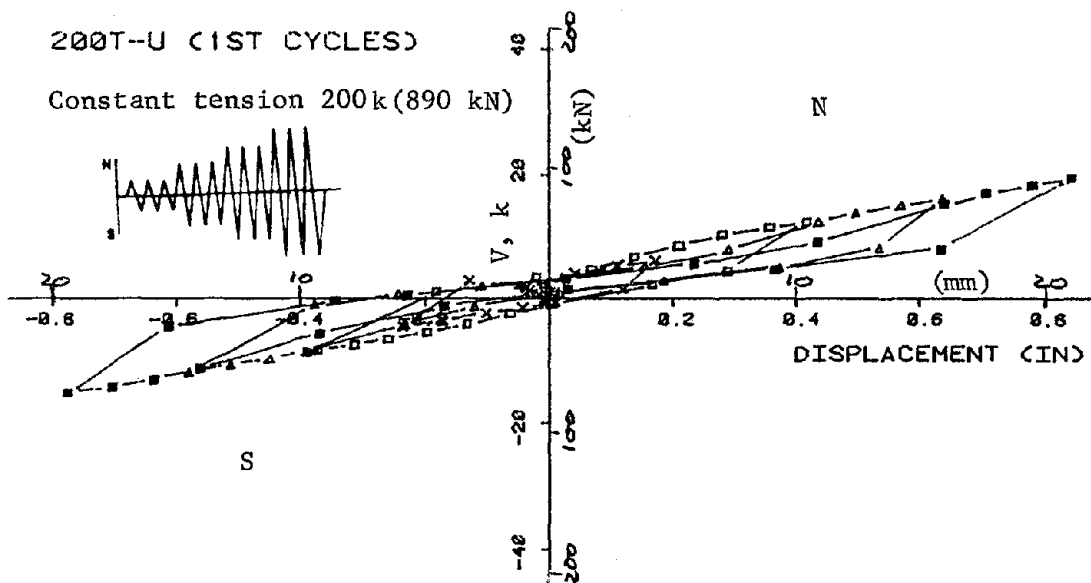


Fig. 6.4 Load-deflection curve, test 200T-U

decrease in applied shear and stiffness for low levels of deformation but no appreciable shear deterioration at large deformations. The observed decrease in applied shear and stiffness was proportional to the level of tension.

Pinching of the hysteresis loops was less than that observed under compressive axial loads (Fig. 5.1). The area (energy dissipated) within the load-deflection curves decreased as the tensile load increased. In Specimen 200T-U the load-deflection curves fell within a very narrow band.

The load-deflection curves for test 50T-B are shown in Fig. 6.5. Some shear decay was observed in both directions of loading, whereas no shear decay was observed under unidirectional loading (50T-U, Fig. 6.1).

Envelopes of Load Deflection. In Fig. 6.6 the envelopes of first and last peaks of normalized shear for tests with constant tension and unidirectional deformation history are presented. Each level of tension is shown and for comparison the envelopes for test 00-U are also shown. From this figure the trends can be clearly visualized. The observation that there is a decrease in applied shear with tension but no deterioration at larger deformations is clear.

Figure 6.7 shows envelopes of peaks to the N and E directions for test 50T-B. Peaks to the N direction for test 50T-U are shown for comparison. In test 50T-U the applied shear remained nearly constant for high levels of deformation, while in test 50T-B shear decay was noted at $4\Delta_i$, especially in the EW direction. It is interesting that the applied shear at $2\Delta_i$ and $3\Delta_i$ levels is greater in 50T-B than in 50T-U. One explanation for this is that main reinforcement used in 50T-B had a higher yield strength than 50T-U. The concrete strength in 50T-B was less than 50T-U; however,

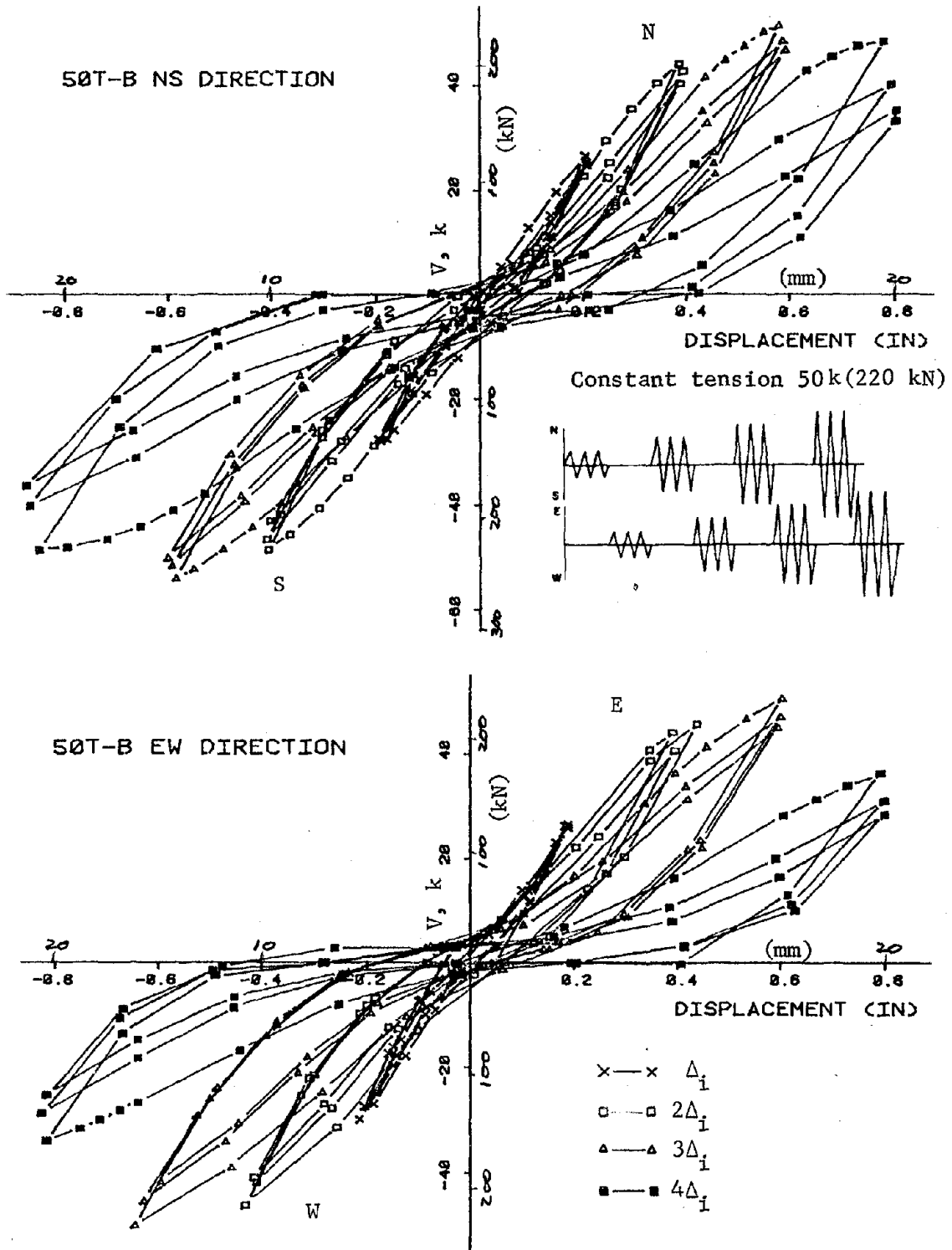


Fig. 6.5 Load-deflection curve, test 50T-B

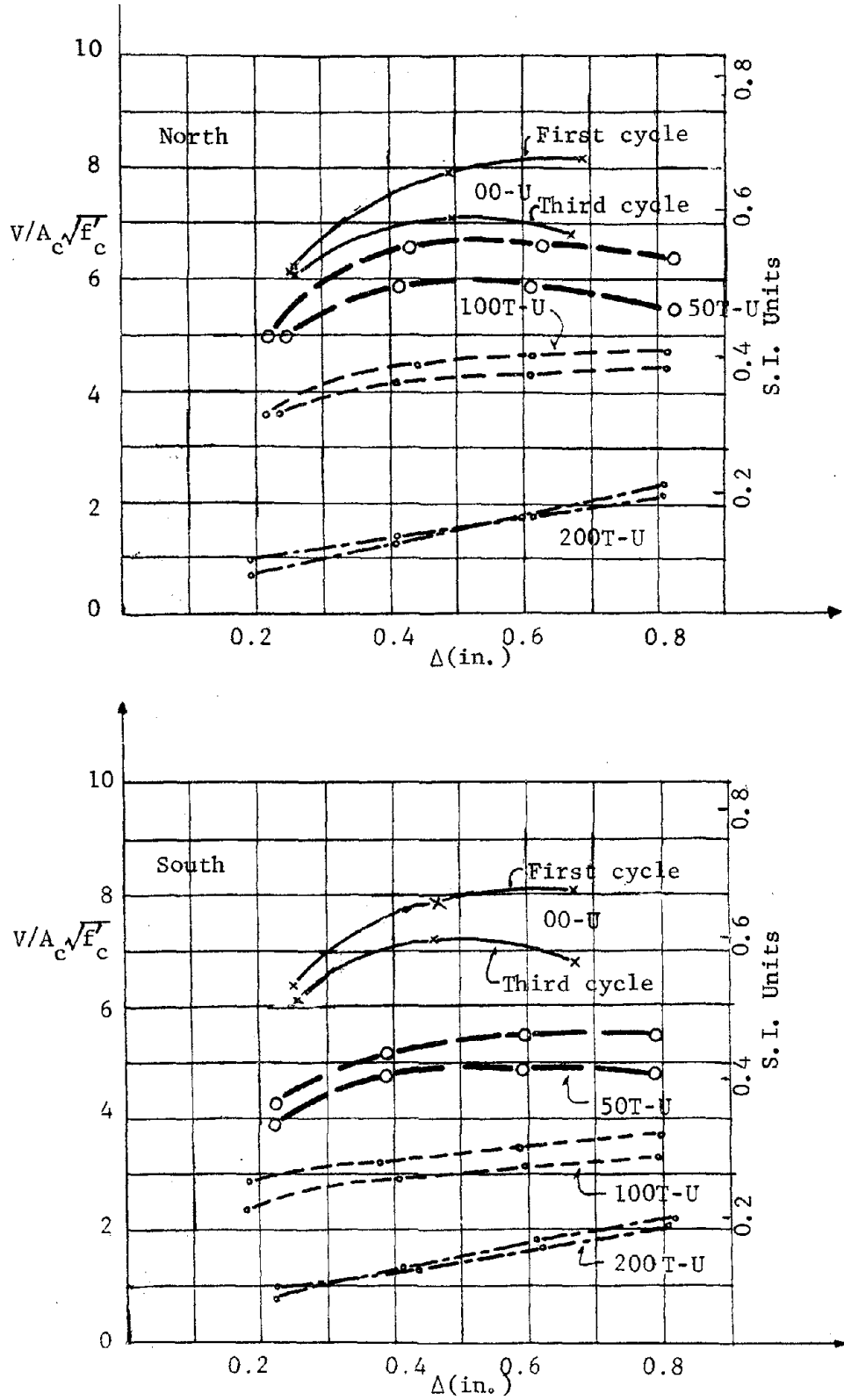


Fig. 6.6 Envelopes of load deflection, tests with constant tension and history U

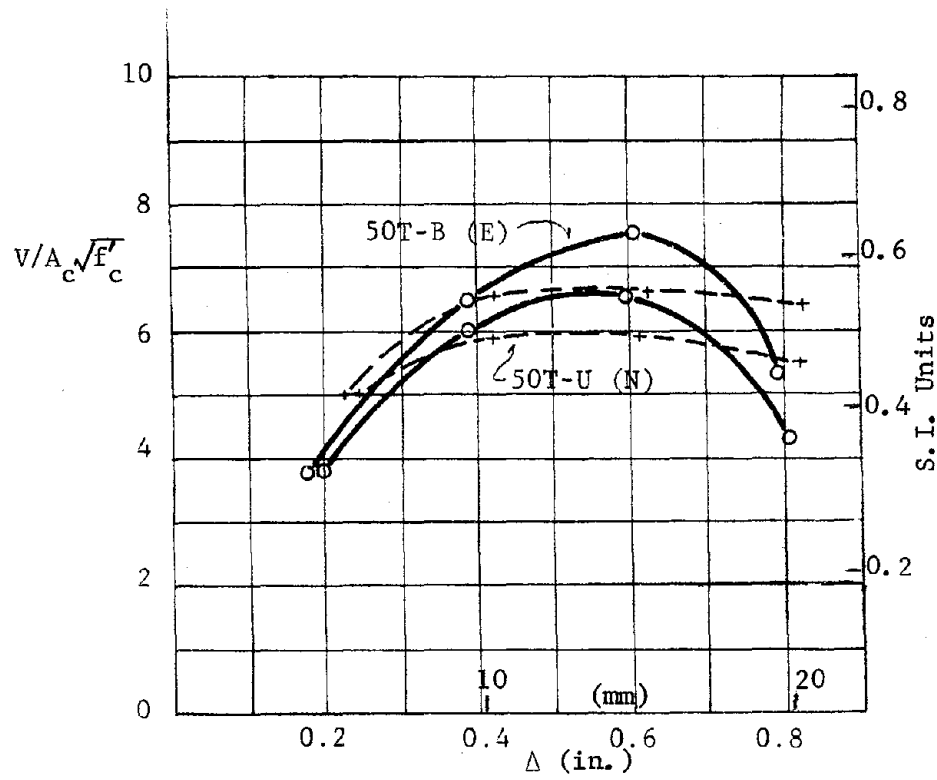
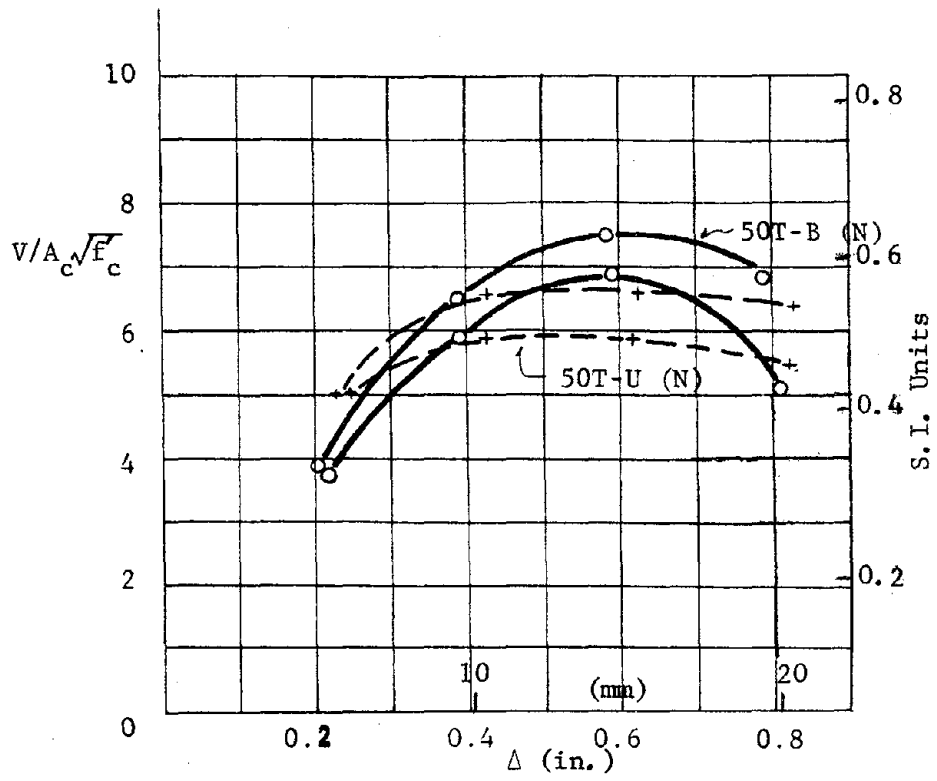


Fig. 6.7 Envelopes of load deflection, tests 50T-U and 50T-B

the influence of concrete strength was not significant when tension was applied.

In Fig. 6.8, the envelopes for test 50T-B are compared with envelopes of peaks to N and E from tests 00-B and 120C-B. Less shear decay was observed in 50T-B than in 00-B and 120C-B for both directions of loading. Considering both strength and energy dissipation per cycle, Specimen 50T-B behaved similarly to 00-B and exhibited better behavior than 120C-B at higher levels of deformation.

Shear Deterioration. Figure 6.9 shows the shear deterioration which occurred in tests 00-U, 50T-U, 100T-U, and 200T-U. Shear deterioration from cycle to cycle at the same level of deformation was most pronounced for 50T-U and 00-U. In 100T-U and 200T-U, the peak normalized shear values remained virtually constant throughout.

The shear deterioration observed in test 50T-B is presented in Fig. 6.10. Peak values from test 00-B are also shown. The shear deterioration at the $3\Delta_1$ and $4\Delta_1$ levels (especially in the EW direction) observed in 50T-B can be attributed to the application of deformations in both NS and EW directions. However, the shear deterioration in 50T-B was less severe than in 00-B.

Strain in Transverse Reinforcement. Figure 6.11 shows peak values of average strain in the ties for test 50T-U. Peaks in the first and third cycles at each deflection level are shown. Figure 6.12 shows similar plots (first cycle peaks only) for tests 100T-U and 200T-U. Strains at the Δ_1 level were larger for low tension than for large tension forces because the axial load was less than that corresponding to tensile cracking of the concrete section. Cracking would occur at a load of 75k, taking $7.5\sqrt{f'_c}$ as an estimate of the tensile strength of the concrete. In the absence of horizontal cracking, inclined cracks were more likely to form. In tests 100T-U and 200T-U, the level of tension was higher than the tensile cracking load and the contribution of the ties

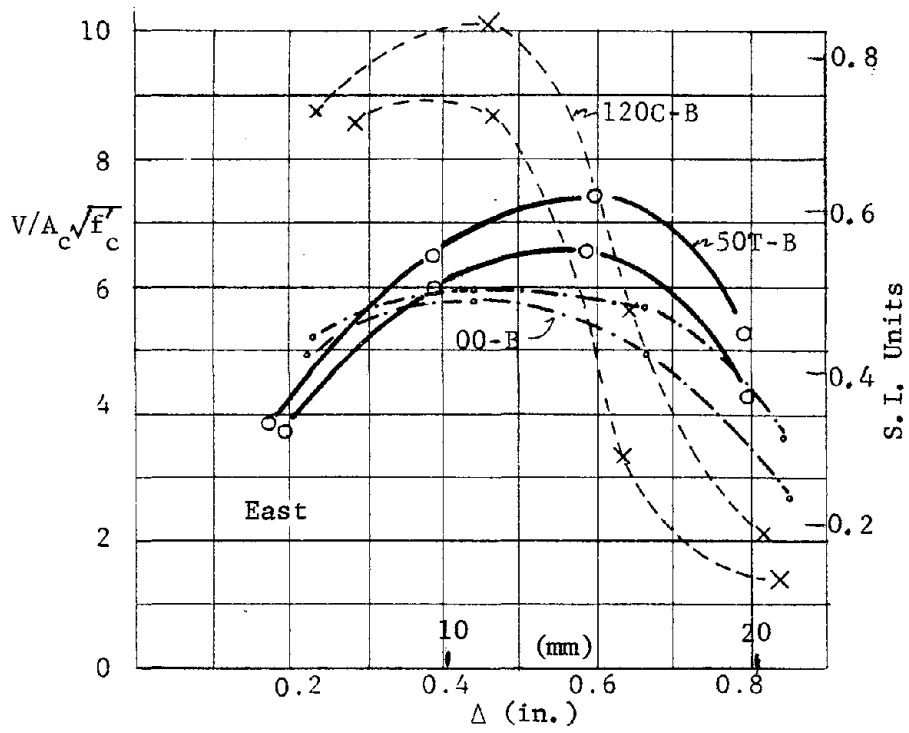
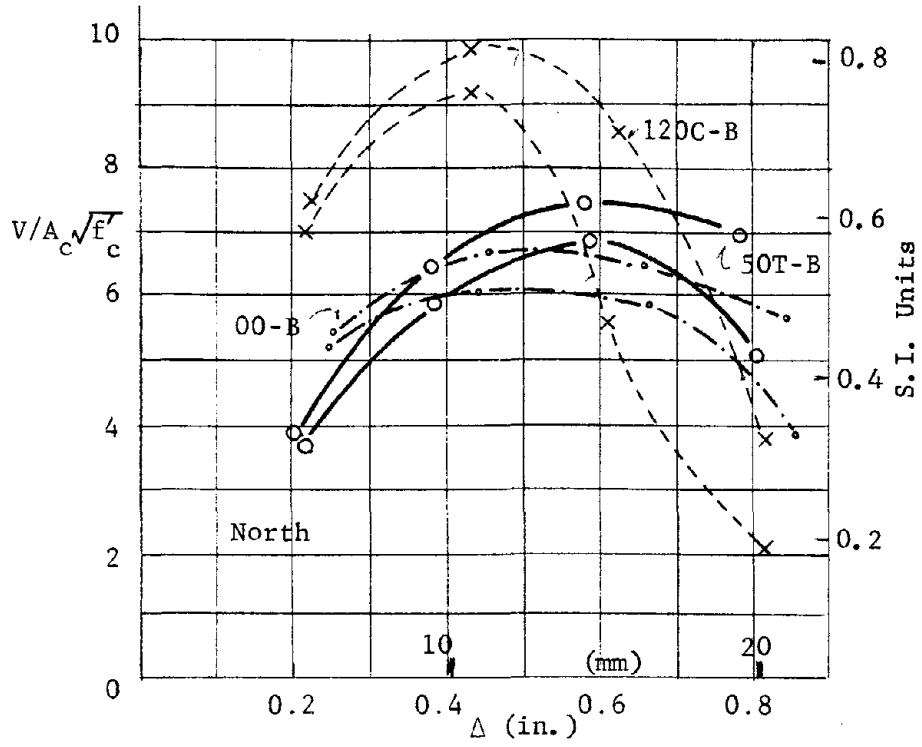


Fig. 6.8 Envelopes of load deflection, tests 50T-B, 00-B, and 120C-B

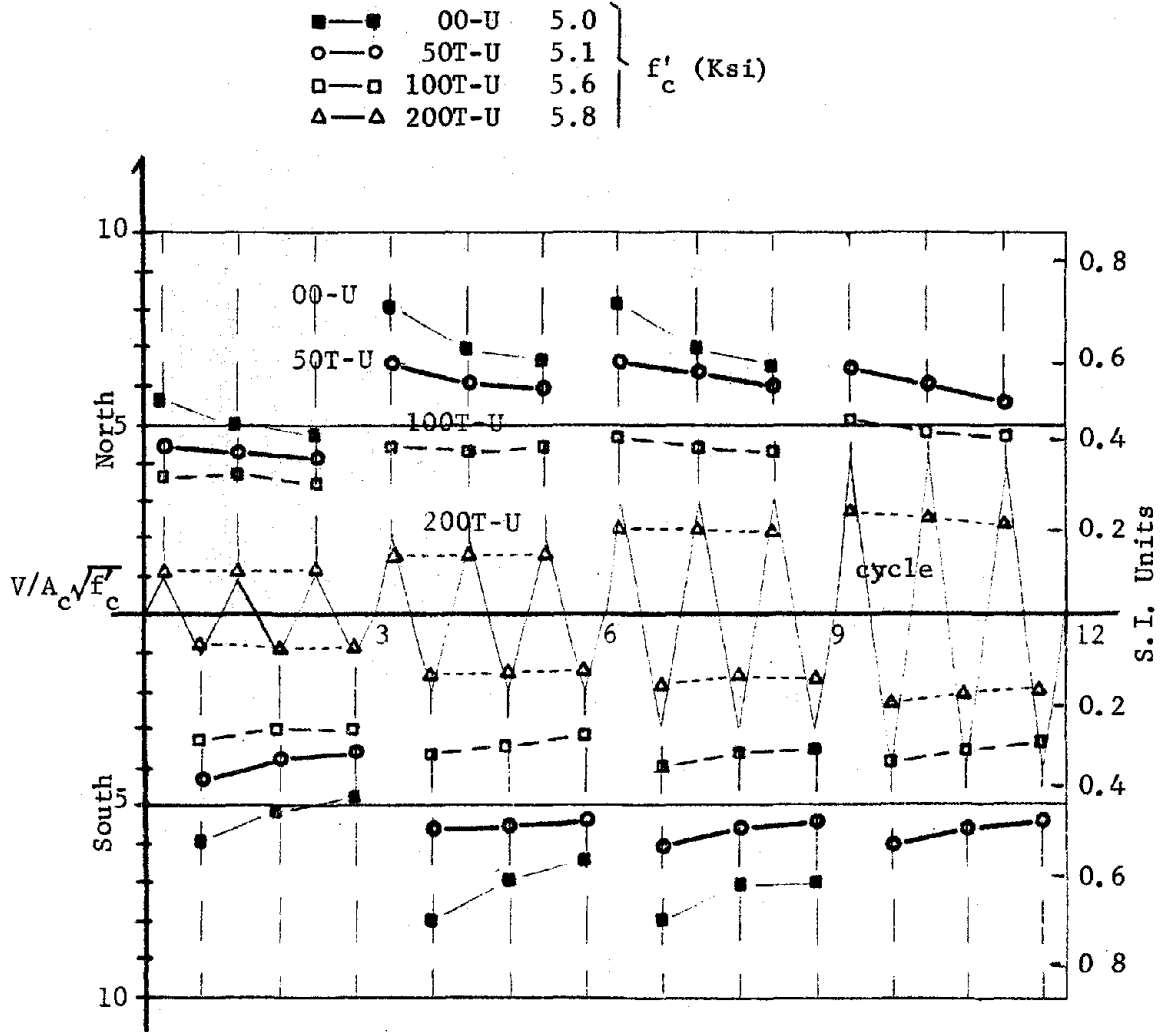


Fig. 6.9 Shear deterioration tests with constant tension and history U

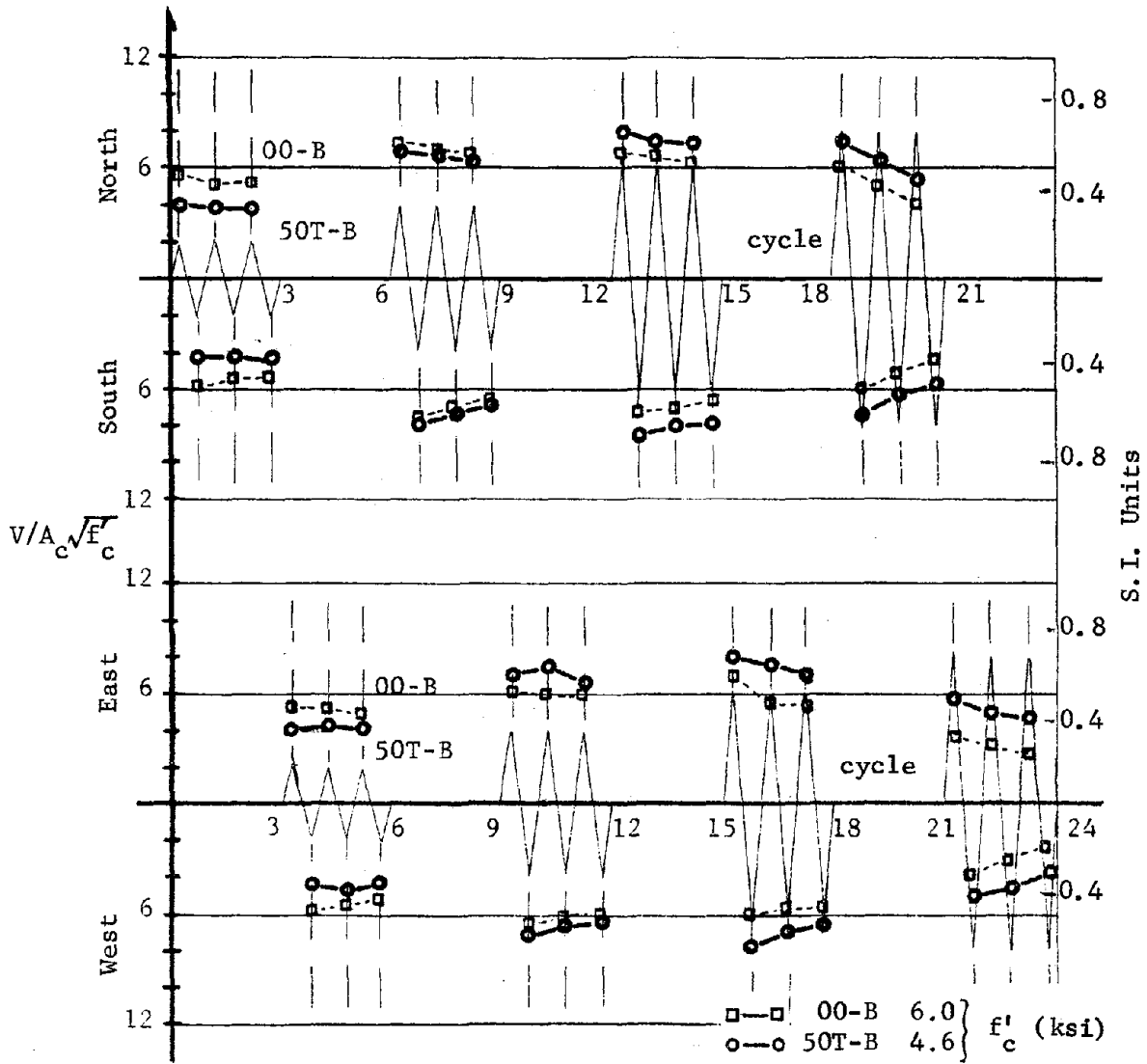


Fig. 6.10 Shear deterioration, tests 00-B and 50T-B

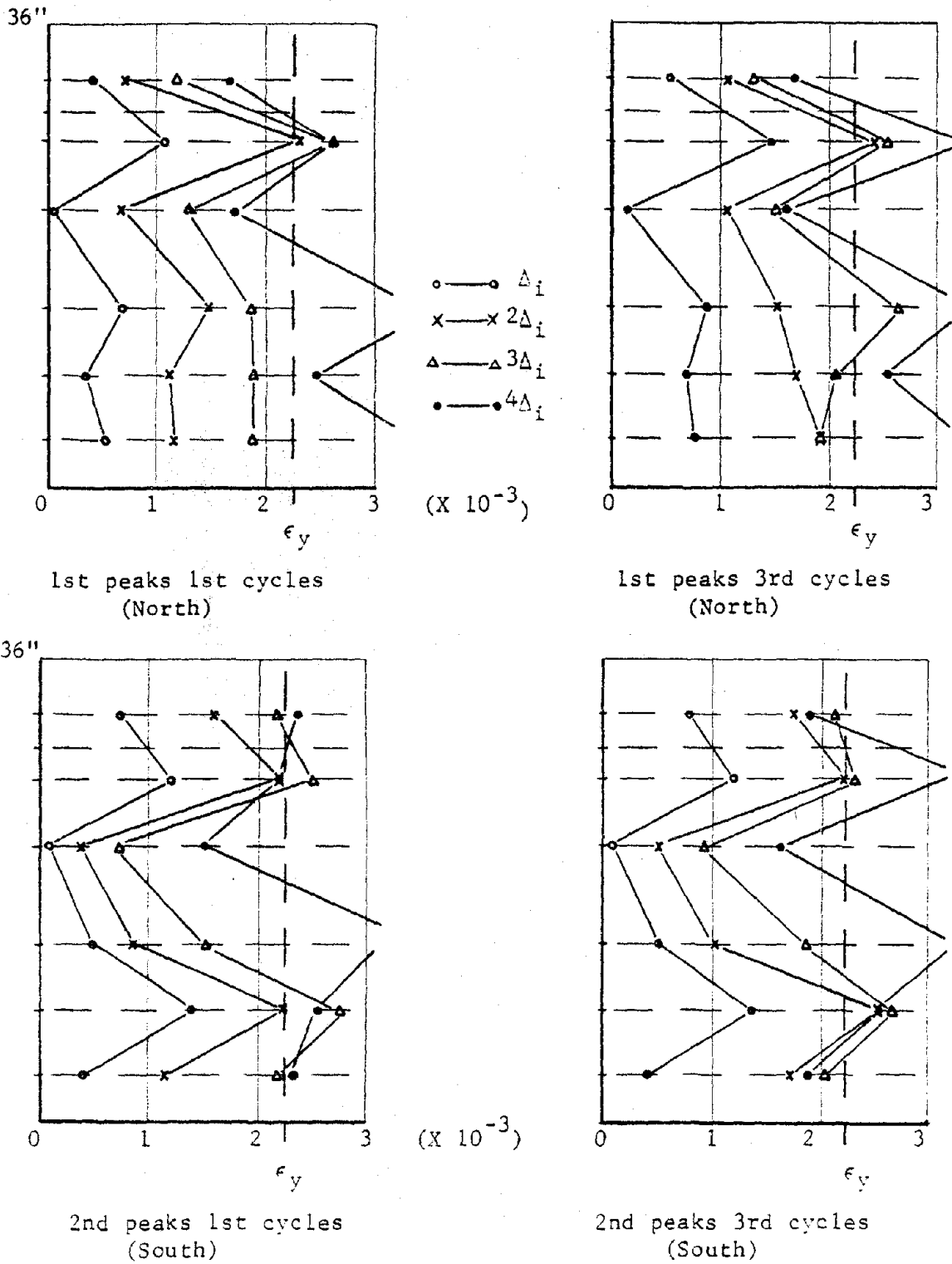


Fig. 6.11 Strain distribution in tie bars, test 50T-U

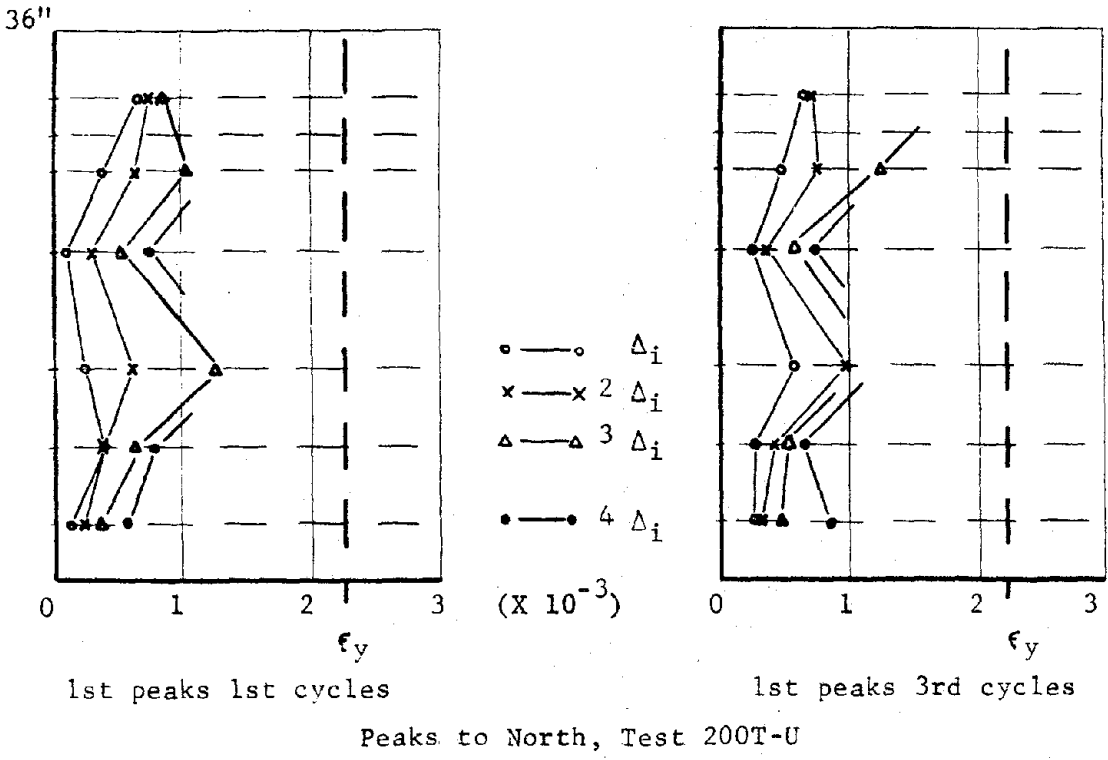
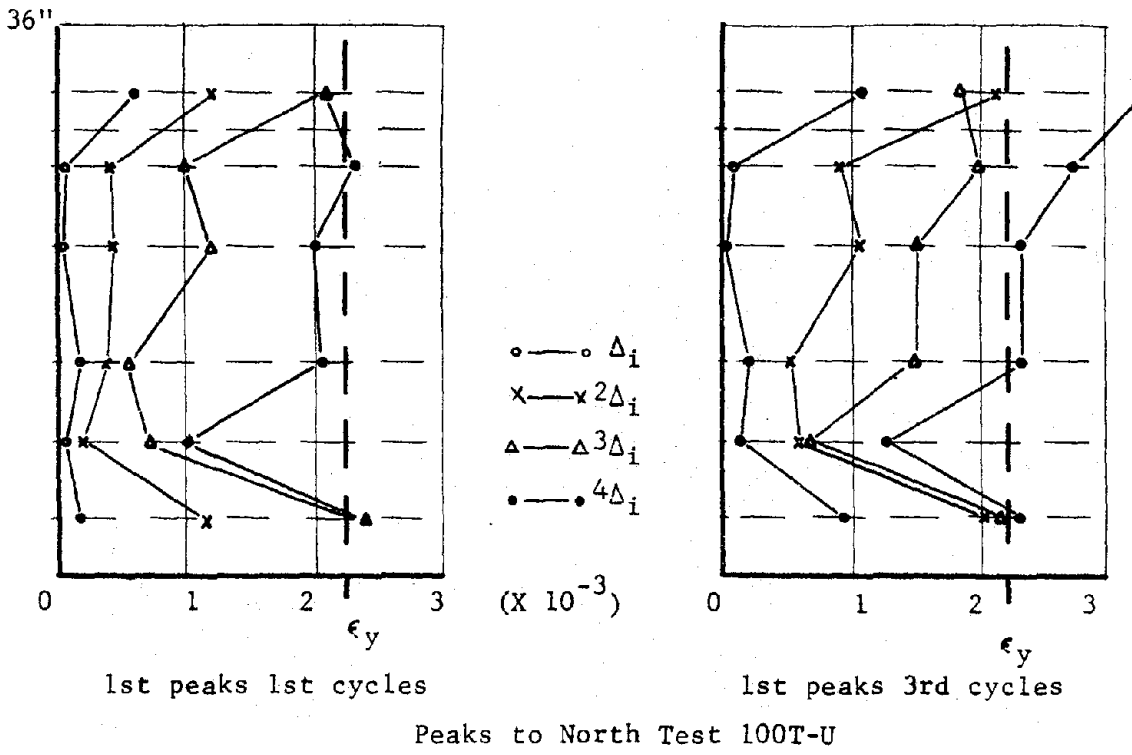


Fig. 6.12 Strain distribution in tie bars, tests 100T-U and 200T-U

started at higher levels of deformation because horizontal cracking across the entire section delayed the formation of inclined cracks.

The strain in the ties increased at a slower rate when tension was applied than when no axial load or compression was present (00-U, Fig. 4.3 and 120C-U, Fig. 5.11). For 200T-U, Fig. 6.12, strains increased at a very slow rate. Figure 6.13 shows the change in strain with unidirectional load history for tests with constant tension. The change in strain between cycles decreased as the level of tension increased.

Figure 6.14 shows progressive strain in two ties in specimens 50T-U and 50T-B. Strains for both directions of loading for test 50T-B are shown. The shape of the strain-cycle curve was similar in both directions of loading of 50T-B.

Crack Patterns. Figure 6.15 shows the crack pattern observed after three cycles of loading at each deflection level for 50T-U. About the same external damage was observed at $2\Delta_1$ and $3\Delta_1$ levels as in Specimen 00-U. However, with tension inclined cracks were not opened as widely as in 00-U and a large number of small noncontinuous cracks (mostly horizontal) were observed. In Fig. 6.16 crack patterns for test 50T-B are shown. Compared with 50T-U (Fig. 6.15), 50T-B exhibited more inclined cracking. Wide inclined cracks developed along well-defined 45° trajectories, with abrasion along the crack.

Crack patterns for test 100T-U are shown in Fig. 6.17. On application of tensile axial load, horizontal cracks formed prior to the application of any lateral deflection. In subsequent stages, inclined cracks changed direction or stopped when crossing previously formed horizontal cracks. As in 50T-U, no appreciable increase in damage was observed after the $2\Delta_1$ level. The crack patterns for 200T-U are shown in Fig. 6.18. Severe cracking was observed under the application of tension and before any lateral load was applied.

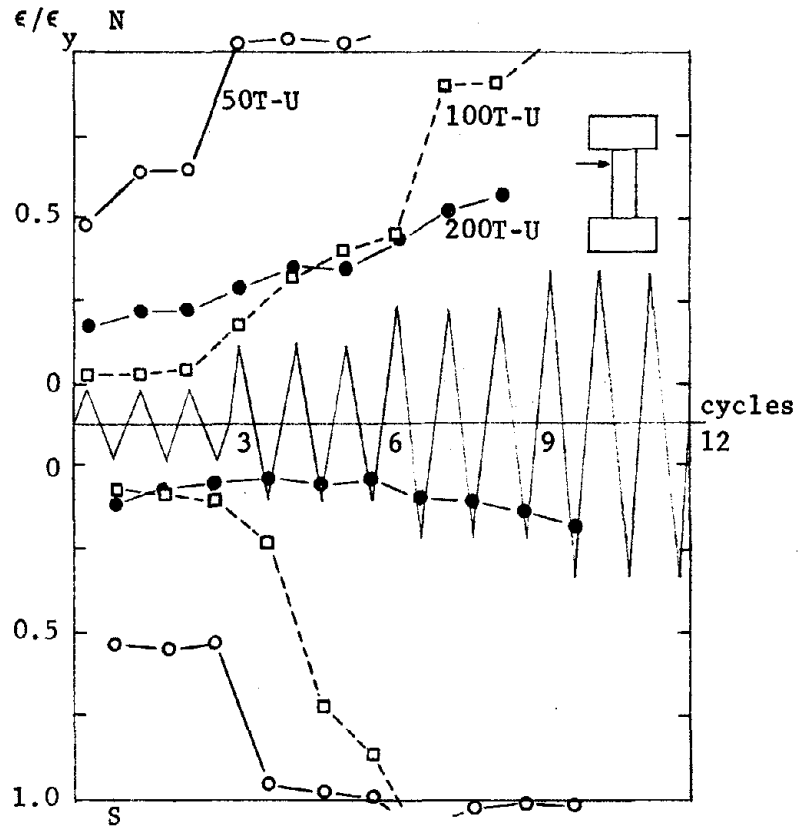


Fig. 6.13 Progressive strain in a tie, tests with constant tension and history U

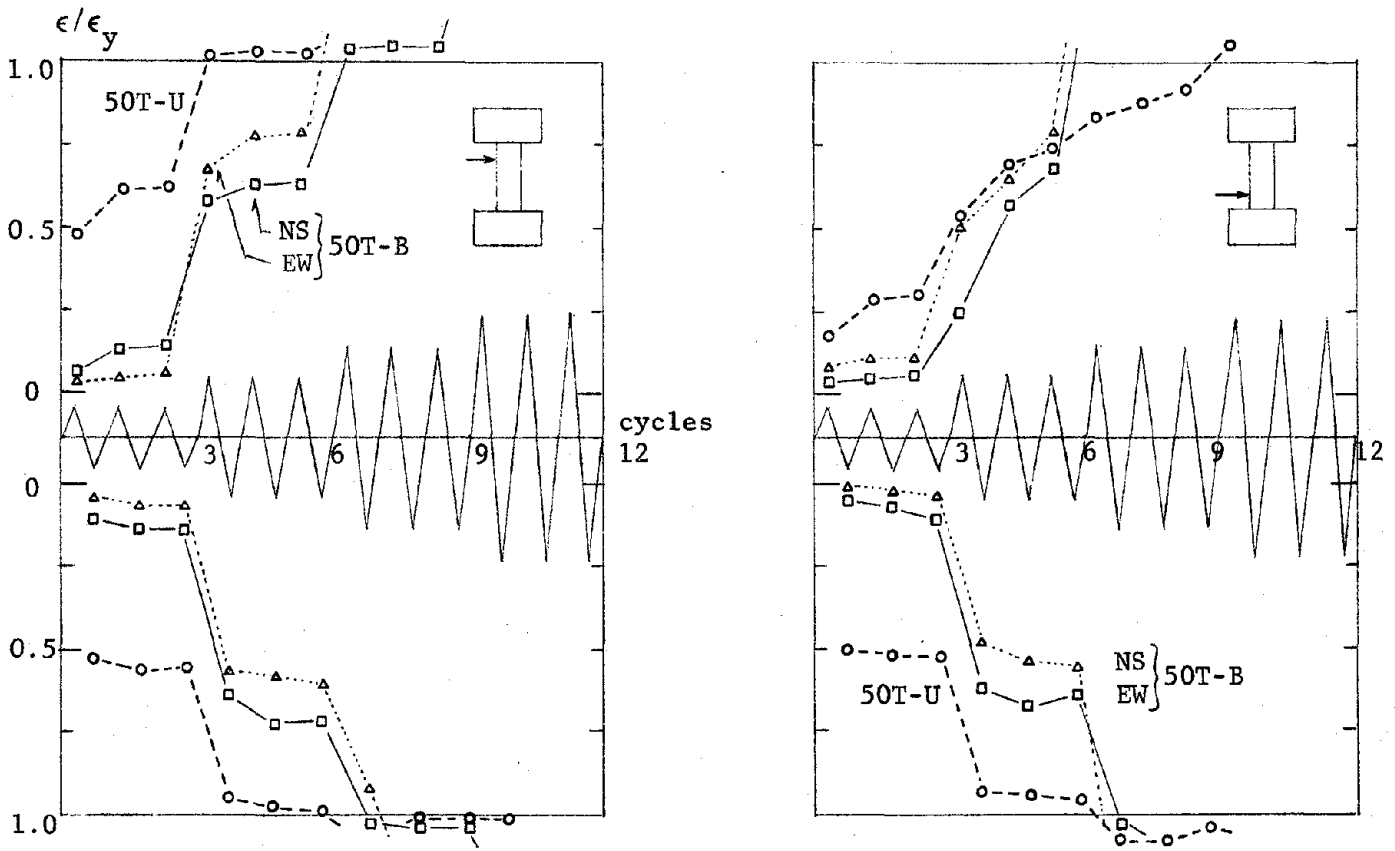
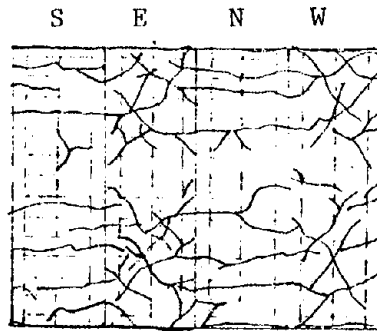


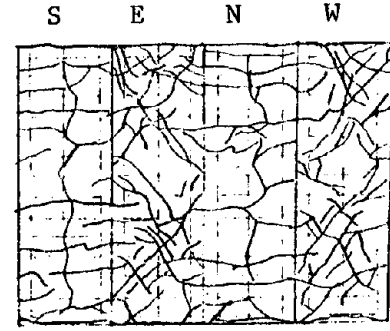
Fig. 6.14 Progressive strain in ties, tests 50T-U and 50T-B



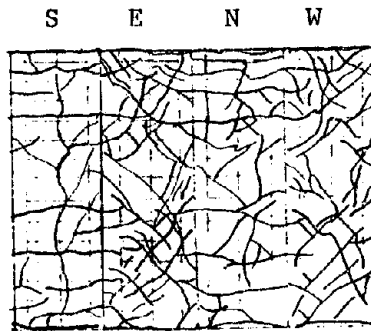
Appearance of specimen after testing



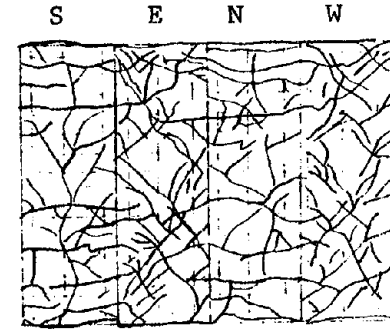
After 3 cycles at Δ_1



After 3 cycles at $2\Delta_1$

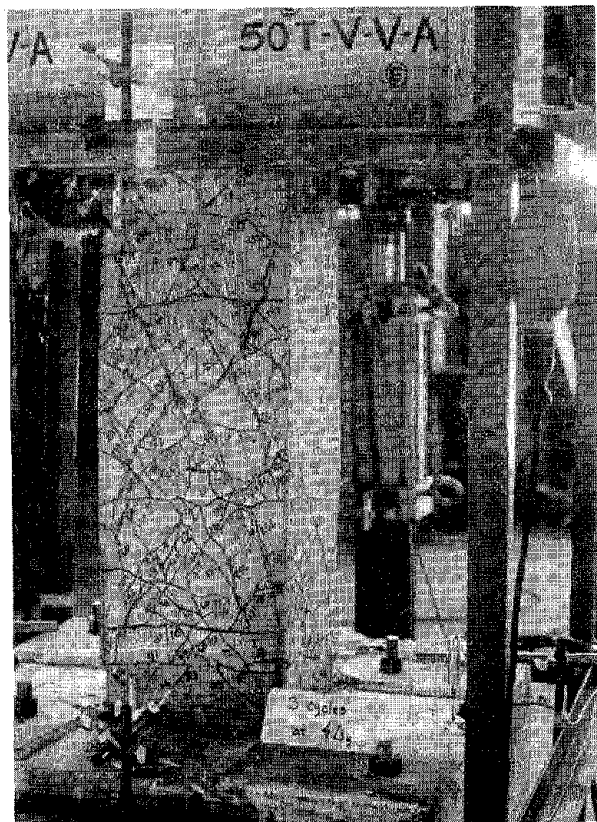


After 3 cycles at $3\Delta_1$

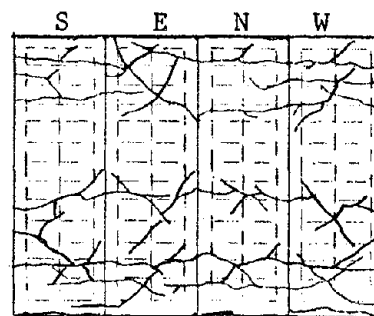


After 3 cycles at $4\Delta_1$

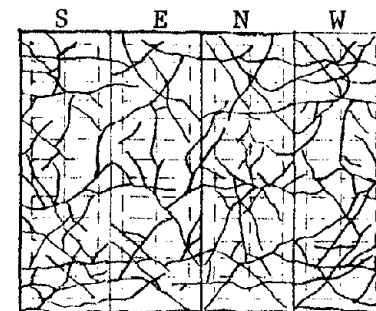
Fig. 6.15 Crack patterns, test 50T-U



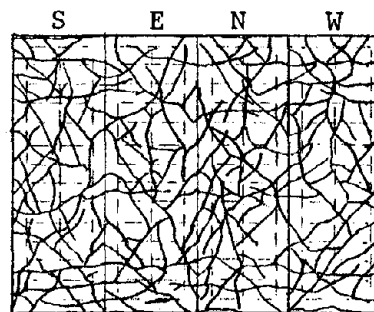
Appearance of specimen at failure



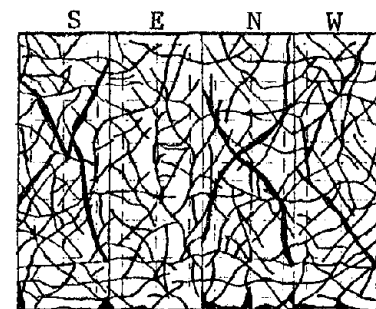
After 3 cycles (each direction) at Δ_i



After 3 cycles (each direction) at $2 \Delta_i$



After 3 cycles (each direction) at $3 \Delta_i$



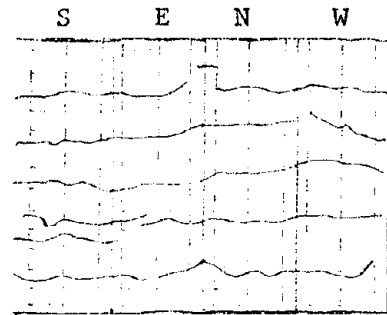
After 3 cycles (each direction) at $4 \Delta_i$

Fig. 6.16 Crack patterns, test 50T-B

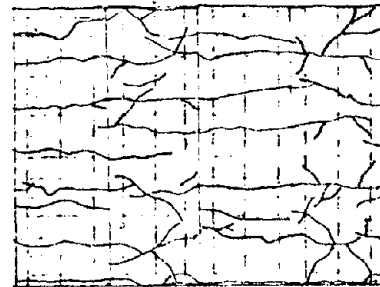


Appearance of specimen after testing

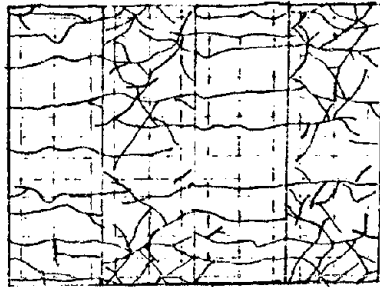
Fig. 6.17 Crack patterns, test 100T-U



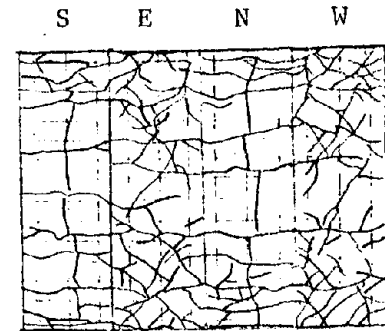
After 100 K tension



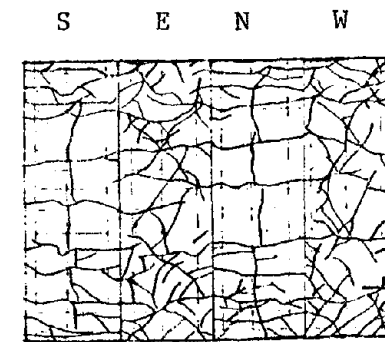
After 3 cycles at Δ_i



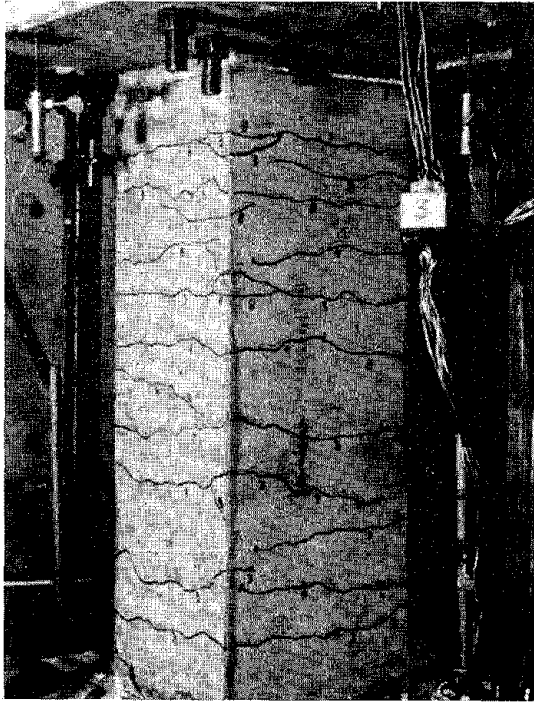
After 3 cycles at $2\Delta_i$



After 3 cycles at $3\Delta_i$



After 3 cycles at $4\Delta_i$



Appearance of specimen after testing

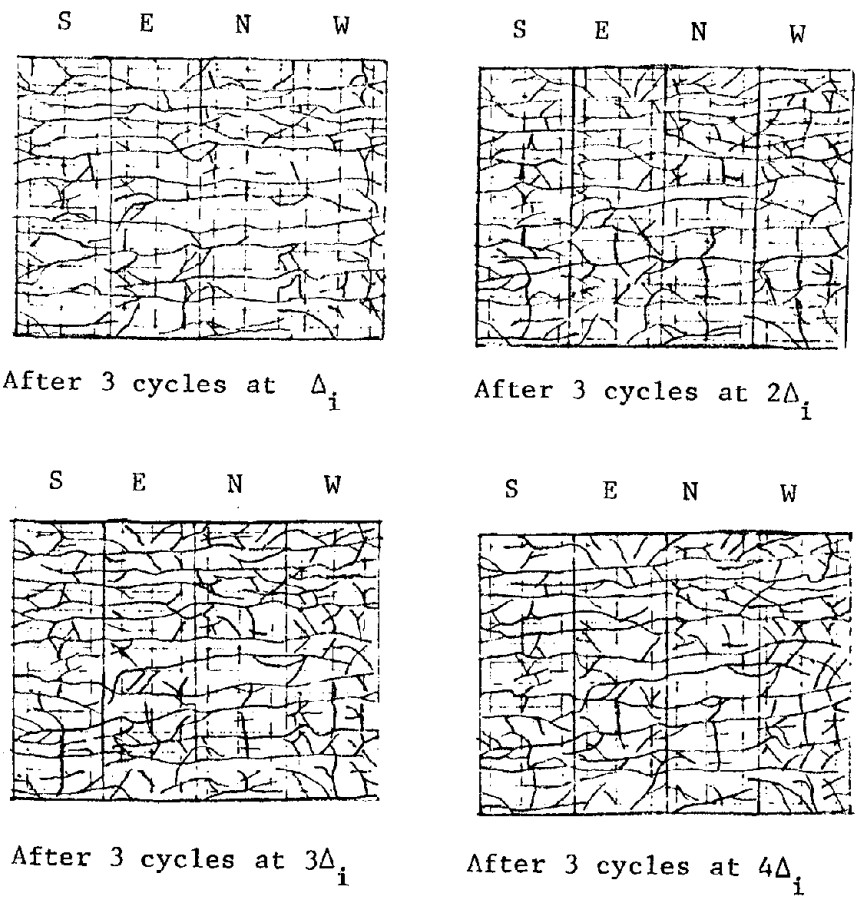


Fig. 6.18 Crack patterns, test 200T-U

Under lateral deformation only short, noncontinuous cracks were formed. There was an increase in axial extension as the test progressed. After the application of the tensile force, axial extension was 0.13 in. and increased to 0.14, 0.27, 0.40, and 0.60 in. at the 1, 2, 3, and $4\Delta_i$ levels, respectively. Little change in damage to the specimen was observed from level to level of lateral deformation.

6.3 Study of the Behavior

Mechanism of Failure. As in the case of constant compression, after a critical deflection was reached, the behavior was dictated by the ability of the ties to confine the core.

Under tension, the ties did not need to provide confinement and were available to carry shear whenever diagonal cracking crossed the tie. It should be noted that forces in the tie were not mobilized until large lateral deformations closed the horizontal tension cracks. With larger axial tension, the cracks were wider and the lateral deformations were greater prior to mobilization of the tie forces. Under tension, the shear strength was less than when compression was present. Maximum shear, V , was $9.4\sqrt{f'_c}A_c$ for 120C-U and $6.6\sqrt{f'_c}A_c$ for 50T-U. Although tension caused the element to have less shear capacity, shear deterioration was controlled, as evidenced by the slow rate of strain in the ties and little damage to the concrete core. Yielding of the ties occurred at higher levels of deformation for tests 50T-U, 50T-B, and 100T-U than in tests with constant compression, and in all tests with constant tension the rate of strain increase was slower than with compression.

Strength Characteristics. The shear required to produce hinges in the test specimen may be utilized as a standard for judging behavior. The shear at hinging is given by $2M_n/L$, where M_n is obtained from interaction diagrams (Figs. 4.5 and 4.6), including the effect of axial tension. Table 6.1 shows the computed

TABLE 6.1 MAXIMUM PEAK SHEAR COMPARED WITH $2M_n/L$
(TENSION)

Test	Maximum Peak			$2M_n/L$	
	V (k)	$V/A_c\sqrt{f'_c}$	Δ (in)	Total	Norm*
00-U	58	8.2	0.69	50	7.1
00-B (NS)	52	6.7	0.46	50	6.5
00-B (EW)	46	5.9	0.45	50	6.5
50T-U	47	6.6	0.43	38	5.3
50T-B (NS)	54	7.9	0.58	46	6.8
50T-B (EW)	51	7.5	0.60	46	6.8
100T-U	36	4.8	0.81	25	3.3
200T-U	18	2.4	0.81	0	0.0

* normalized respect $A_c\sqrt{f'_c}$

TABLE 6.2 ACI NOMINAL SHEAR STRENGTH (TENSION)

Specimen	$\frac{N}{A_c}$ (psi)	V_c (k)	V_s (k)	V_n (k)	$V_n/A_c\sqrt{f'_c}$
50T-U	500	0.0	26.3	26.3	3.7
50T-B	500	0.0	26.3	26.3	3.5
100T-U	1000	0.0	26.3	26.3	3.4
200T-U	2000	0.0	26.3	26.3	3.9

$$V_c = 2 \left(1 - \frac{T}{500A_c} \right) \sqrt{f'_c} A_c$$

$$V_s = \frac{A_v f_{sy} d}{s}$$

$$V_n = V_c + V_s$$

values of $2M_n/L$ for tests with tension as well as for tests with zero axial load. For comparison, values of the measured maximum shear and the deflection at which the peak occurred are also listed. In all the tests with tension, the applied shear reached the value required to form plastic hinges. The deflection level at which the maximum peak shear was reached increased as the level of tension is increased.

The nominal shear strength according to the ACI Code is $V_n = V_c + V_s$. For members subjected to axial tension the contribution of the concrete V_c is given by Eq. (11.9):

$$V_c = 2 \left(1 + \frac{N_u}{500A_g} \right) \sqrt{f'_c} b_w d$$

where N_u is negative for tension. Considering core area only (A_c instead of A_g), the contribution of the concrete is zero for all levels of tension because the average stress produced was 500 psi or more. Values of the nominal shear computed as $V_n = V_s$ are listed in Table 6.2, according to Eq. (11.17) of the ACI Code. For the low level of tension (50T-U and 50T-B) the nominal shear predicted by the ACI equations is reached for cycles at Δ_1 (Figs. 6.1 and 6.5), and for higher levels of deformation peak shears are equal to or greater than the nominal shear. Based on tests conducted with shear span-to-depth ratios of 1.5 (1.8 using core dimensions), elements subjected to tension loads producing a stress of 500 psi or less on the concrete core area may be adequately designed assuming $V_n = V_s$.

For higher levels of tension the applied shear may not reach the shear computed as $V_n = V_s$ for any level of deformation or reach it at very high levels of deformation. For instance, in test 100T-U, V_s is reached at $3\Delta_1$ in the south direction and in test 200T-U, V_s is not reached for any of the deformation levels considered. Therefore, a criterion based on strength considerations

only may not be adequate for columns under cyclic loads. Deformation characteristics and energy dissipation must be taken into account.

Summary of the Influence of Constant Tension. Comparing the results of tests with constant compression, zero axial load, and constant tension the following differences in the behavior were discerned:

- (a) The required shear to attain a given deformation decreases as the level of tension increases but less shear deterioration with cycling and with large deformations is observed.
- (b) The adverse effect of alternate deformations in the orthogonal direction decreases with the presence of constant tension as compared with tests with compression and no axial load.
- (c) Hysteresis loops for low levels of tension show about the same amount of energy dissipation as similar tests with compression or no axial load, especially for first cycles.
- (d) The shear deterioration from cycle to cycle at the same level of deformation decreases with the level of tension.
- (e) With tension, distress in the concrete occurs at large deformations while with compression similar distress is apparent at low deflections.

CHAPTER 7

ALTERNATE TENSION AND COMPRESSION

7.1 Introduction

In this chapter the influence of alternate application of tension and compression is discussed. Results from tests with alternating axial loads (ATC-U and ATC-B) are compared with the results of tests with similar lateral deformation history and equal levels of constant axial load (120C-U and 100T-U are compared with ATC-U, and 120C-B and 50T-B are compared with ATC-B).

7.2 Load-Deflection Curves and Shear Deterioration

Figure 7.1 shows the complete load-deflection relationship and Fig. 7.2 shows the first cycle at each deflection level, for test ATC-U. Figure 7.3 shows the shear deterioration which occurred in test ATC-U compared with 120C-U and 100T-U.

In test ATC-U, alternate tension and compression was applied during the first three cycles at the Δ_i level, and afterward constant compression was applied. The sequence of application of axial loads, with respect to the lateral deflection history is included in Fig. 7.3 for reference.

Comparing Figs. 7.1 and 7.2 with the respective load-deflection curve for test 120C-U (Fig. 5.1), it is observed that for all cycles except those in the N direction at the Δ_i level, the response is similar. Comparing ATC-U with 100T-U (Fig. 6.2), only in the cycles to the N direction at the Δ_i level are the curves similar. The effect of tension is reflected as a reduction in shear and stiffness, but only during that part of the loading

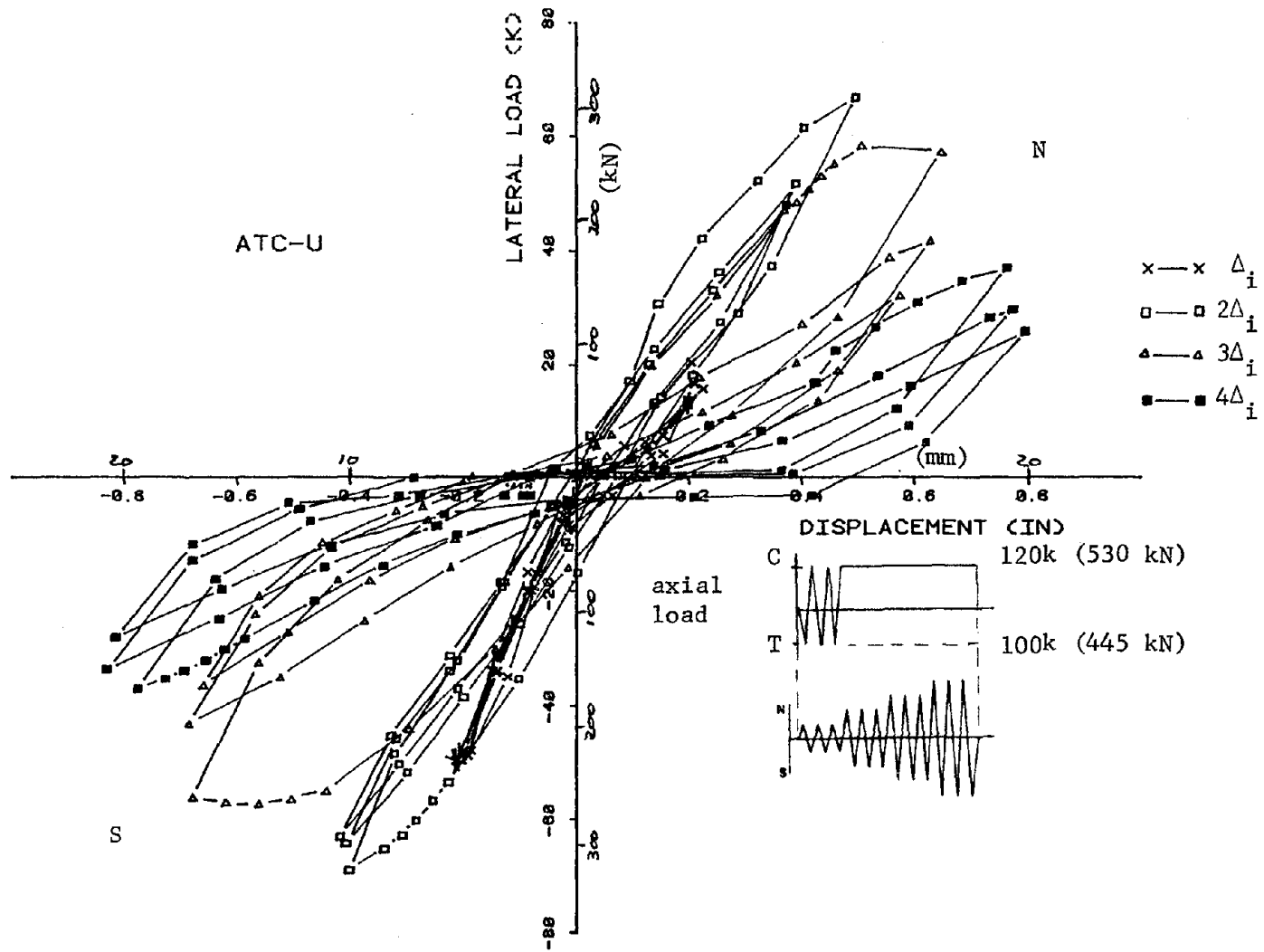


Fig. 7.1 Load-deflection curve, ATC-U

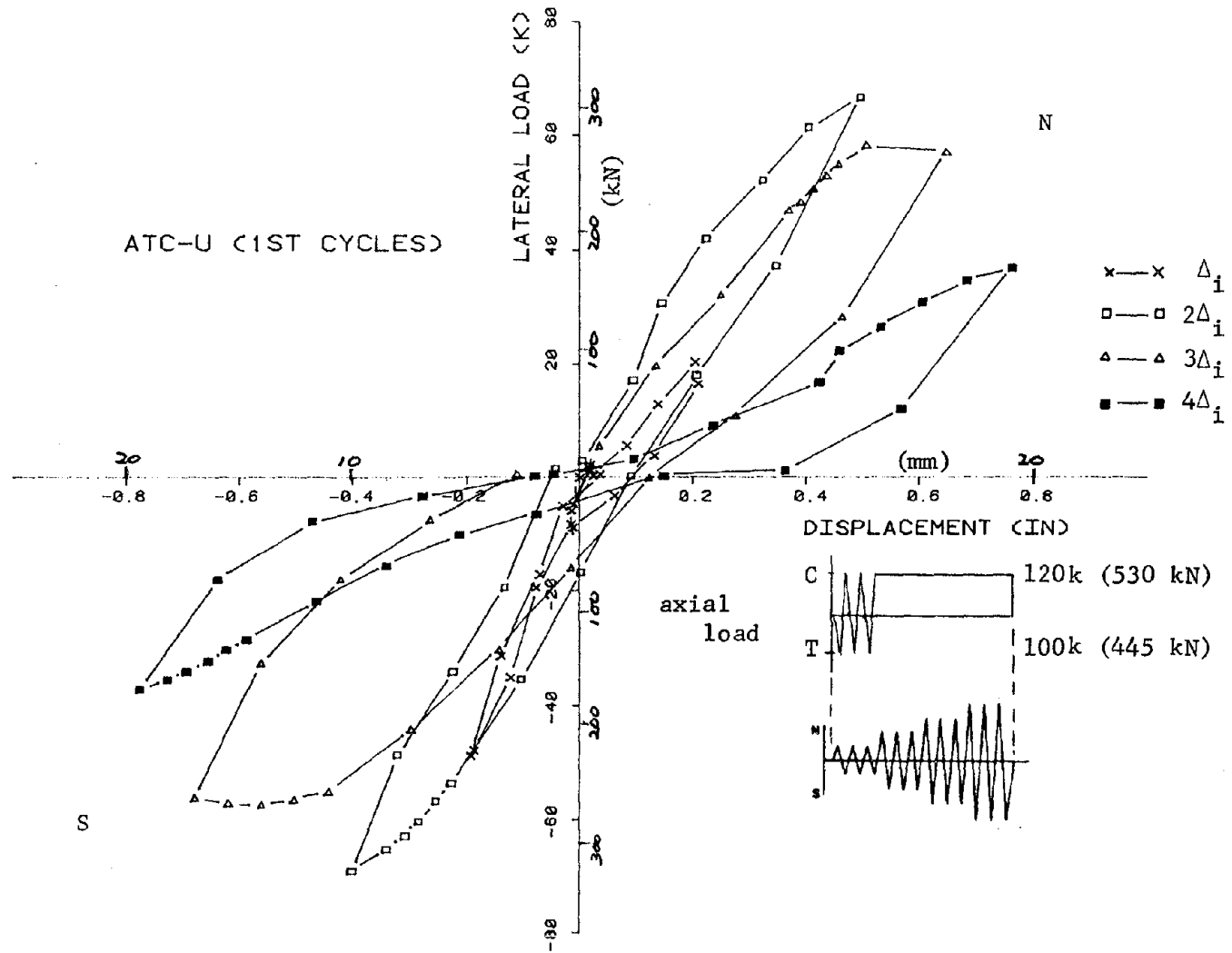


Fig. 7.2 Load-deflection curve, ATC-U first cycles

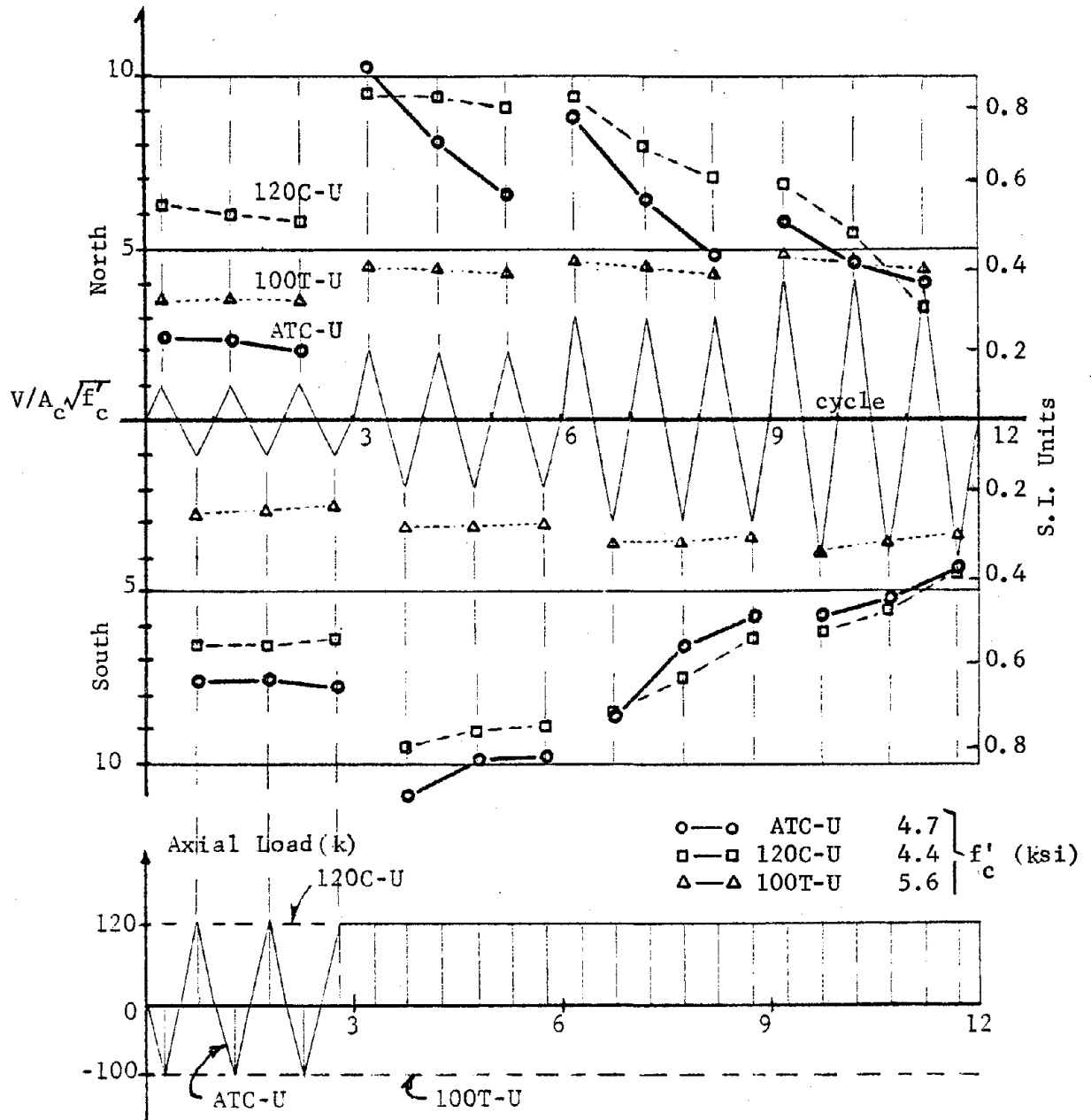


Fig. 7.3 Shear deterioration, tests ATC-U, 100T-U, and 120C-U

history where tension was imposed. This effect can also be seen in Fig. 7.3, where the shear deterioration in the S direction is similar in tests ATC-U and 120C-U. In the N direction, ATC-U shows shear deterioration at the Δ_i level similar to that of 100T-U and somewhat greater shear deterioration with cycling at deflection levels 2, 3, and $4\Delta_i$ produced by the effects of tension applied at Δ_i .

The load-deflection curves for test ATC-B are presented in Fig. 7.4 (NS direction) and Fig. 7.5 (EW direction). The shear deterioration observed in test ATC-B is shown in Fig. 7.6. For comparison tests, 50T-B and 120C-B are included.

In test ATC-B, alternate tension and compression was applied for cycles in the NS direction, while in the EW direction constant compression was applied. The sequence of application of axial loads with respect to the lateral deflection history is included in Fig. 7.6.

Comparing the load-deflection curves for test ATC-B (Figs. 7.4 and 7.5) with the load-deflection curves for test 120C-B (Figs. 5.2 and 5.3), a similarity is observed except for peaks to the N direction where tension was applied.

From Fig. 7.6, more shear deterioration is observed in test 120C-B than in test ATC-B, which means that constant compression is more severe than alternate tension and compression. The beneficial action of tension in reducing shear decay observed in tests with constant tension remains when tension is applied alternately with compression.

7.3 Envelopes of Load Deflection

Envelopes of peak values of shear and deflection are plotted in order to extend the observations from the load-deflection and shear-deterioration curves.

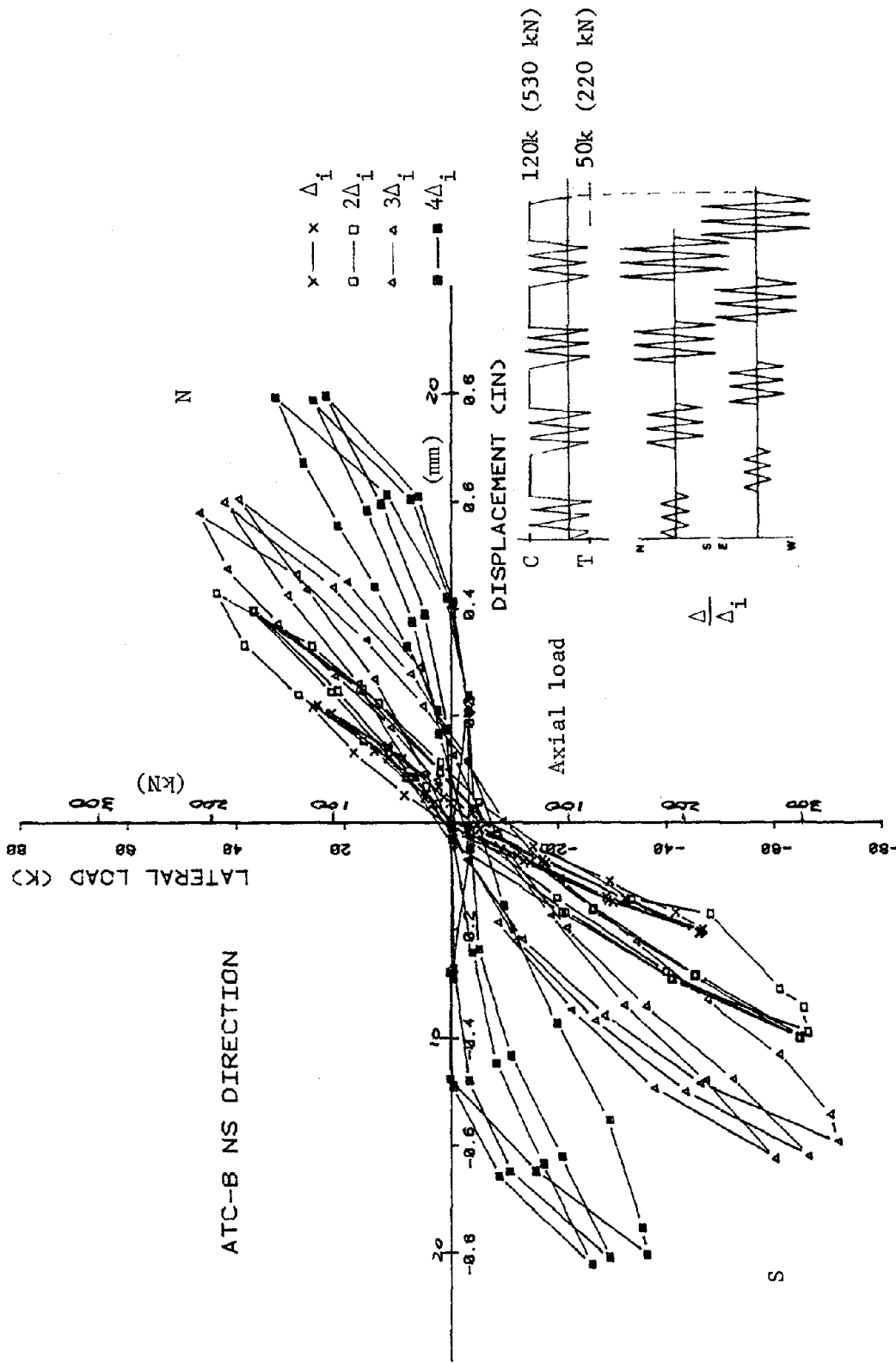


Fig. 7.4 Load-deflection curve, ATC-B - NS direction

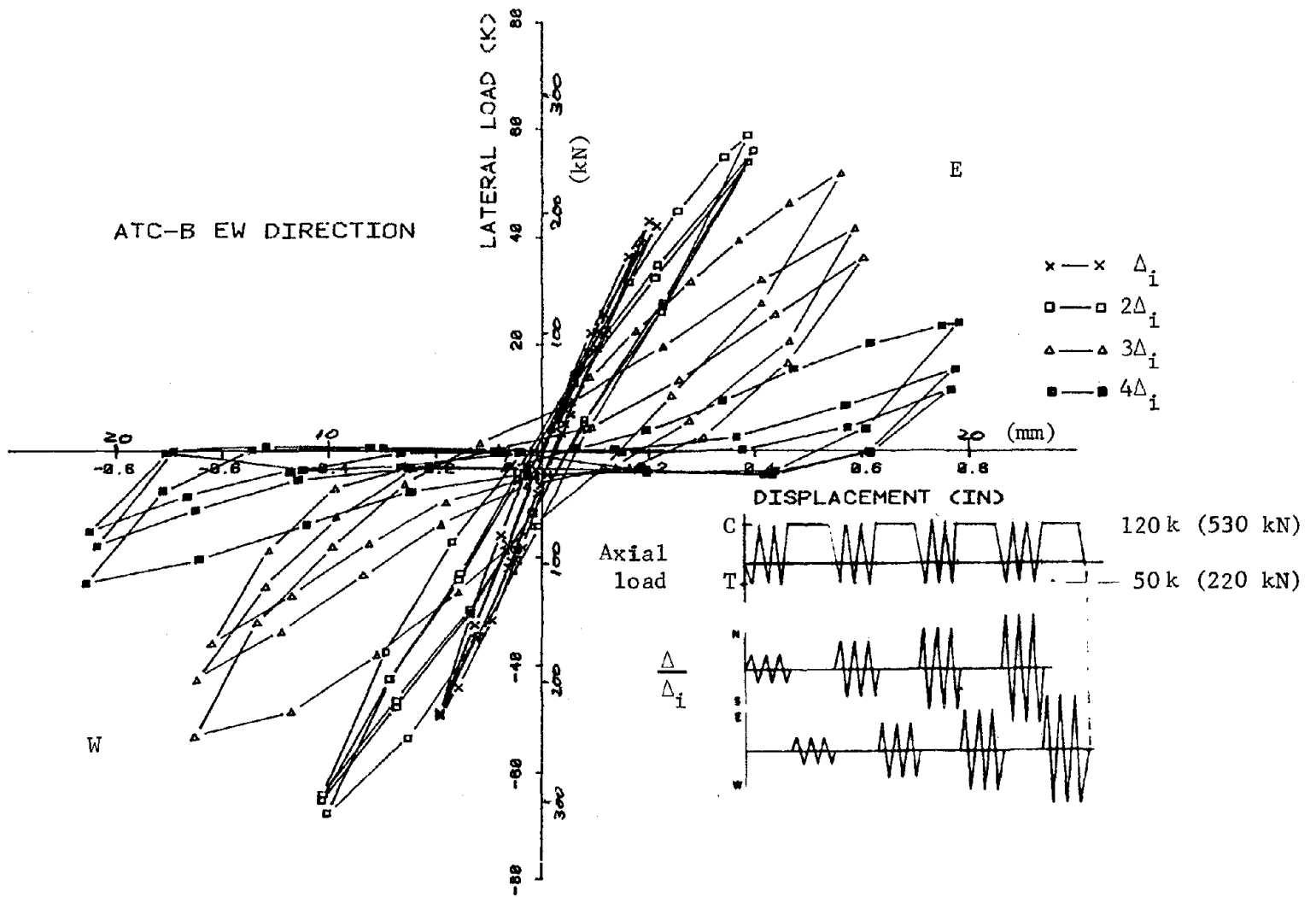


Fig. 7.5 Load-deflection curve, ATC-B - EW direction

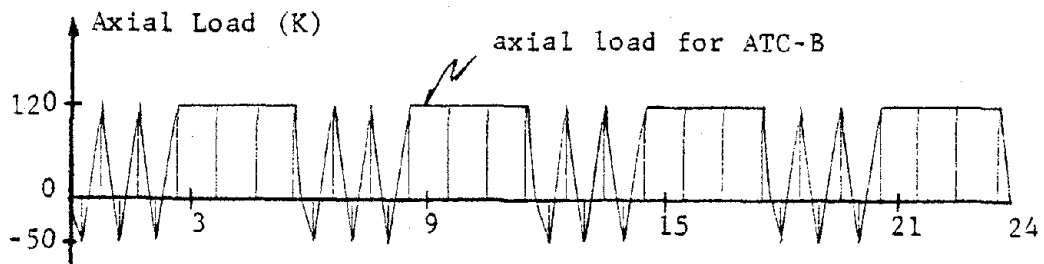
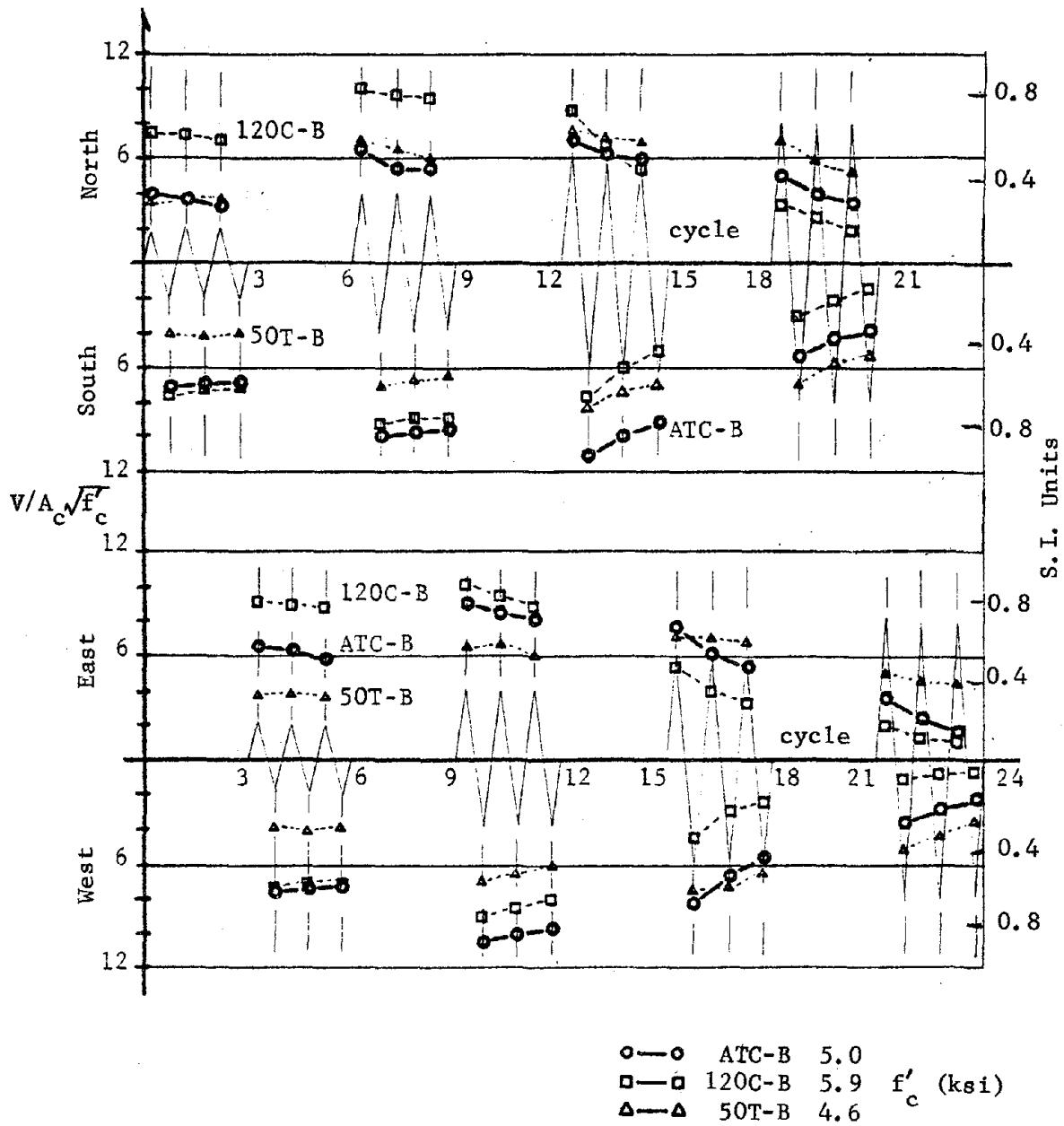


Fig. 7.6 Shear deterioration, tests ATC-B, 50T-B, and 120C-B

Envelopes of first and last peaks from tests ATC-U, 120C-U, and 100T-U are shown in Fig. 7.7. For peaks to the N direction at the Δ_i level in which tension was applied, peak shears are less than observed in 100T-U (same level of tension but constant in all cycles). However, for higher levels of deformation the peaks to the N direction in ATC-U approximate those in 120C-U (constant compression in both). In the N direction, ATC-U shows more shear deterioration from cycle to cycle at the same level of deformation than 120C-U. Envelopes for tests ATC-U and 120C-U are very similar in the S direction. The effect of alternately applying tension and compression in the first three cycles is not apparent in the south direction of loading. The effect of tension is limited mainly to the peaks in which tension was applied. In the overall behavior, the effect of tension is apparent as shear deterioration from cycle to cycle only in the direction in which tension was applied.

Figures 7.8 (NS direction) and 7.9 (EW direction) show first and last peak envelopes of tests ATC-B, 50T-B, and 120C-B. The shape of the envelopes in the N direction is similar in tests ATC-B and 50T-B, but peak values in ATC-B are lower than in 50T-B. This is due to the alternate mode of application of tension and the application of compression in the EW direction in ATC-B. For peaks to the S direction, test ATC-B shows behavior similar to 120C-B except that higher shears and less shear deterioration are observed in ATC-B. Peaks to the E direction (Fig. 7.9) in ATC-B are lower than in 120C-B for Δ_i and $2\Delta_i$ levels; however, for larger deformations the peaks are similar. For peaks to the W direction, similar behavior is observed, but ATC-B shows less deterioration than 120C-B.

In Fig. 7.10, envelopes in the NS direction of test ATC-B are compared with envelopes of peaks to the N direction from 50T-U and of peaks to the S direction from 120C-U. Peaks values for ATC-B are approximately equal to peaks for 50T-U in the N direction and

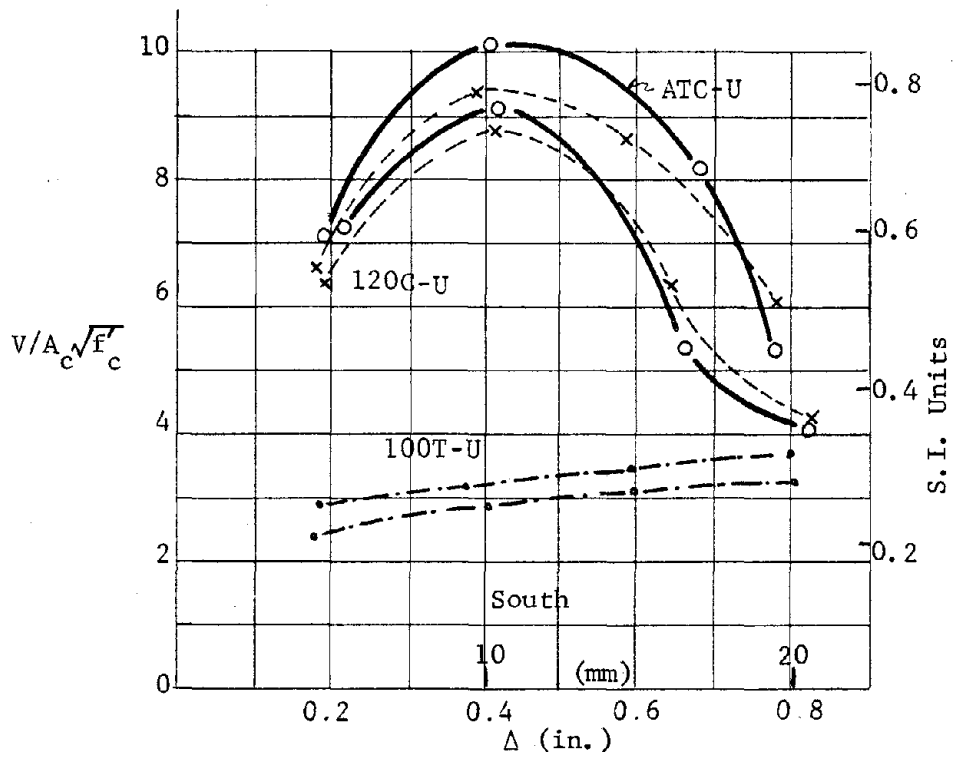
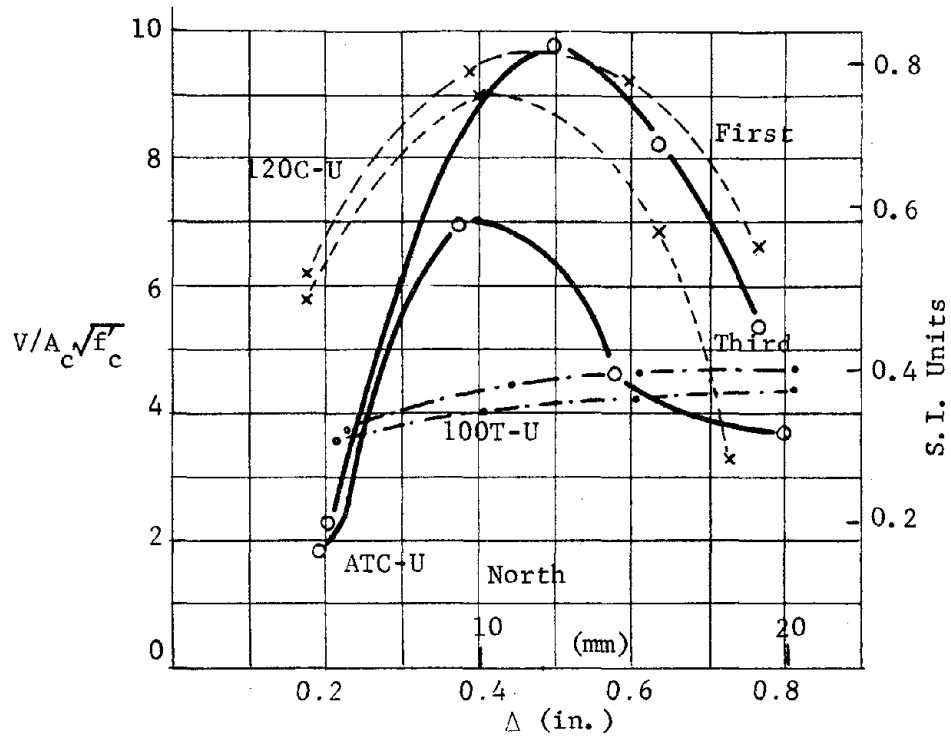


Fig. 7.7 Envelopes of load deflection, ATC-U, 100T-U, and 120C-U

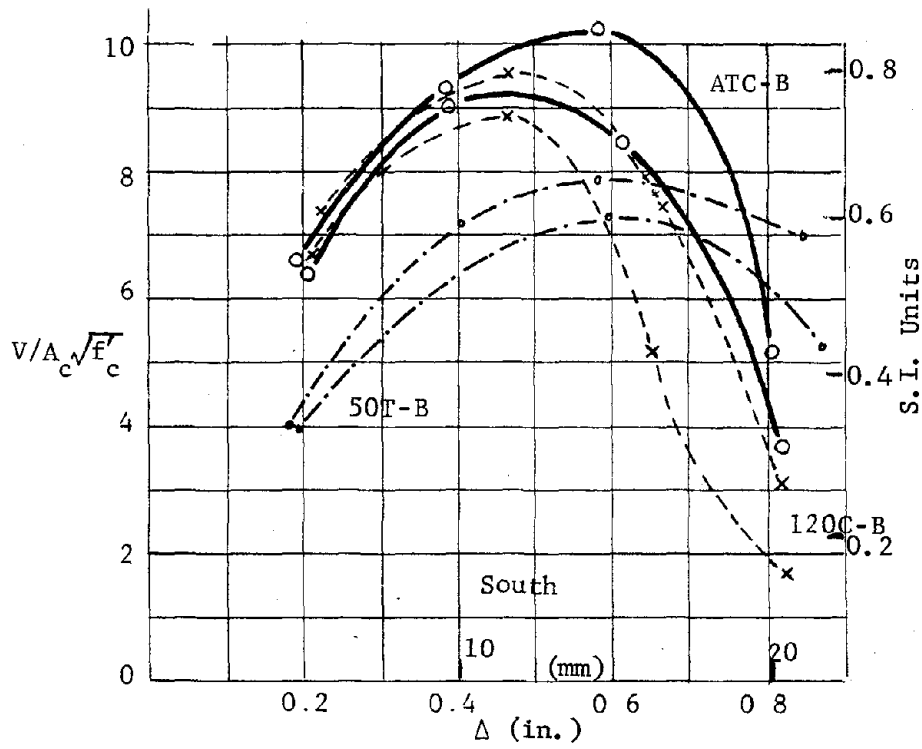
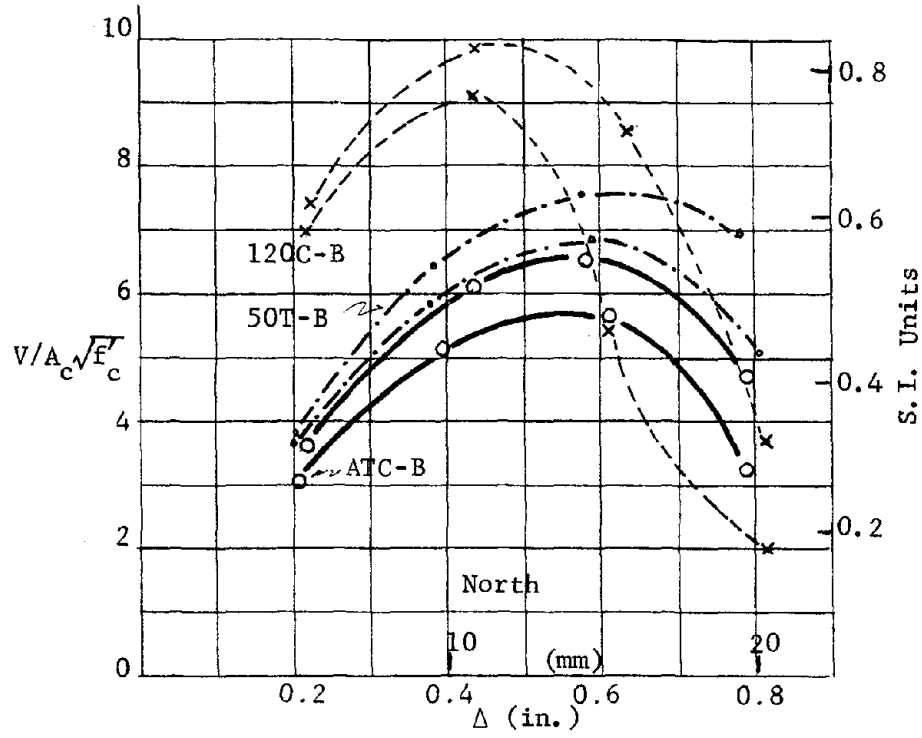


Fig. 7.8 Envelopes of load deflection, tests ATC-B, 50T-B, and 120C-B (NS direction)

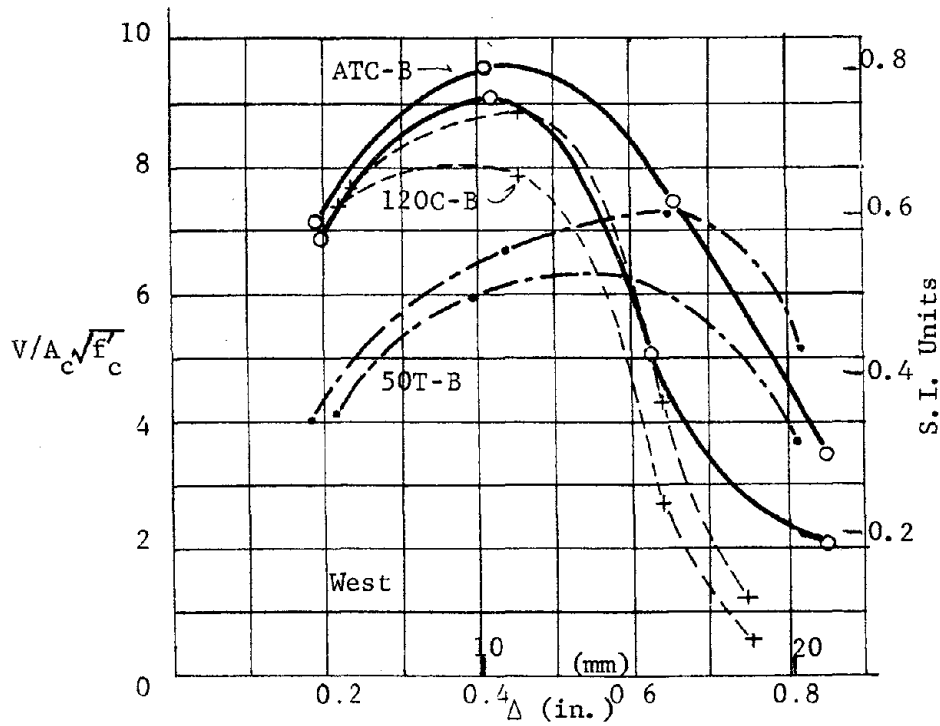
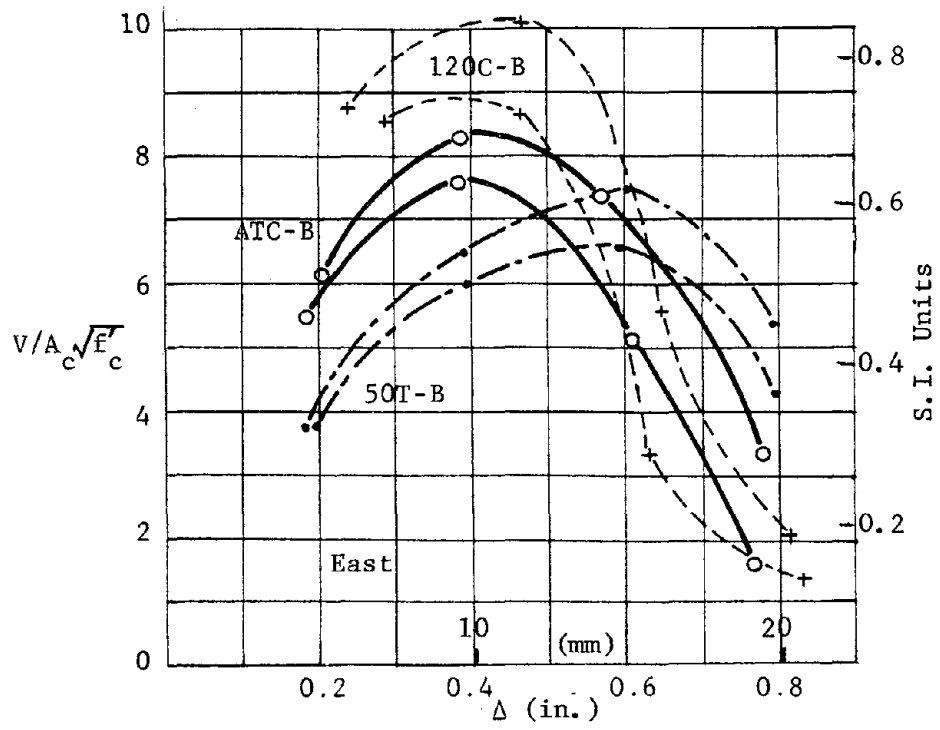


Fig. 7.9 Envelopes of load deflection, tests ATC-B, 50T-B, and 120C-B (EW direction)

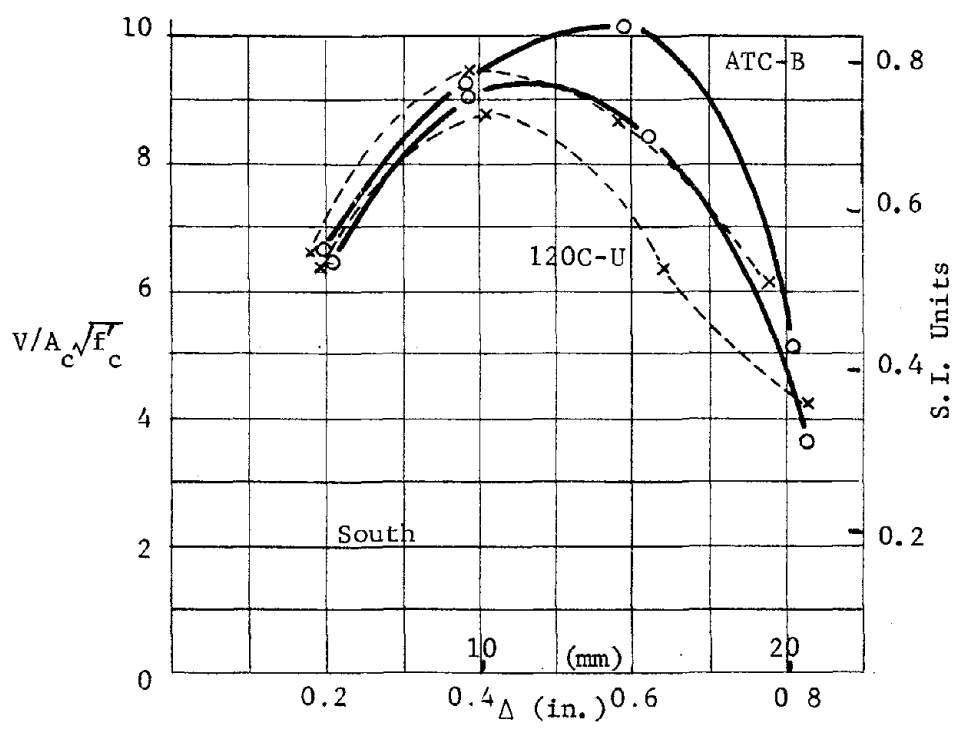
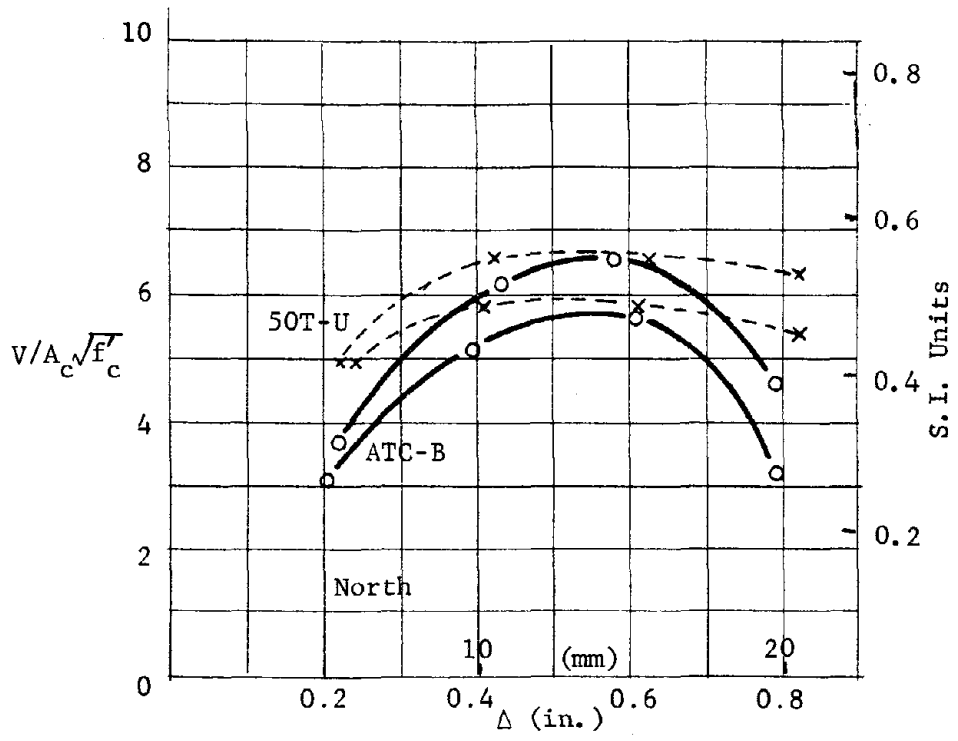


Fig. 7.10 Envelopes of load deflection, tests ATC-B, 50T-U, and 120C-U (NS direction)

peaks for 120C-U in the S direction. Thus, in this direction of loading the effect of alternate deformations is not noticeable.

Figure 7.11 shows envelopes of ATC-B in the EW direction compared with envelopes from test 120C-U (both constant compression). Envelopes to the west in ATC-B are similar to those in the south direction in 120C-U, except for high levels of deformation. Envelopes to the east in ATC-B are lower than envelopes to the north in 120C-U. Thus, ATC-B behaves as an individual unidirectional test in the NS direction and the effect of alternate deformations is not as noticeable as in test 120C-B.

7.4 Strain in Transverse Reinforcement

Figure 7.12 shows peak values of average strain in the ties for test ATC-U. Peaks of first and third cycles at each deflection level are shown. Figure 7.13 shows similar plots for the first cycle at each deflection level for both directions of loading on ATC-B. The strain in the ties increased at similar rates in tests ATC-U and 120C-U (Fig. 5.11), but strains remained below yield for larger deformations in ATC-U. From Fig. 7.12, it can be seen that after $2\Delta_1$ deformation not much increase in strain was observed. The distribution of strain in the ties in tests ATC-B (Fig. 7.13) and 120C-B (Fig. 5.13) were similar, especially for the Δ_1 and $2\Delta_1$ levels. However, strains tended to remain below yield for larger deformations in ATC-B, especially when compared to the NS direction of loading of both tests.

Figure 7.14 shows the change in strain with lateral history for two ties in ATC-U and 120C-U. Similar change is observed in both tests up to the $2\Delta_1$ level, but after $2\Delta_1$ strains in ATC-U remained near the yield level while strains in 120C-U reached yield at the $2\Delta_1$ level. Figure 7.15 shows progressive strain in a tie for both directions of loading of test ATC-B and 120C-B. Similar change in strain is observed for both directions. Again, the

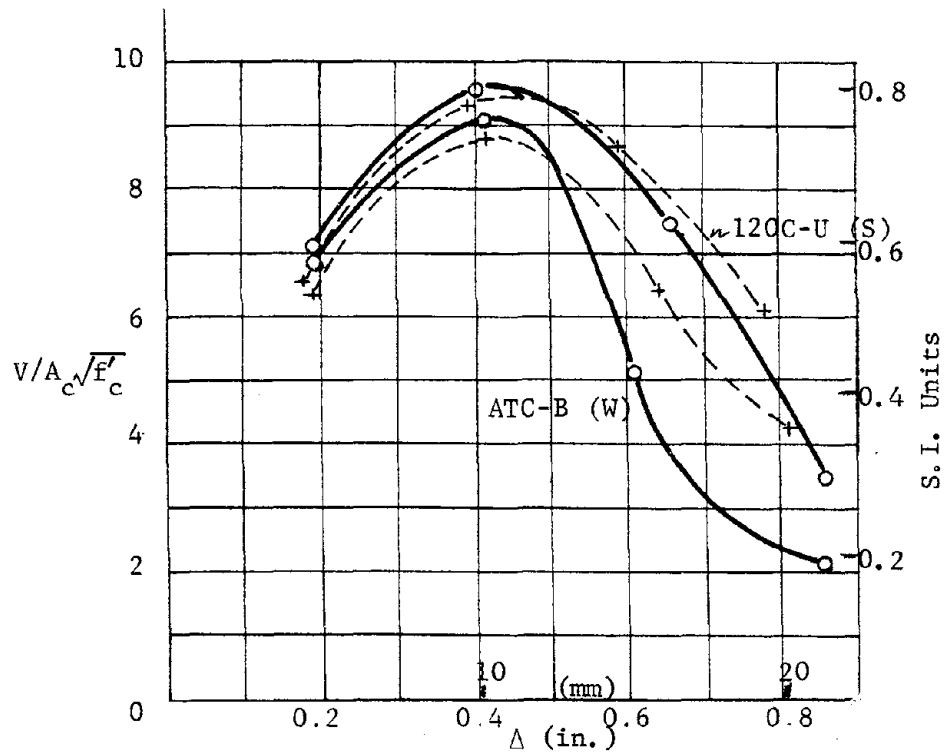
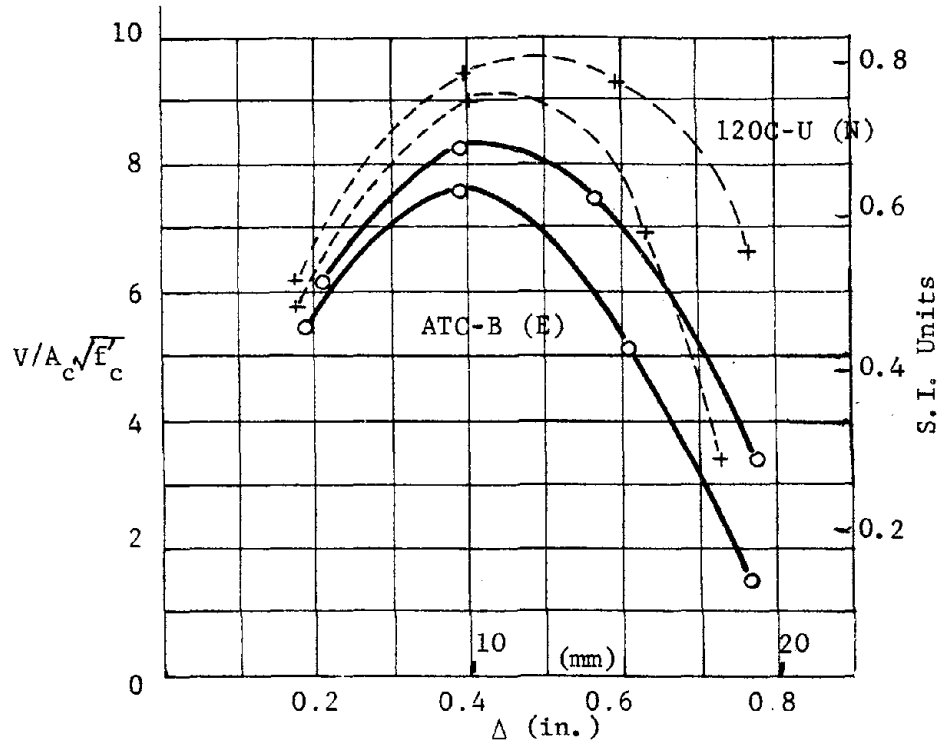
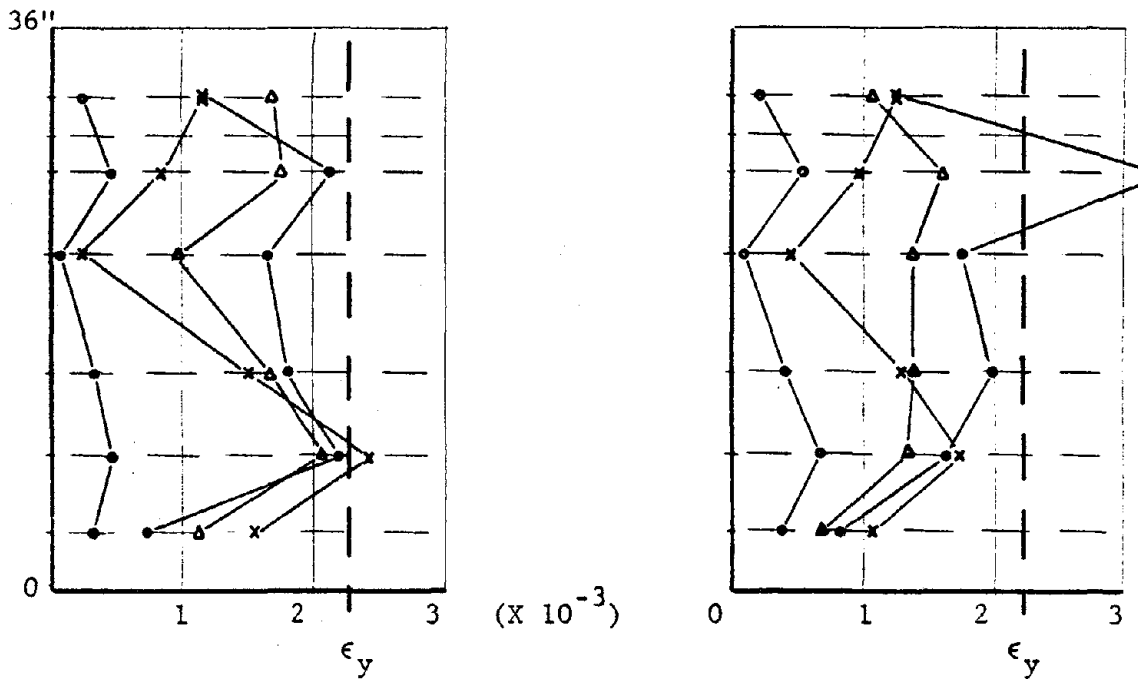
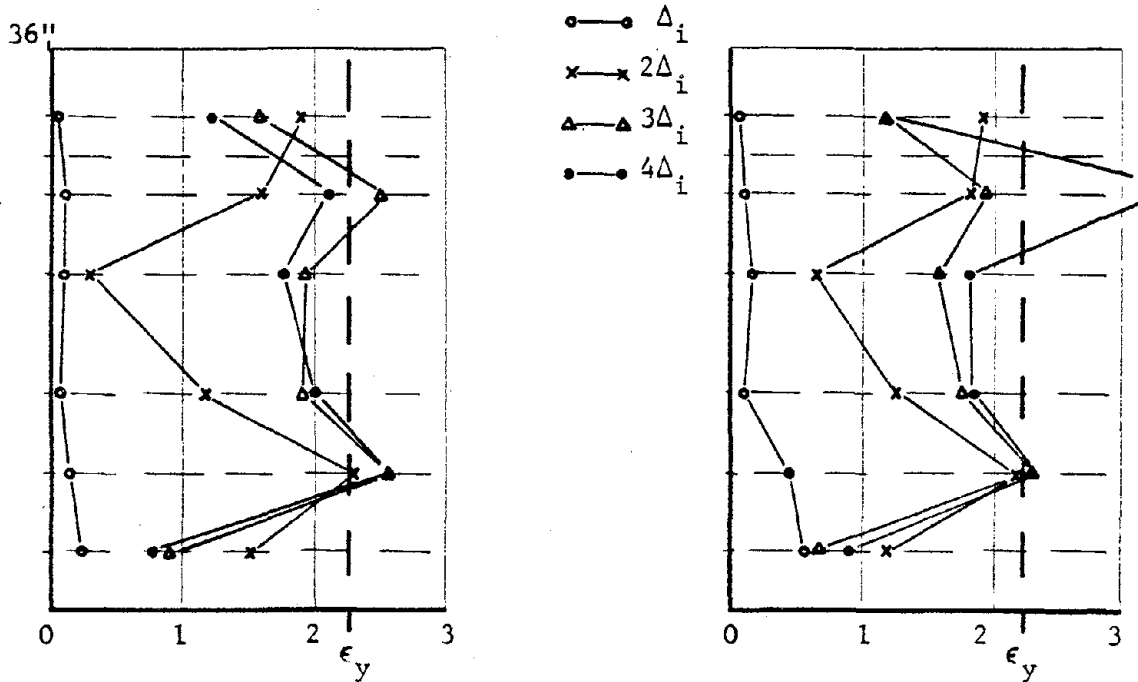


Fig. 7.11 Envelopes of load deflection, tests ATC-B and 120C-U



1st peaks 1st cycles
(North)

1st peaks 3rd cycles
(North)



2nd peaks 1st cycles
(South)

2nd peaks 3rd cycles
(South)

Fig. 7.12 Strain distribution in ties, ATC-U

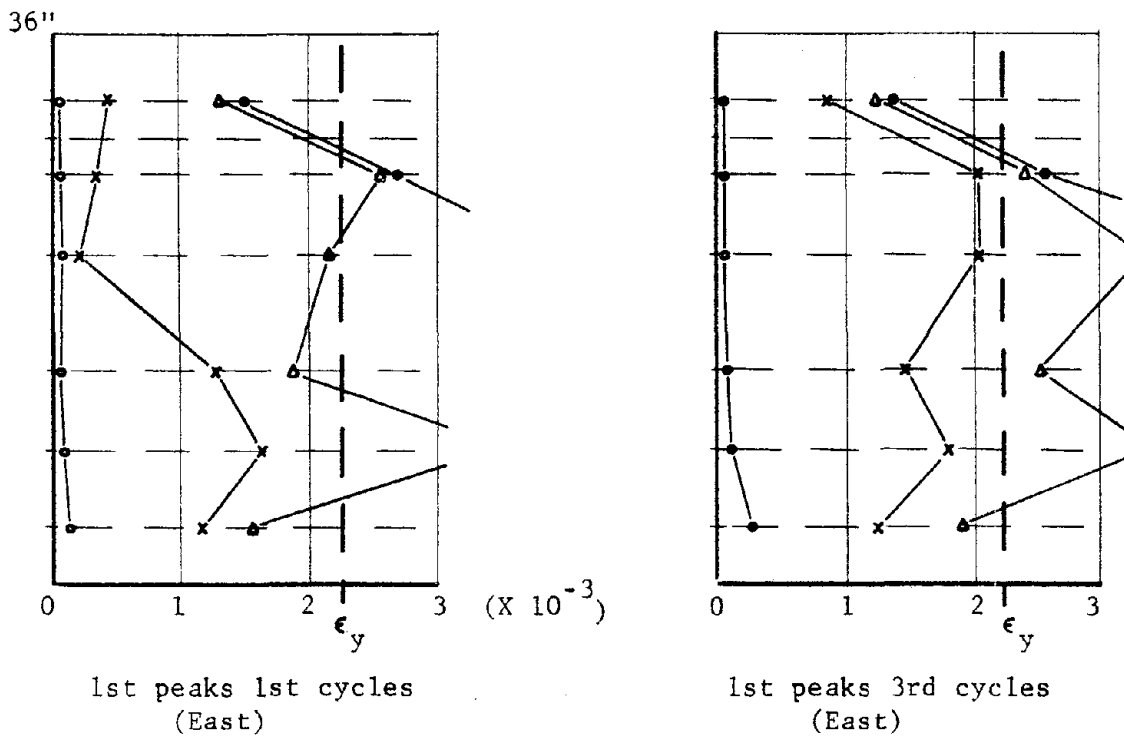
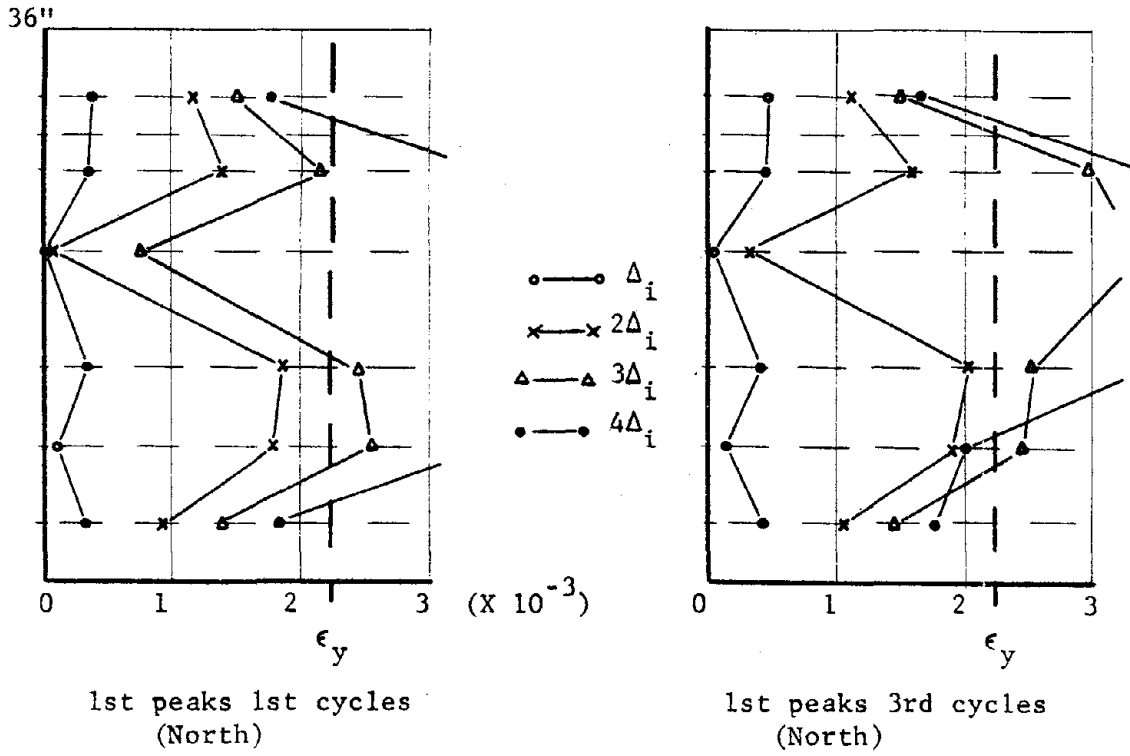


Fig. 7.13 Strain distribution in ties, ATC-B

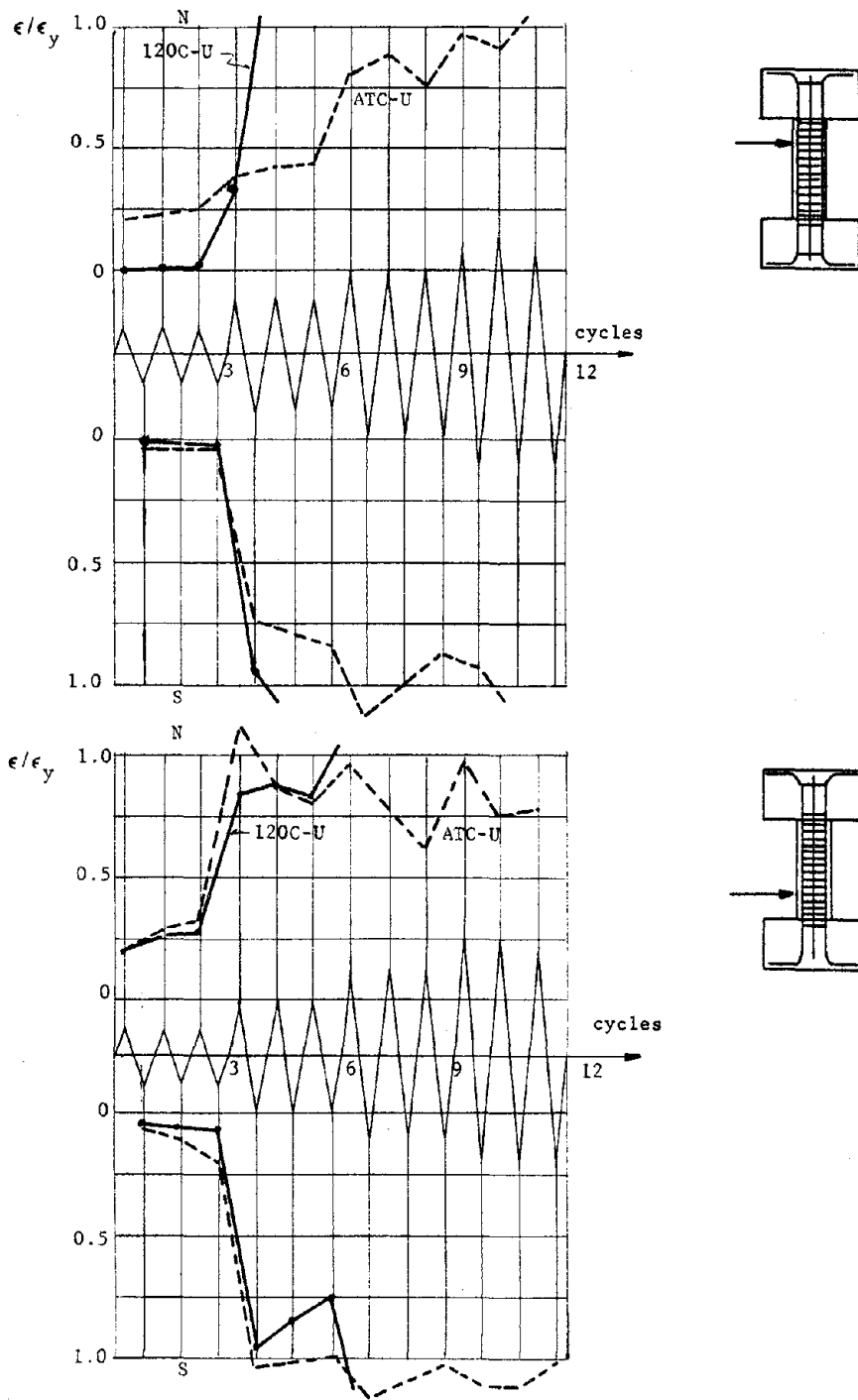


Fig. 7.14 Progressive strain in two ties, ATC-U and 120C-U

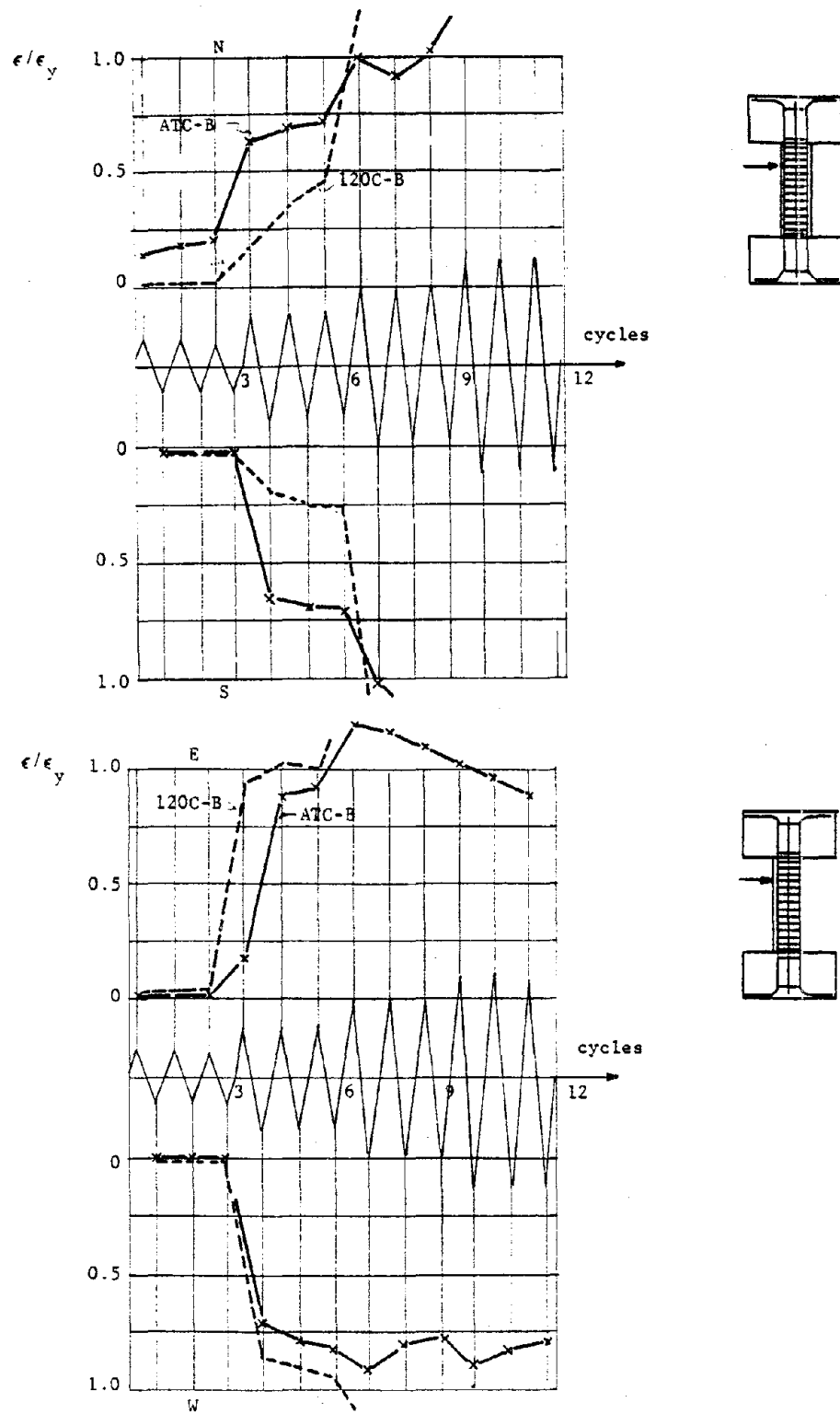


Fig. 7.15 Progressive strain in a tie, ATC-B and 120C-B

tendency of the strains to remain below yield under alternate application of axial loads is clear.

7.5 Commentary

In terms of shear deterioration and area within the load-deflection curves, the behavior of tests with alternate axial loads (ATC-U and ATC-B) was similar to that observed in tests with the same lateral deformation history and constant compression (120C-U and 120C-B). Shear deterioration for high levels of deformation was reduced in ATC-B as compared with 120C-B. In tests with constant tension, the reduction in shear decay observed with respect to tests with constant compression was attributed to less damage of the concrete core. According to the study of the strain distribution in tests ATC-U and ATC-B (Figs. 7.14 and 7.15), the beneficial aspects of tension are also observed when tension is applied alternately with compression.

The tendency of tensile axial forces to decrease shear decay may be explained using the idealization presented in Fig. 7.16. The portion of the concrete section resisting shear is smaller under tensile loads than under compressive loads. The reduction in area of contact between cracked sections in the concrete core reduced the shear strength and stiffness. The crack surfaces not in contact will likely not be damaged as severely. Because shear is low and confinement is not needed, the ties will remain in condition to provide confinement at high levels of deformation. In addition, the concrete core will have some reserve (undamaged surface area) capacity to resist shear in subsequent loadings.

External evidence of less damage in the concrete core in tests ATC-U and ATC-B, as compared with tests 120C-U and 120C-B, can be observed in Figs. 7.17 and 7.18 showing photographs of the specimens after testing.

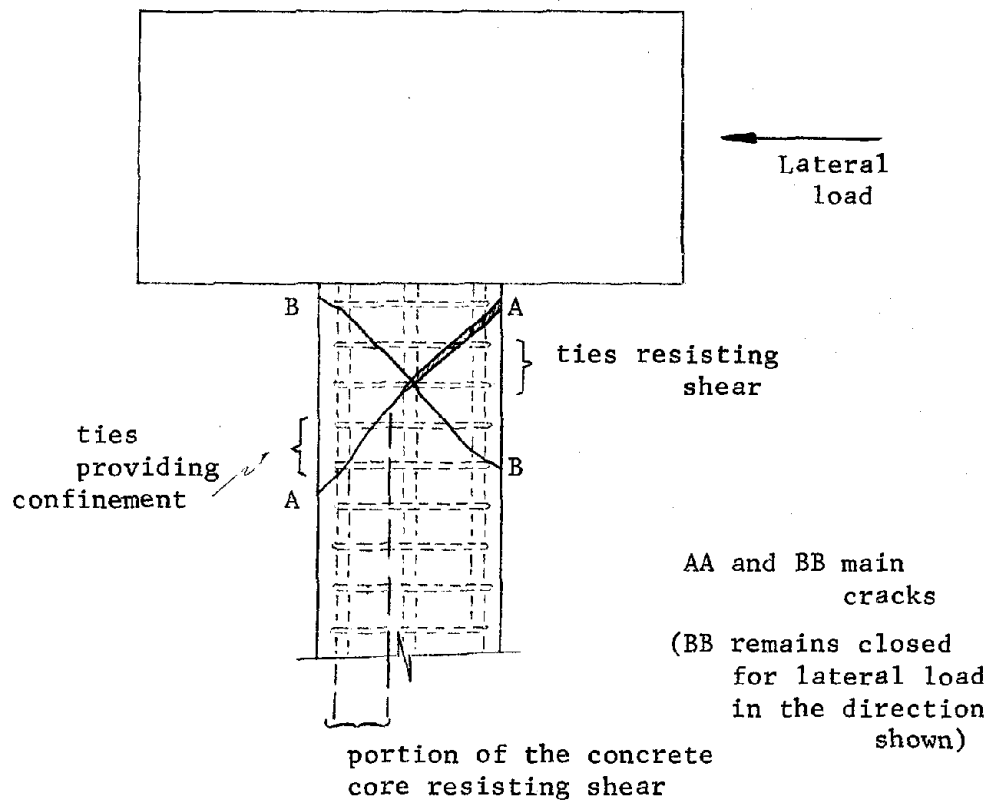
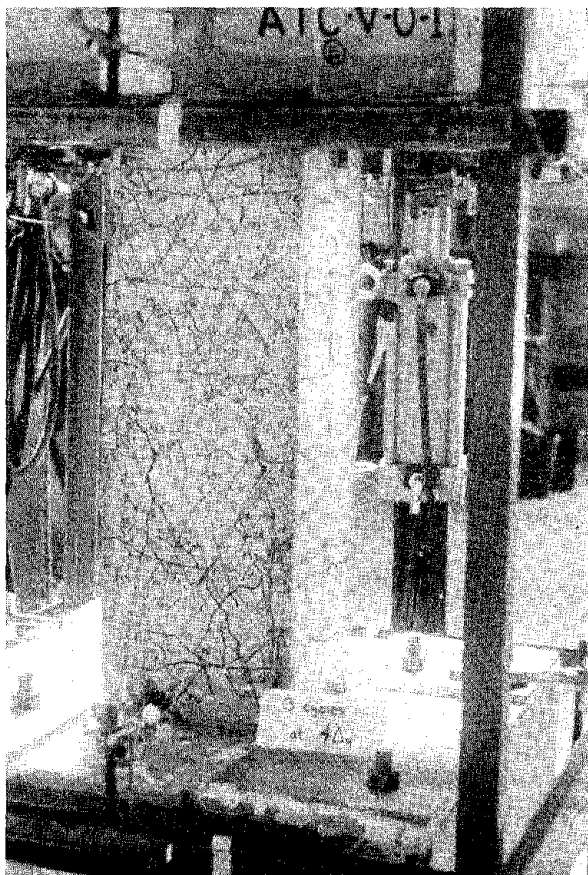
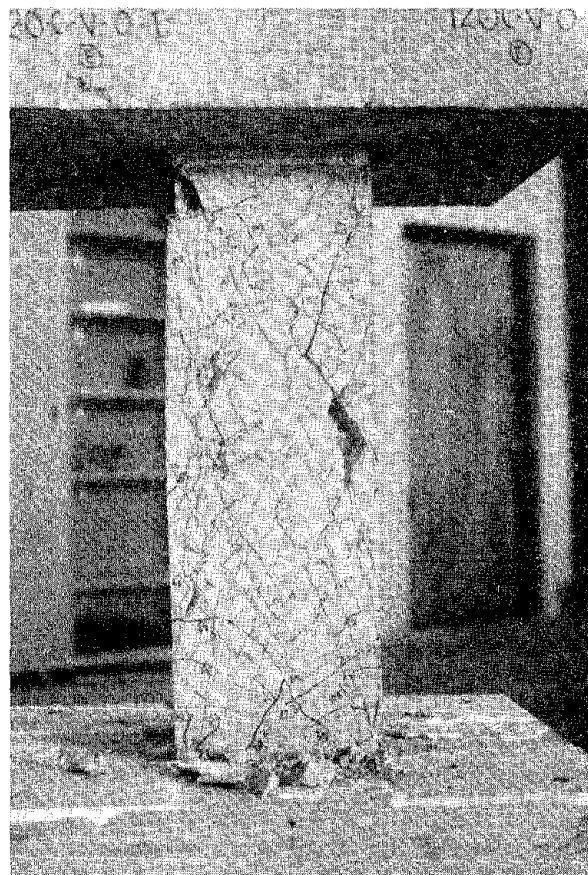


Fig. 7.16 Idealization of inclined cracks

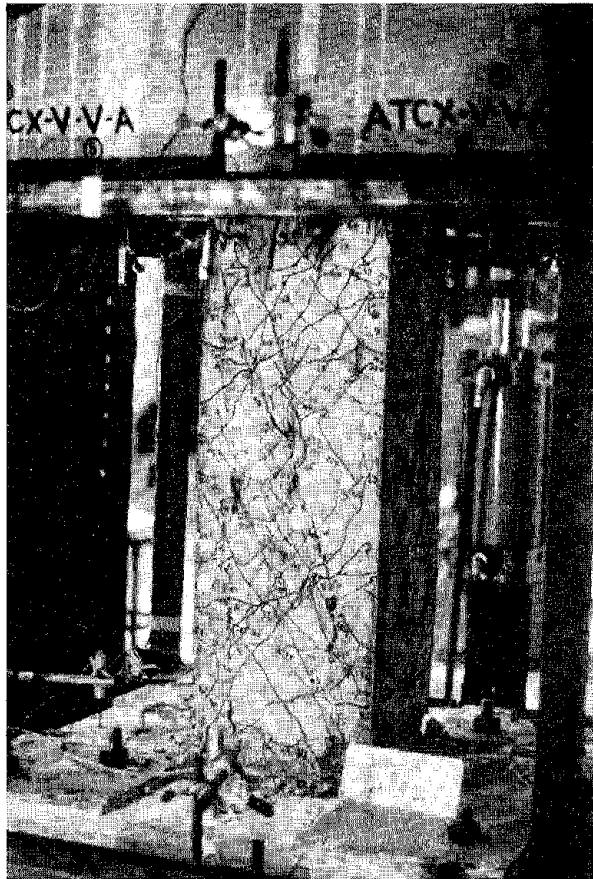


ATC-U

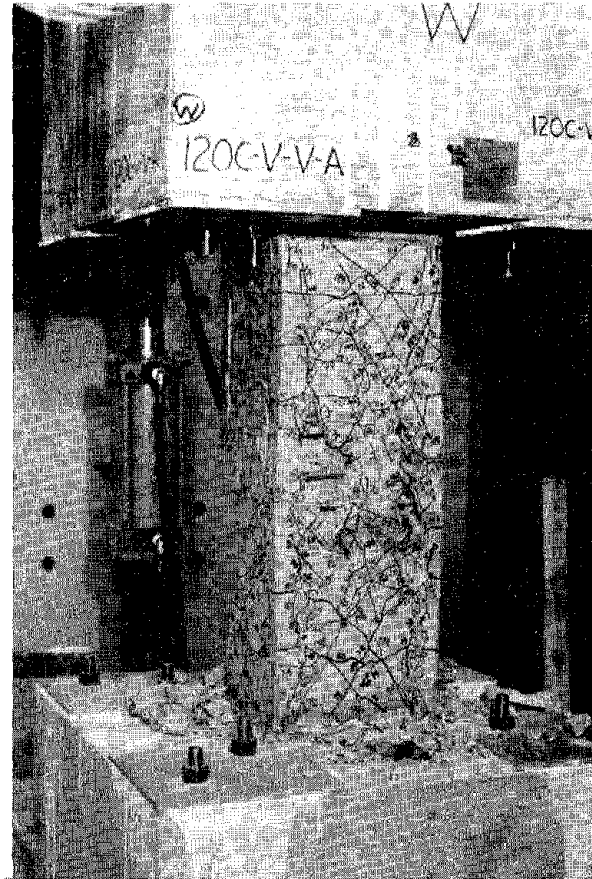


120C-U

Fig. 7.17 Appearance of Specimens ATC-U and 120C-U after testing



ATC-B



120C-B

Fig. 7.18 Appearance of Specimens ATC-B and 120C-B after testing

124

124

C H A P T E R 8

A DESIGN APPROACH FOR COLUMNS WITH DIFFERENT LEVELS OF AXIAL LOAD

8.1 Introduction

In this chapter a design approach is formulated based on the observed behavior from tests described herein and the results from other analytical and experimental studies. The data from this study refer to one element with constant geometry and reinforcement. Only one level of compression and three levels of tension were considered for two lateral deflection histories. The limited data preclude the development of design recommendations which can be considered inclusive of all types of members. The intention was to develop a frame of reference for the design of columns failing in shear which can be improved when more data become available.

One of the main considerations in the development of a design approach was to incorporate available knowledge regarding members failing in flexure and to extend that knowledge to members failing in shear. It was also desired to incorporate the level of axial force in the design recommendations.

Because of the low energy dissipating capacity of short columns observed in this experimental study as well as in other experimental studies [29,36,37], the use of such elements must be avoided where possible in seismic regions. The design approach discussed here is intended primarily for cases where the length-to-thickness ratio cannot be changed to ensure flexural failure. It may be useful also for short columns in which deformation capacity is required or desired (zones with moderate or low seismic risk).

The proposed design approach is developed primarily for short columns subjected to cyclic loads in one direction and constant levels of axial, tensile, or compressive forces. A discussion is included for adapting the design approach to alternating axial loads. Implications of bidirectional lateral loads are also discussed.

8.2 Basic Requirements for Columns with Constant Compression

Based on the observed behavior, the design of short columns subjected to cyclic deformations beyond yielding may not be adequate in terms of strength only. The column specimens tested exhibited low energy dissipating capacity.. Noticeable shear deterioration was observed when axial compression was imposed.

The deformability characteristics must also be taken into account. Ductility ratios as well as design recommendations are generally based on Δ_y , the deformation at first yield, which is based on flexural computations. In short columns, the deflection calculated at first yield may not have meaning for columns failing in bending. Moreover, the quantity of web reinforcement influences the hysteretic behavior of short columns. As more confinement is provided, flexural behavior is expected to be dominant and as a result the specimen dissipates more energy and exhibits ductile behavior.

In accordance with the observed behavior, a design criterion for short columns subjected to lateral deformations and compressive axial loads must include the following variables: lateral displacement history, axial load level, shear span ratio, and quantity of reinforcement--both longitudinal and transverse. The influence of the lateral displacement history (unidirectional vs bidirectional) and level of axial load (zero vs 120k) has been studied in this investigation. The effect of the other variables has been reported

elsewhere [30,31]. It would be desirable to base shear requirements for short columns subjected to load reversals on a criterion which permits a certain level of shear decay for a given number of load reversals in accordance with the level of energy absorption needed.

Gosain, Brown, and Jirsa [32] proposed a criterion in which an element must be capable of withstanding at least five cycles at a deformation level of 4 to $6\Delta_y$ without a decrease in the strength of more than 25 percent. This criterion was based on a work index which was a measure of the energy dissipation and with the primary assumption that the element is capable of forming hinging regions maintaining both flexural and shear capacity. The work index was defined as $I_w = n(\Delta/\Delta_y)$, where n is the number of cycles at a deflection level Δ , in which the load P is at least equal to or greater than $0.75P_y$. This parameter was modified to account for different span lengths and axial loads, as follows:

$$I'_w = I_w(1 - d_c/a)(1 + 0.0005 N/A_c) \quad (8.1)$$

Based on reported experimental data and assuming values of I'_w of 10 to 50 for satisfactory performance, they concluded that the ultimate shear stress in the core must be limited to 6 to $7\sqrt{f'_c}$ and that the transverse reinforcement should be designed to carry a shear not less than the maximum shear imposed on the section.

In short columns failing in shear, however, it is difficult to establish a criterion of this type because the formation of hinging regions is not ensured and as a consequence Δ_y and P_y are not well defined. In this case, Δ_y and P_y depend not only on section parameters and axial load, but on ρ_w and a/d as well. The hysteric behavior will be different from that in an element forming hinging regions. Figure 8.1 shows cycles at 2 and $3\Delta_i$ from test 120C-U compared with the hypothetical behavior of a similar element governed by flexure [33] (confined core). Point B represents the

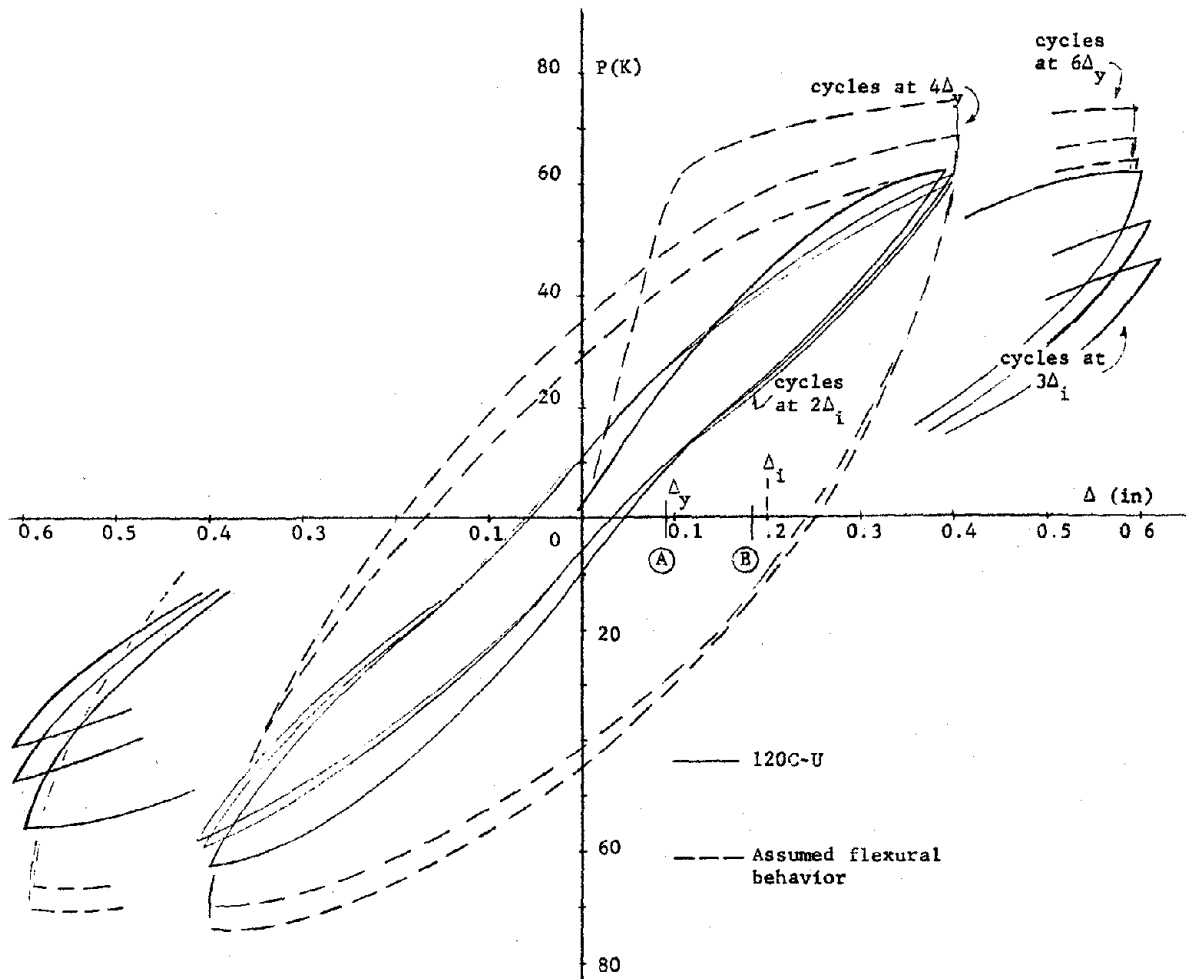


Fig. 8.1 Shear behavior vs flexural behavior

observed deflection at first yield of the main steel for 120C-U and Point A the computed yield deflection assuming flexural behavior. Point B does not represent plastic hinge formation as does A in the assumed flexural case. The lateral load increases after reaching first yield, but deteriorates very rapidly due to shear decay. The strength is maintained through large deformation when flexure governs. Assuming that the flexural behavior shown in Eq. 8.1 is representative, the energy dissipated per cycle is lower in the case governed by shear compared with the case governed by flexure.

If the ductility factor of an element failing in shear is estimated using Δ_y (assuming flexure controls), it will not represent the same area under the load-deflection curve as for an element forming plastic hinges because the load at any level of deformation may be below that defined as P_y in flexure. The factor $(1 - d_c/a)$ in the work index, I'_w , may not be sufficient to account for reduced energy dissipation in very short columns and more conservative considerations may be needed.

8.3 A Proposed Design Criterion

Reinforced concrete columns forming part of a structural frame must meet a number of limitations to ensure satisfactory performance under cyclic loads. The limitations for flexural hinging regions failing in shear are summarized in Ref. 32 and are based on reported experimental and analytical work. The limitations can be stated as follows:

- The ultimate shear stress must be limited to 6 to 7 $\sqrt{f'_c}$.
- The transverse reinforcement must be designed to carry a shear not less than the maximum shear imposed on the section.
- Shear is resisted by the core only.

- Spacing of transverse reinforcement must be limited to six longitudinal bar diameters, in order to prevent buckling of the main steel.
- The average compressive stress on the core area should not exceed 1500 psi. (No data are available for specimens with more than 1500 psi in compression.)

In short columns, the requirements for transverse reinforcement may need to be increased and the strength provided may not always be utilized if large deformations are imposed and shear decay is likely.

Identification of Shear-controlled Behavior. To propose specific design recommendations for short columns consistent with the observed behavior, a means of identifying shear behavior is first required. For this purpose, a critical shear-span ratio, defined by Yamada [29], was obtained by equalizing flexural and shear strengths, and assuming that the shear failure was governed by an elliptical failure criterion of the concrete under combined normal and tangential stresses. The expression for the critical shear-span ratio accounts for level of compressive axial load, longitudinal reinforcement and material properties. Good correlation was found with experimental work related to short columns with a/d ratios near one. With an a/d ratio of about two for the tests in this program, the behavior could no longer be predicted satisfactorily using the elliptical failure criterion for the concrete.

Instead of using the critical shear-span ratio, a parameter $L_f = 2M_n/V_n$ will be introduced in this study. The nominal flexural strength M_n can be obtained from interaction diagrams or tables ($\phi = 1$) and the nominal shear strength V_n is computed as $V_s + V_c$ in accordance with the ACI Code. The interpretation of L_f is the length of a fixed end column with given cross section required to reach both flexural and shear strengths at the same time under

monotonic load. With a length of L_f , an element will be able to form a plastic hinge under monotonic load and using the limitations mentioned above the column should perform satisfactorily under cyclic loads (Fig. 8.1).

The computation of L_f provides a reference for defining the likely mode of failure. There is likely to be a transition zone from shear to flexural behavior due to the contribution of transverse reinforcement to the shear strength. The contribution of the transverse reinforcement is likely to vary with the arrangement of the transverse and longitudinal reinforcement, column geometry, axial load, and material properties. Therefore, a performance criterion for cyclic behavior must be based on a reference which is not rigidly defined. Another consideration is that L_f should be computed using routine design equations for shear and flexural capacity. In this regard, M_n is a function of axial load and longitudinal steel; V_c is a function of axial load and V_s is a function of the transverse steel.

If the length of a column is equal to or greater than L_f , the design proceeds with a criterion which ensures flexural behavior (sufficient transverse reinforcement to ensure formation of plastic hinges), as in Ref. 32. If the length of a column is less than L_f , shear failure is anticipated. In this case it is proposed that the transverse steel designed using Eq. (11.17) of the ACI Code for the maximum shear imposed be increased by the ratio L_f/L in order to provide deformation capacity. Therefore, the shorter the column the more transverse reinforcement will be required without any increase in strength.

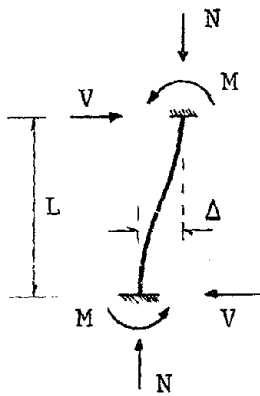
The transverse reinforcement can be computed using Eq. (11.17) of the ACI Code which is based on the truss analogy. In the truss analogy the transverse steel is required to resist diagonal tension across inclined cracks. For cyclic load reversals, the transverse

steel may be required to provide a certain amount of deformation capacity. In this context, it is recognized that the confinement must be dictated by considerations of the amount, strength, and arrangement of both transverse and longitudinal steel, because both contain the core and provide confinement to maintain the integrity of the core under large deformations. Thus, it is anticipated that a more complex expression may be required for the general case as more data become available.

Design Options. To take into account the observed behavior of short columns ($L < L_f$)--mainly the shear decay after reaching a certain deformation level and the low energy dissipated per cycle--an additional adjustment in the shear strength may be required. Two basic approaches may alleviate the problems which occur in design. The designer could

- (a) Limit the deflections to avoid shear decay and design the section for the total shear. By limiting the deflections, less energy will be dissipated than in a column failing in flexure. The deflection at maximum load considering monotonically increasing lateral load may be used as the value of the deflection limit in this case.
- (b) If the deflections are not limited, the usable shear strength may have to be adjusted downward. For example, if large axial loads are present, shear decay is accelerated and a reduction in shear capacity is required. As the ratio of shear strength to shear required for the formation of hinges at the ends of the column falls below unity, shear failure is more likely and the shear strength will need to be reduced.

In accordance with these considerations, the flow chart in Fig. 8.2 represents a general approach that may be followed in designing a fixed end column under cyclic loadings. In the case



LIMITATIONS

$$V_u \leq 6 \sqrt{f'_c} A_c$$

$$V_s = V_u$$

$$s \leq 6d_b$$

$$N/A_c = 1500 \text{ psi}$$

$$L_f = \frac{2M_n}{V_n}$$

M_n - from interaction diagram, $\phi = 1$

$$V_n = V_s + 2 \left[1 + \frac{N_u}{2000A_c} \right] \sqrt{f'_c} A_c$$

$L < L_f$

Shear behavior

Transverse reinforcement to provide deformation capacity

$$A_v = \frac{V_s (L_f/L) s}{d_c f_{sy}}$$

or

$$\rho_w = \frac{V_s (L_f/L)}{f_{sy} A_c}$$

II. Deflections not limited

Reduce shear strength, as

$$V_u (L/L_f) (1 - N/N_o)$$

$$N_o = 0.85 f'_c A_c + A_s f_{sy}$$

$L \geq L_f$

Flexural behavior

Provide transverse reinforcement to ensure formation of plastic hinges but not less than required to carry V_u

I. Limitation in deflections or reduction in the ductility factor

shear strength V_u

Fig. 8.2 Design of R/C columns under cyclic loads

of flexural behavior no further details are given and the criteria from Ref. 32 are proposed. When the lateral forces for design are not reduced for ductility as in a ductile frame (alternative I), the strength of the column may be taken as V_u and the deformation limited to that occurring when the maximum capacity of the column is reached. It is assumed that the column can withstand several cycles of load reversal provided that the deflection is less than that occurring at maximum capacity under monotonic load. A general method for computing such deflections is not available. Ductility factors may be used instead. If lateral forces are computed with reduction for ductility [34], the reduction may be a function of the number and distribution of the short columns in the structure. A similar approach is the use of K-factors as defined in the SEAOC Code [35]. For instance, if short columns are used as components of a ductile moment-resisting space frame but column behavior or failure do not impair the vertical or lateral load-resisting ability of the entire frame, then K may be taken as 0.80. In a frame without rigid elements, i.e., short columns, K may be taken as 0.67 and in a building with shear walls, $K = 1.33$.

Deflection Limits. It may be possible to utilize experimental data to obtain a limit for the lateral deflection to be used in alternative I. Figure 8.3 shows a deflection index, $\Delta d/L^2$, plotted against axial stress on the section for selected data on cyclic loads on short columns [29,36,37], in which specimens with varying values of ρ_w were tested. The parameter $\Delta d/L^2$ was obtained from the relative story displacement angle $R = \Delta/L$, where Δ is the deformation at which shear decay is first observed and L is the story height and the shear span-to-depth ratio a/d , with a expressed as function of the member length L. The deflection index is $\frac{\Delta/a}{L/d}$. The combination of Δ/L and a/d accounts for column section and story height variations. From Fig. 8.3 a limit to the deflection for different percentages of transverse reinforcement ρ_w may be stated as follows:

Ref. No.

- △ 29
- 36
- 37
- 00-U, 120C-U

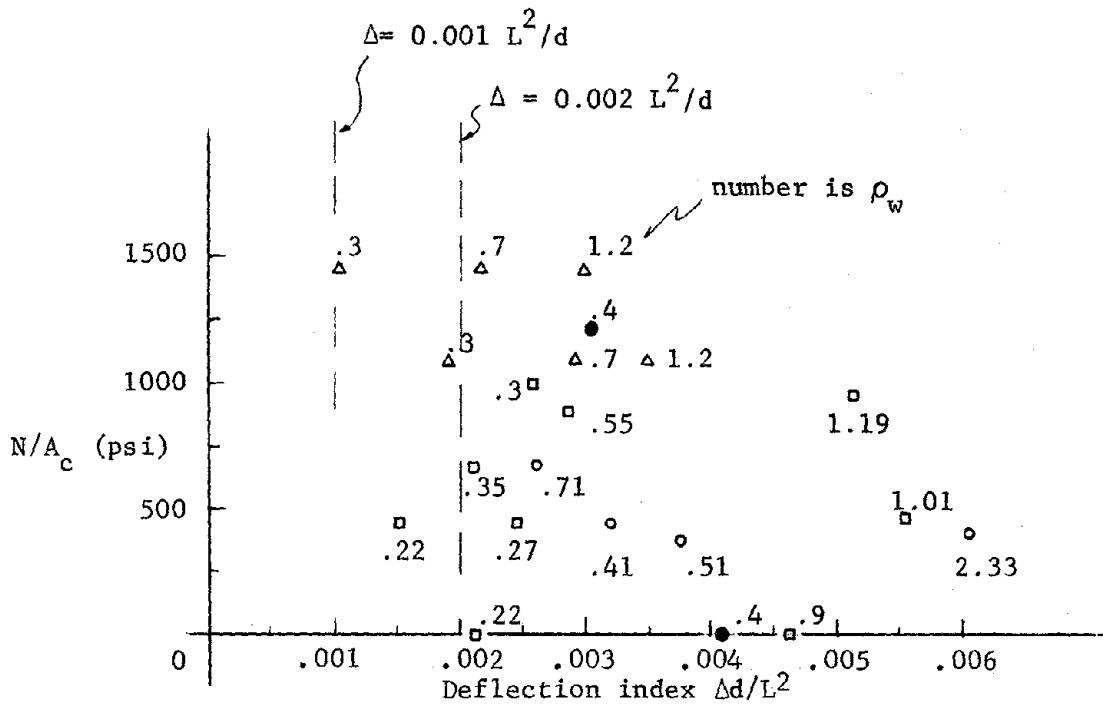


Fig. 8.3 Lateral deflection limit

$$\Delta = 0.002 L^2/d ; \rho_w \geq 0.7\%$$

$$\Delta = 0.001 L^2/d ; 0.3\% < \rho_w < 0.7\%$$

The limit appears to also be influenced by the axial load; however, there is considerable scatter in the data and an insufficient number of tests is available to define this relationship.

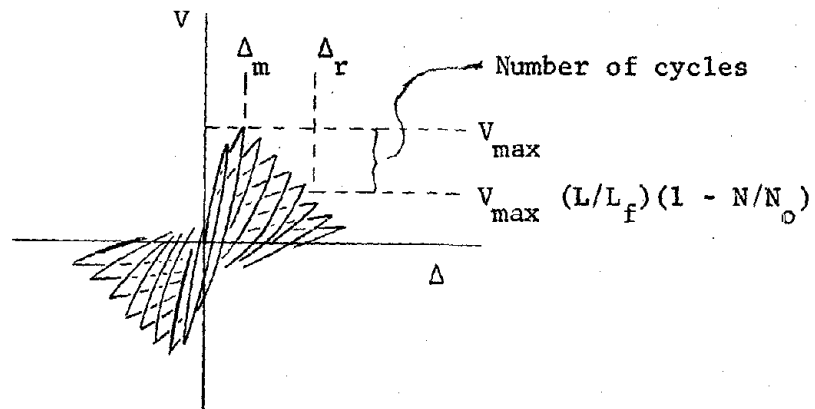
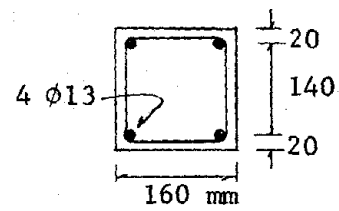
In alternative II, the short column is used as a component of a ductile frame. The reduction in strength is formed by two terms. The first term L/L_f accounts for the length of the element, the shorter the column the more shear decay is expected. The second term, $1 - N/N_o$, accounts for the axial load level which tends to increase the shear decay at large deflections.

Table 8.1 shows values of the proposed reduction $L/L_f(1 - N/N_o)$ for a series of tests reported by Yamada [29]. The tests were conducted for cyclic loads under increasing lateral deformation on columns with $a/d = 1.2$. Two different levels of axial load for two percentages of transverse reinforcement were considered. Applying the reduction to the maximum shear observed, values of the ratio of the deflection at the reduced shear to deflection at maximum shear (Δ_r/Δ_m) and the number of cycles imposed from maximum to reduced shear were determined from the test data and are included in Table 8.1. A sketch is included showing the definition of Δ_r, Δ_m , and number of cycles.

At least four cycles were imposed beyond the cycle in which maximum shear was observed before the reduced shear was reached. The deflection at the reduced shear was at least two times the deflection at maximum observed shear. Thus, the reduction factor seems to be satisfactory for estimating the shear which can be relied on during cyclic loading. The proposed design criterion (Fig. 8.2) is considered to be conservative because the reduction is applied to the design ultimate shear which is based on $6 \sqrt{f'_c} A_c$ and not to the

TABLE 8.1 DATA FROM REF. 29

Test	ρ_w (%)	L/L_f	$1 - N/N_o$	Δ_r/Δ_m	No. of Cycles
1/6 N_o e1	1.18	0.60	0.83	5	11
1/6 N_o e2	0.71	0.48	0.83	3	8
1/3 N_o e1	1.18	0.62	0.67	2	6
1/3 N_o e2	0.71	0.48	0.67	2	4



maximum measured shear which was at least $11 \sqrt{f'_c} A_c$ in the four tests listed in Table 8.1.

8.4 Bidirectional Effects

If deformations in both principal directions are considered, the design approach may need to be modified. In this study bidirectional alternate lateral deformations in orthogonal directions were considered. From the data, the effect of bidirectional loading was reflected as more rapid shear decay at higher deformations. For this reason it appears that the criteria must be modified if the element is to form a part of a ductile frame. Two possibilities may be adequate in that case:

- (a) Multiply ρ_w by a factor greater than one, no increase in usable shear strength.
- (b) Multiply the usable shear strength by a factor less than one without increasing ρ_w .

It should be noted that the data are for the case of deflections applied in orthogonal directions alternately and other load histories were not considered in the experimental program. Thus, there was not enough data to evaluate a factor which takes into account bidirectional lateral movements.

8.5 Evaluation of the Design Approach

In order to compare the transverse reinforcement provided in the test specimen to that computed using the proposed criterion, Specimens 120C-U and 00-U were analyzed.

120C-U. Figure 8.4 shows calculations for Specimen 120C-U presented in the same sequence as shown in the flow chart in Fig. 8.2. From Fig. 4.6, $M_n = 1380$ in.-k. Assuming a maximum shear capacity of $V_u = 6\sqrt{f'_c} A_c = 40k$, $V_n = 61.4k$, and $L_f = 45$ in., which is greater than the actual length of 36 in. Thus, shear failure is anticipated

$$\underline{V_u = 6 \sqrt{f'_c} A_c = 40 \text{ K}}$$

$$V_s = 40 \text{ K}$$

$$s_{\max} = 6d_b = 4.5 \text{ in}$$

$$\underline{N/A_c = 1200 \text{ psi} < 1500 \text{ psi}}$$

$$L = 36 \text{ in}$$

$$f'_c = 4.45 \text{ Ksi}$$

$$f_y = 65.2 \text{ Ksi}$$

$$f_{sy} = 67.5 \text{ Ksi}$$

$$M_n = 1380 \text{ in-K} \quad \text{from Fig. 5.6}$$

$$V_n = V_s + 2(1 + N_u/2000A_c) \sqrt{f'_c} A_c = 6\sqrt{f'_c} A_c + 3.2\sqrt{f'_c} A_c$$

$$= 61.4 \text{ K}$$

$$L_f = \frac{2M_n}{V_n} = \frac{2(1380)}{61.4} = 45 \text{ in}$$

$$\underline{L = 36 \text{ in} < 45 \text{ in}}$$

Shear failure

$$\rho_w = \frac{V_s (L_f/L)}{f_{sy} A_c} = \frac{40 \frac{45}{36}}{67.5(100)}$$

$$\underline{\rho_w = 0.0074}$$

II

$$N_o = 0.85 f'_c A_c + A_s f_y = 608 \text{ K}$$

$$(L/L_f) (1 - N/N_o) = (36/45) (1 - 120/608) = 0.64$$

$$\text{reduced strength} \quad 40(0.64) = 26 \text{ K}$$

I Deflection limited
to
 $0.002 L^2/d = 0.25 \text{ in}$
shear strength = 40 K

Fig. 8.4 Example of calculations, redesign of 120C-U

and the transverse steel required to ensure satisfactory behavior under load reversals should be not less than 0.74 percent, which is about twice the transverse reinforcement provided (0.39 percent).

If the deflection is limited (0.25 in. with $0.002 L^2/d$) the strength may be taken as 40k, otherwise the permissible shear for a ductile frame is 26k. It should be noted that for 120C-U, if the same amount of transverse reinforcement had been provided but no axial load was compared, the specimen would likely be governed by flexure and the assumed strength over 60 percent greater.

00-U. From Fig. 4.5, M_n is 900k, $V_n = 57k$, and $L_f = 32$ in., which is less than the column length of 36 in. Therefore, flexural behavior is anticipated. With the shear capacity $V_u = 6\sqrt{f'_c} A_c = 42k$, the percentage of transverse reinforcement to carry the total shear is 0.63 percent and that required to form plastic hinges at the ends is 0.74 percent. In this case the transverse reinforcement is controlled by the requirement that plastic hinges form at the ends and the shear strength can be taken as 42k.

The calculations indicate that if the specimen had twice the transverse reinforcement provided, its ductility would be comparable to that of a longer element. This is in accordance with the observed behavior of Specimen 00-U, in which the flexural strength was reached but was not stable. With $\rho_w = 0.74$ percent, the strength is assumed to be stabilized.

To illustrate further the proposed criterion, two extreme cases are considered: a long column and a very short column. Material properties, section dimensions, longitudinal steel, and axial load are assumed to be as in 120C-U.

- (a) Long column - assume $L = 112$ in. for $a/d_c = 5.6$:
 For $V_u = 6\sqrt{f'_c} A_c = 40k$, $V_n = 61k$ and $L_f = 45$ in.
 Flexural behavior controls and the percentage of transverse reinforcement required is 0.59 percent to

carry the total shear (0.37 percent is required for plastic hinge formation but without consideration of cyclic reversals or deflection limits).

Thus, for long columns the transverse steel will be greater than required for the formation of plastic hinges but may be less than required in ACI Code Appendix A for confinement of the core in many cases.

(b) Very Short Column - assume $L = 24$ in. for $a/d_c = 1.2$:

For $6\sqrt{f'_c} A_c = 40k$, $V_n = 61k$, and $L_f = 45$ in. Shear behavior controls and the percentage of transverse reinforcement required is 1.11 percent.

Yamada [29], studying columns with $a/d = 1.2$, concluded that in order to attain a good behavior under cyclic loading, ρ_w must be greater than 1 percent, which compares favorably to the approach in Fig. 8.2.

For the short column, the permissible strength is 17 kips if no limitation in deflection is considered. If the strength of the element is reduced for design purposes, the designer will tend to search for more economical solutions. This reflects current practice in which the use of very short columns in seismic regions is avoided where possible.

8.6 Columns with Constant Axial Tension

The observed behavior under axial tension was controlled by flexural behavior where plastic hinges form (the moment resisted by the hinge is reduced for the effects of tension). The criterion utilized for axial compression (Fig. 8.2) can be applied to axial tension. It can be used to define L_f if nominal values of moment and shear are adjusted for axial tensile stress. The low values of M_n after reduction for tension would indicate that the columns should be as controlled by flexural as observed. However, for high levels of tension on short columns, the assumption of hinging at

the ends may result in shear values which are unrealistically high. In those cases, the shear strength should be reduced according to the level of axial tension applied. For very short columns with moderate axial tension, shear failure would be expected and a reduction in the shear strength for the effects of tension must be made.

To determine shear reduction in the presence of tension, the following procedure was used:

- (a) Using an existing program for multivariate regression analysis, a curve was obtained to represent the ratio of peak shear for each of the levels of tension considered to peak shear for 00-U (S_R). This ratio was used to calibrate the reduction in shear due to tension. The result was:

$$S_R = 0.98 - 0.70 \frac{T}{T_y} + 0.222 \frac{T}{T_y} \left(\frac{\Delta}{\Delta_i}\right)^2 - 0.092 \left(\frac{T}{T_y}\right)^2 \frac{\Delta}{\Delta_i}$$

- (b) The deflection level at which the maximum reduction is reached was obtained by taking

$$\frac{\partial S_R}{\partial \left(\frac{\Delta}{\Delta_i}\right)} = 0 \Rightarrow 0.044 \frac{T}{T_y} \frac{\Delta}{\Delta_i} - 0.092 \left(\frac{T}{T_y}\right)^2 = 0$$

$$\frac{\Delta}{\Delta_i} = 2.08 \frac{T}{T_y} \approx 2 \frac{T}{T_y}$$

- (c) Substituting, an expression for the maximum reduction was obtained.

$$S_{R \max} = 0.98 - 0.70 \frac{T}{T_y} - 0.096 \left(\frac{T}{T_y}\right)^3$$

This may be simplified, as shown in Fig. 8.5, using $S_{R \max} = 1.0 - 0.8 \frac{T}{T_y}$. A conservative approximation is

$$S_{R \max} = 1 - \frac{T}{T_y}$$

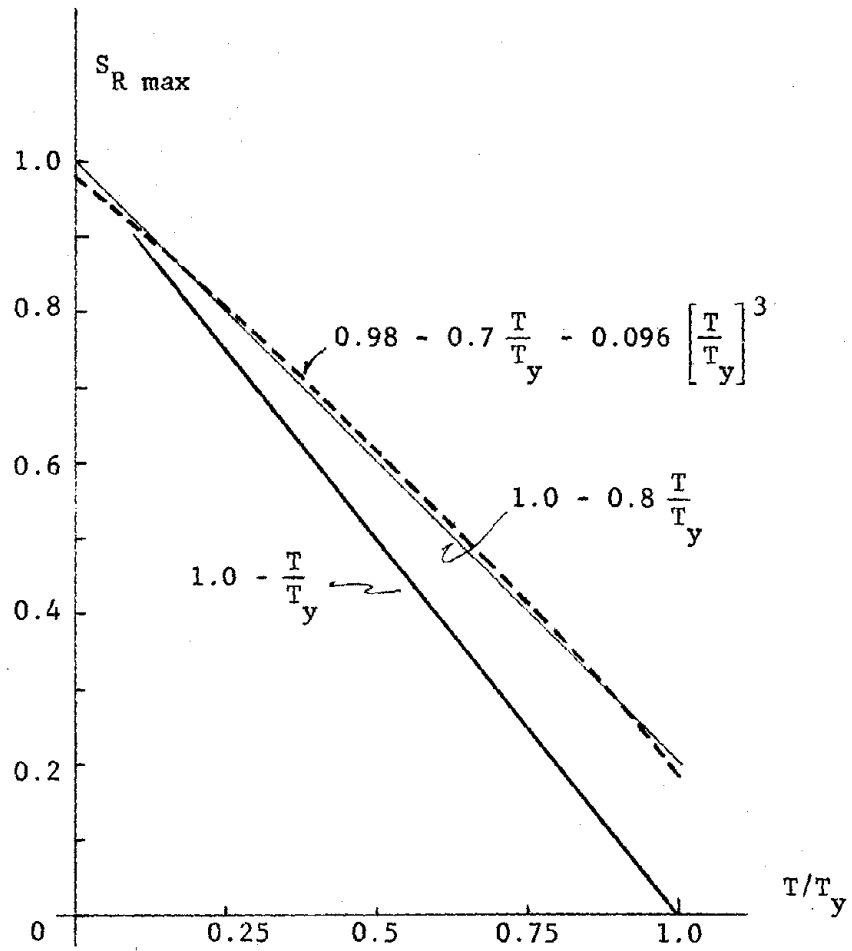


Fig. 8.5 Reduction due to axial tension

Data from five tests, 120C-U, 00-U, 50T-U, 100T-U, and 200T-U were utilized to obtain empirical equations for each cycle. For four levels of deformation, 20 data points were available. S_R is the ratio of the peak shear value at a given deflection and axial load level (tension or compression) to the peak shear in test 00-U at the same deformation level. Table 8.2 shows measured and calculated values of S_R for 50T-U, 100T-U, and 200T-U.

TABLE 8.2 MEASURED AND PREDICTED VALUES OF S_R

Test	Δ/Δ_i	S_R	
		Measured	Predicted
50T-U	1	0.82	0.80
	2	0.84	0.82
	3	0.81	0.84
100T-U	1	0.61	0.61
	2	0.61	0.62
	3	0.60	0.66
200T-U	1	0.11	0.20
	2	0.18	0.19
	3	0.24	0.21

The regression analysis was conducted studying several polynomial forms and selecting that which best fit the measured data.

Using the equation $1 - T/T_y$ for the reduction in shear due to axial tension, a general approach that may be followed in the design of fixed end columns under constant axial tension and cyclic lateral loads is presented in Fig. 8.6. The influence of shear span is assumed as in the case of axial compression presented in Section 8.2 and the transverse steel requirements follow the same guidelines. In this case there are no data available to check the accuracy of the assumptions.

LIMITATIONS

$$V_u \leq 6\sqrt{f'_c} A_c$$

$$V_s = V_u$$

$$s \leq 6d_b$$

$$L_f = \frac{2 M_n}{V_n}$$

M_n - from interaction diagram, $\phi = 1$ (considering the tension T)

$$V_n = V_s + 2 \left[1 - \frac{T}{500A_c} \right] \sqrt{f'_c} A_c$$

if $T/A_c > 500$, $V_n = V_s$ (T in lb)

$L < L_f$

Shear behavior

Permissible shear strength:

$$V_u \left(\frac{L}{L_f} \right) \left(1 - \frac{T}{T_y} \right)$$

where $T_y = A_s f_y$

if transverse reinforcement is providing deformation capacity

$$A_v = \frac{V_u (L_f/L) s}{f_{sy} d_c}$$

or

$$\rho_w = \frac{V_u (L_f/L)}{f_{sy} A_c}$$

$L \geq L_f$

Flexural behavior

-Transverse reinforcement to ensure formation of plastic hinges but not less than required to carry V_u

-The permissible shear strength is the shear corresponding to plastic hinge formation or the reduction for cyclic loading

$$V_u \left(1 - \frac{T}{T_y} \right)$$

whichever is less

Fig. 8.6 Design of R/C columns under cyclic loads and constant axial tension

It is difficult to imagine a column subjected to cyclic lateral loads and a high level of constant axial tension. Although the approach is theoretically valid for any level of tension, it may not represent practical situations. The reduction in shear strength is intended to cover the cases where the energy dissipated is low due to high axial tension. Because no noticeable shear decay is present when tension is applied, no limitation in deflections or ductility factor is required.

The approach proposed for cases with tension (Fig. 8.6) and compression (Fig. 8.2) converges to the same solution if no axial load is present.

Bidirectional Effects. If deformations in both orthogonal directions are considered, some modifications may be required in the proposed criterion. However, data are available only at the low level of tension and one history of lateral deformations.

The energy dissipation per cycle for bidirectional deformations (50T-B, Fig. 6.5) seemed to be lower than for unidirectional deformations (50T-U, Fig. 6.1) because the pinching effect was more accentuated. On the other hand, the proposed criterion is conservative and the differences may not be significant; therefore, the assumption of similar behavior for unidirectional and bidirectional deformations seems to be adequate for low levels of axial tension. However, if other bidirectional movements and/or levels of axial load are considered an increase in the amount of transverse steel and/or a decrease in the assumed strength may be needed. No specific modifications can be offered until sufficient data are available.

8.7 Evaluation of the Design Approach for Axial Tension

In order to compare the transverse reinforcement used with that required using the proposed approach, specimens for 50T-U and 100T-U were examined.

50T-U. Detailed calculations for this case are presented in Fig. 8.7. The maximum shear capacity, V_u , is taken as $6\sqrt{f'_c} A_c = 42.8k$. With $M_n = 680$ in.-k from Fig. 4.5 and $V_n = V_s = V_u = 42.8k$, $L_f = 32$ in., indicating flexural behavior. The transverse reinforcement must carry the total shear. The shear corresponding with the formation of plastic hinges is greater than the reduced strength due to the effect of tension, thus the permissible shear strength must be the reduced strength of $31.6k$ or $4.42\sqrt{f'_c} A_c$.

The level of shear, $4.42\sqrt{f'_c} A_c$, is less than the peak shears observed in test 50T-U (Fig. 6.9), which means that the approach is conservative.

100T-U. For $V_u = 6\sqrt{f'_c} A_c = 44.9k$, $V_s = 44.9k$. $M_u = 450$ in.-k from Fig. 4.5, and $V_n = 44.9k$, then $L_f = 20$ in. Flexural behavior is anticipated because the actual length, 36 in., is greater than L_f . The percentage of transverse reinforcement to attain plastic hinges is 0.37 percent and that required to carry the total shear is 0.66 percent. Therefore, the transverse reinforcement is $\rho_w = 0.0066$ and the permissible strength is $V_u(1 - T/T_y) = 21.4k$, or $2.85\sqrt{f'_c} A_c$ ($2M_n/L = 25k$).

Again, this level of shear is less than peak shears observed in test 100T-U (Fig. 6.9). In this case L_f must depend on the flexural capacity of the section because the nominal shear is maintained at about the same level. Although the section is provided with high shear resistance, the axial tensile load does not permit the development of that resistance. Only for very short columns with low or moderate levels of tension is it likely that shear will control.

In order to illustrate the proposed approach, two idealized cases for two levels of tension in each case are examined.

- (a) A long column with tension of 50k, $L = 112$ in. The same section and material properties of Specimen 50T-U are

$$V_u = 6 \sqrt{f'_c} A_c = 42.8 \text{ K}$$

$$V_s = 42.8 \text{ K}$$

$$s_{\max} = 6(0.75) = 4.5 \text{ in}$$

$$M_n = 680 \text{ in-K} \quad \text{from Fig.5.5}$$

$$\begin{array}{l} L = 36 \text{ in} \\ f'_c = 5.1 \text{ Ksi} \\ f_y = 54.2 \text{ Ksi} \\ f_{sy} = 67.5 \text{ Ksi} \\ T = 50 \text{ K} \\ A_c = 100 \text{ si} \end{array}$$

$$V_n = V_s + 2 \left[1 - \frac{T}{500A_c} \right] \sqrt{f'_c} A_c = V_s = 42.8 \text{ K}$$

$$L_f = \frac{2 M_n}{V_n} = \frac{2(680)}{42.8} = 32 \text{ in}$$

$$L = 36 \text{ in} > 32 \text{ in} \quad \longrightarrow \quad \text{Flexural behavior}$$

Transverse reinforcement to attain plastic hinges:

$$\rho_w = \frac{2 M_n}{L f_{sy} A_c} = \frac{2(680)}{36(67.5)(100)} = 0.0055$$

Transverse reinforcement to carry the total shear:

$$\rho_w = \frac{V_s}{f_{sy} A_c} = \frac{42.8}{67.5(100)} = 0.0063 \quad \leftarrow$$

Shear corresponding with the formation of plastic hinges:

$$\frac{2 M_n}{L} = \frac{2(680)}{36} = 38 \text{ K}$$

Reduced shear under cyclic loading due to tension:

$$V_u \left(1 - \frac{T}{T_y} \right) = 42.8 \left(1 - \frac{50}{191} \right) = 31.6 \text{ K} \quad \leftarrow$$

Fig. 8.7 Example of calculations, redesign of 50T-U

assumed. For $V_n = V_s = V_u = 6\sqrt{f'_c} A_c = 42.8k$, $L_f = 32$ in. and flexural behavior is anticipated. The percentage of transverse reinforcement is that required to carry the total shear, 0.63 percent (0.18 percent for $2M_n/L$). The shear strength is $2M_n/L = 12.1k$, because in this case the shear corresponding with the formation of hinges is less than $V_n(1 - T/T_y) = 31.6k$. As in the case of compressive axial loads, the shear strength in long columns is dictated by the hinging condition but the transverse steel must be greater than that corresponding to flexural hinging in order to ensure the maintenance of the hinge for alternate and repeated lateral loads.

- (b) A long column with tension of 100k, $L = 112$ in. The same section and material properties of Specimen 100T-U are assumed. $V_u = 6\sqrt{f'_c} A_c = V_s = V_n = 44.9k$, $L_f = 20$ in. and flexural behavior is anticipated. The required percentage of transverse steel is 0.66 percent and the shear strength is $2M_n/L = 8k$. High tensile load decreases the moment capacity at hinge and results in the low shear strength.
- (c) Very short column with tension of 50k, $L = 24$ in., and the same section and material properties as in test 50T-U. For $V_u = 6\sqrt{f'_c} A_c = V_s = V_n = 42.8k$, $L_f = 32$ in., shear behavior is anticipated. The required percentage of transverse steel is

$$\rho_w = \frac{V_u (L_f/L)}{f_{sy} A_c} = 0.0084$$

and the reduced strength is $V_u(L/L_f)(1 - T/T_y) = 23.7k = 3.3\sqrt{f'_c} A_c$. A similar element subjected to 120k in compression will require $\rho_w = 1.04$ percent for a reduced strength of $3\sqrt{f'_c} A_c$, which shows that for short columns the case with tension may not be as unfavorable as the case with compression.

- (d) Very short column with tension of 100k, $L = 24$ in. and the same section and material properties as in test 100T-U. $V_u = 6\sqrt{f'_c} A_c = V_s = V_n = 44.9k$, $L_f = 20$ in., flexural behavior is anticipated. $\rho_w = 0.66$ percent and $V_u(1 - T/T_y) = 21.4k = 3\sqrt{f'_c} A_c$ (the shear required to form hinges is $2M_n/L = 37.5k$). In this case, high tension indicates flexural behavior, but the element is so short that the shear corresponding to the formation of hinges is still higher than the shear reduced to reflect the effects of tension.

8.8 Columns with Alternating Tension and Compression

Constant compression causes an increase in applied shear and stiffness for low levels of deformation and a noticeable shear decay for higher levels. The effect of constant tension is reflected in a reduction in shear and stiffness but with less shear decay than with constant compression. Compression causes a more noticeable pinching effect in the hysteretic loops, while under tension there is less tendency toward pinching, especially in the first cycles at each deflection level. When tension is applied alternately with compression the effects of both are present. Under tension the shear and stiffness are reduced, the amount of shear decay is reduced, and the shape of the hysteretic loops is improved. The result is that in terms of the behavior throughout the load history and the total amount of energy dissipated, the application of tension alternately with compression is not different from the behavior under constant compression if the lateral displacement history is the same. Therefore, the behavior of test ATC-U is similar to that of 120C-U and the behavior of ATC-B is similar to 120C-B. Because a design criterion for columns subjected to cyclic loadings is based on energy dissipation considerations, a design recommendation for columns that may be subjected to alternating axial load could

be designed as if the column were subjected to constant compression.

For an isolated column, the above recommendation would not be adequate because under lateral displacement accompanied by tension, the stiffness of the element will be very low and the lateral deflection may be excessive. The most typical case is the columns in a story of a building frame subjected to equal deformation--the interstory drift for the frame. Because of overturning of the frame, some columns will be in tension while others are in compression, a behavior similar to that studied in the experimental program is expected. Because only two tests were conducted, a general recommendation may be inadequate for other cases. Further discussion of the applicability of the design approach in relation to tests ATC-B and ATC-U may be helpful.

Test ATC-U was designed to represent the case of a column which is subjected to a high level of tension alternating with compression for the first cycles of seismic motion. Assuming that the sequence of application of loads in the test is representative, the amount of energy dissipation as well as the overall behavior is expected to be similar to that when the column is subjected to constant compression. The utilization of the design criterion for columns with constant compression seems to be justified.

Test ATC-B was designed to represent an exterior column in which, due to its location in a three-dimensional structural frame, variable axial loads are present in one of the principal directions while a constant level of compression is developed under lateral movement in the perpendicular direction. Assuming that the sequence of application of loads in the test is representative, the shear capacity for peaks in the direction in which tension is present will be lower than in a similar case where constant compression at the same level is applied. However, the shear decay will not be as

great. The reduction in shear decay is not significant in the general context of the proposed design criterion. Thus, the energy dissipated will be comparable to that present in a column with the same lateral displacement history but with constant compression.

In conclusion, columns subjected to lateral movements in both principal directions and with the possibility of variable axial loads may be designed as if the axial load were constant compression. The approach stated in Section 8.2 may be applicable if a modification (more transverse reinforcement and/or lower permissible shear strength) to account for bidirectional lateral movements is adopted. As a corollary, if only unidirectional lateral displacements are considered with alternating axial loads, it appears to be adequate to design the column using the criterion presented in Fig. 8.2 without any modification. In the case where some of the columns in a story are in tension while others are in compression, the total lateral shear resistance of the entire story under cyclic deformations must be evaluated with due consideration of the axial forces on each column, even though the design may be based on the case where axial compression is considered.

CHAPTER 9

SUMMARY AND CONCLUSIONS

9.1 Summary of the Investigation

The influence of axial loads on the behavior of reinforced concrete short columns under cyclic lateral deformations was studied. The experimental program on which the analysis was based consisted of ten tests of short column specimens subjected to pre-determined load sequences.

Test Specimen. All specimens had the same geometry and reinforcement. The specimen had a 12 in. (30 cm) square cross section with eight #6 bars (19 mm) for the longitudinal reinforcement, #2 (6 mm) closed stirrups at 2.6 in. (65 mm) as transverse reinforcement and 1 in. (25 mm) cover. The specimen cross section was a 2/3-scale model of an 18 in. (46 cm) prototype column section. The shear span was 1.5 times the thickness of the cross section. The spacing of the transverse reinforcement was greater than required to prevent shear failure. The intent was to test columns that might not perform satisfactorily under the imposed load histories, but would represent typical practice in column design in seismic regions. The shape of the specimen was selected to permit simulating a short stiff column framing into a relatively stiff floor system.

Lateral Load History. The lateral loading was controlled by monitoring deformations. Two basic histories were selected: one with displacement variation in only one direction and the other with displacements applied alternately in orthogonal directions. Three cycles at each peak deflection level of one, two, three, and

four times a selected initial value were considered. This resulted in a total of 12 continuous cycles for the unidirectional history and 24 for the bidirectional.

Axial Load History. Axial load variations were selected with the intention of developing basic information that might be useful for further experimental studies. In order to study the effect of constant compression, constant tension and alternate tension and compression, axial loads were held constant in some tests and variable in others. Only one level of constant compression ($N_u/A_c = 1200$ psi [8MPa]) was considered. Because no data have been reported regarding cyclic lateral loads in combination with axial tension, three levels of constant tension were considered. Two sequences simulated loads varying from tension to compression.

9.2 Test Results

Effect of Constant Axial Compression. The main effect of axial compression was to accelerate the shear deterioration at higher levels of deformation compared with the deterioration of a specimen without axial loads. Lateral deformations in the orthogonal direction caused more shear deterioration at higher levels of deformation but no noticeable effect for deformation levels lower than that at maximum observed peak shear. An increase in shear strength was noted with compressive axial loads as compared with no load.

Effect of Constant Axial Tension. In tests with constant tension, the shear capacity and the stiffness were reduced, as compared with tests with constant compression or with no axial load, but the shear deterioration was decreased. The required shear to attain a given deformation decreased as the level of tension was increased. The adverse effects of alternate deformations in the

orthogonal direction decreased with the application of constant tension as compared with tests with compression or with zero axial load. The required level of lateral deformation to produce yield in the ties increased with the level of tension. With tension, distress in the concrete occurred at large deflections, while with compression similar distress was apparent at low deflections.

Effect of Alternate Axial Load. The effect of tension alternate with compression was reflected as a reduction in shear and stiffness but only during that part of the loading history where tension was imposed. The influence of tension in reducing shear decay observed in tests with constant tension was also true when tension was applied alternately with compression. In terms of overall behavior and total amount of energy dissipated, the effect of alternate axial loads on response was no more severe than the effect of constant compression when the same lateral deformation history was considered.

9.3 Design Approach

In order to develop a design approach for columns failing in shear, it was necessary to define a parameter identifying shear behavior and to define rules for satisfactory performance in terms of energy dissipation. The influence of the material and section properties, the amount and type of transverse steel, and the axial load on the member were considered. The design criterion included adjustments to strength and stiffness to account for shear decay and loss of energy absorbing capacity.

Guidelines for satisfactory performance for the general case of cyclic lateral deformations and axial loading are not available. In this study general considerations (based on the observed behavior and results from other analytical and experimental studies) for a design approach were established. The basic concept was that for satisfactory performance the shear stress in the core

should be limited and the transverse reinforcement designed to carry an amount of shear reflecting the requirement for energy dissipation. The procedure was found to reflect adequately the influence of the main variables and was in agreement with observed behavior. However, it was based on data from a limited number of tests and may not be adequate for other geometries, lateral histories, or shear spans.

9.4 Recommendations for Future Work

In order to reach a better understanding of the problem of columns under 3D cyclic loads failing in shear, more analytical and experimental studies are required. The influence of variables considered in this experimental program require some verification and others not directly considered need to be incorporated. Variations in spacing and type of transverse steel in the shear span and in the cross section geometry, keeping the lateral history and axial load sequence constant, should be studied. Using a model representing observed shear behavior, analytical investigations of 3D frames should be conducted to determine loading sequences for future experimental studies.

Some specific recommendations can be made using the results of this investigation.

Axial Loads - Constant compression seems to be the most representative axial load sequence. Constant tension is not likely to be encountered often. Alternate sequences of tension and compression may be assumed to be similar to constant compression.

Transverse Reinforcement - To improve the concept of critical length, variations in the spacing above and below the one used in this study should be considered. Spacing selected in accordance with the design criterion proposed herein should be examined to see if more energy dissipating capacity is improved.

Shear Span - In order to incorporate this variable, values above and below that of the present study should be considered. Also, variations in the amount of longitudinal steel to produce different flexural strengths in combination with different shear spans need to be considered.

Behavioral Model - The results of the present investigation in conjunction with other reported results may provide sufficient data to develop a model representing shear behavior of columns. Such a model could be used for the seismic analysis of structural systems.

9.5 Conclusions

Based on tests conducted in this investigation, the following conclusions were made:

- (a) Constant compression produced an increase in shear capacity with respect to similar tests with no axial load for low levels of deformation. The increase in shear capacity was about equal to that predicted using Eq. (11.14) of the ACI Code [28]. The shear capacity started to deteriorate after the maximum peak shear was reached. Compared with companion tests with zero axial load, the effect of constant compression was to accelerate shear deterioration and reduce the energy dissipating capacity of the column.
- (b) The effect of constant tension was to decrease the shear deterioration but at the same time to substantially reduce the shear capacity and the stiffness near the origin. The observed reduction in shear capacity was equivalent to the reduction estimated using Eq. (11.9) of the ACI Code [28] for a column subjected to 50 kips tension. For higher levels of axial tension, the reduction in shear capacity was more than predicted because horizontal cracking produced a drop

in the stiffness and delayed participation of the ties in carrying shear.

- (c) The application of tension alternately with compression reduced some of the damage to the concrete core which occurred under constant compression. The shear capacity provided by the ties improved as compared with constant compression using the same lateral deformation history. In terms of total response both cases were similar.
- (d) The overall response of the specimens was dictated by the confinement and shear strength provided by the ties. The efficiency of the ties to confine the core decreased with compressive axial load, with the number of cycles at a given deflection level, and with the application of lateral deflections in the perpendicular direction.
- (e) The approach suggested for design of short columns was dependent on establishing a satisfactory performance criterion in terms of energy dissipation. A limit on the shear stress in the core was established and the transverse reinforcement was proportioned in terms of the energy dissipation or deformation that the column might be expected to sustain.

REFERENCES

1. Burns, N. H., and Siess, C. P., "Plastic Hinging in Reinforced Concrete," Proceedings, ASCE V. 92, ST5, Oct. 1966, p. 45.
2. Burns, N. H., and Siess, C. P., "Repeated and Reversed Loading in Reinforced Concrete," Proceedings, ASCE V. 92, ST5, Oct. 1966, p. 65.
3. Park, R., and Sampson, R. A., "Ductility of Reinforced Concrete Column Sections in Seismic Design," ACI Journal, Proc. V. 69, No. 9, Sept. 1972, p. 543.
4. Gulkan, P., and Sozen, M. A., "Inelastic Responses of Reinforced Concrete Structures to Earthquake Motions," ACI Journal, Proc. V. 71, No. 12, Dec. 1974, p. 604.
5. Hiroswawa, M., Ozaki, M., and Wakabayashi, M., "Experimental Study on Large Models of Reinforced Concrete Columns," Session 2D: Dynamic Behavior of Structural Elements, No. 96, Fifth World Conference on Earthquake Engineering, Rome, 1973.
6. Shimazu, T., and Hirai, M., "Strength Degradation of Reinforced Concrete Columns Subjected to Multi-Cycle Reversals of Lateral Loads at Given Amplitudes of Post-Yielding Deformations," Session 3D: Dynamic Behavior of Structural Elements, No. 139, Fifth World Conference on Earthquake Engineering, Rome, 1973.
7. Wight, J. K., and Kanoh, Y., "Shear Failure of Reinforced Concrete Columns Subjected to Cyclic Loadings," Session 2D: Dynamic Behavior of Structural Elements, No. 94, Fifth World Conference on Earthquake Engineering, Rome, 1973.
8. Selna, L. A., Morrill, K. B., and Ersoy, O. K., "Shear Collapse, Elastic and Inelastic Biaxial Studies of the Olive View Hospital Psychiatric Day Clinic," U.S.-Japan Seminar on Earthquake Engineering, University of California at Berkeley, Sept. 1973.
9. Pecknold, D. A. W., and Sozen, M. A., "Calculated Inelastic Structural Response to Uniaxial and Biaxial Earthquake Motions," Session 5B: Response of Structures to Ground Shaking, No. 223, Fifth World Conference on Earthquake Engineering, Rome, 1973.

10. Karlsson, B. I., Aoyama, H., and Sozen, M. A., "Spirally Reinforced Concrete Columns Subjected to Loading Reversals Simulating Earthquake Effect," Session 2D: Dynamic Behavior of Structural Elements, No. 93, Fifth World Conference on Earthquake Engineering, Rome, 1973.
11. Aktan, A. E., and Pecknold, D. A., "Response of a Reinforced Concrete Section to Two-Dimensional Curvature Histories," ACI Journal, Proc. V. 71, No. 4, May 1974, p. 246.
12. Aktan, A. E., Pecknold, D. A. W., and Sozen, M. A., "Effect of Two-Dimensional Earthquake Motion on a Reinforced Concrete Column," Structural Research Series No. 399, Civil Engineering Studies, University of Illinois at Urbana, May 1973.
13. Okada, T., Seki, M., and Asai, S., "Response of Reinforced Concrete Columns to Bi-Directional Horizontal Force and Constant Axial Force," Bull. ERS, No. 10, 1976.
14. Fintel, M. "Resistance to Earthquakes, Philosophy, Ductility and Details," Response of Multistory Concrete Structures to Lateral Forces, SP-36, American Concrete Institute, Detroit, 1973, p. 75.
15. Diaz de Cossio, R., and Rosenblueth, E., "Reinforced Concrete Failures During Earthquakes," ACI Journal, Proc. V. 58, No. 5, Nov. 1961.
16. Lew, H. S., Leyendecker, E. V., and Dikkers, R. D., "Engineering Aspects of the 1971 San Fernando Earthquake," Building Science Series 40, National Bureau of Standards, U.S. Department of Commerce, Dec. 1971.
17. "Observations on the Behavior of Buildings in the Romania Earthquake of March 4, 1977," NBS Special Publication 490, U.S. Department of Commerce, Sept. 1977.
18. ACI Committee 318, Building Code Requirements for Reinforced Concrete (ACI 318-71), American Concrete Institute, Detroit, 1971.
19. EERI Investigation Team I, Behavior of RC Building during the Managua Earthquake, Proc. EERI Conference on 1972 Managua Earthquake, San Francisco, 1973.
20. Sozen, M. A., "The Caracas Earthquake of July 29, 1967," ACI Journal, Proc. V. 65, No. 5, May 1968, p. 394.

21. Umemura, H., Hirosawa, M., and Eudo, T., "Experimental Research on Ductility of Reinforced Concrete Columns," U.S.-Japan Seminar on Earthquake Engineering, University of California at Berkeley, Sept. 1973.
22. Higashi, Y., Ohkubo, M., and Ohtsuka, M., "Influence of Loading Excursions on Restoring Force Characteristics and Failure Modes of Reinforced Concrete Columns," Sixth World Conference on Earthquake Engineering, Preprints Vol. II, New Delhi, 1977.
23. Wight, J. K., and Sozen, M. A., "Strength Decay of RC Columns under Shear Reversals," Proceedings, ASCE, V. 101, ST5, May 1975.
24. Newmark, N. M., and Rosenblueth, E., Fundamentals of Earthquake Engineering, Prentice-Hall, Inc., Englewood Cliffs, New Jersey, 1971.
25. Marques, J. L. G., and Jirsa, J. O., "A Study of Hooked Bar Anchorages in Beam-Column Joints," ACI Journal, Proc. V. 72, No. 5, May 1975.
26. Yamada, M., and Kawamura, H., "Resonance Capacity Criterion for Evaluation of the Aseismic Capacity of Reinforced Concrete Structures," Reinforced Concrete Structures in Seismic Zones, SP-53, American Concrete Institute, Detroit, 1977, p. 81.
27. Maruyama, K., "Behavior of Reinforced Short Columns under Bidirectional Lateral Loading," Ph.D. dissertation, The University of Texas at Austin, 1979; also, CESRL Report 79-1, Aug. 1979.
28. ACI Committee 318, Building Code Requirements for Reinforced Concrete (ACI 318-77), American Concrete Institute, Detroit, 1977.
29. Yamada, M., "Shear Strength, Deterioration and Explosion of Reinforced Concrete Short Columns," Shear in Reinforced Concrete, SP-42, American Concrete Institute, Detroit, 1973, p. 617.
30. Bertero, V. V., and Popov, E. P., "Hysteretic Behavior of Ductile Moment-Resisting Reinforced Concrete Frame Components," Report No. EERC 75-16, University of California, Berkeley, Apr. 1975.
31. Wight, J. K., and Sozen, M. A., "Shear Strength Decay in Reinforced Concrete Columns Subjected to Large Deflection Reversals," Structural Research Series No. 403, Civil Engineering Studies, University of Illinois, Urbana, Aug. 1973.

32. Gosain, N. K., Brown, R. H., and Jirsa, J. O., "Shear Requirements for Load Reversals on RC Members," Proceedings, ASCE, V. 103, ST7, July 1977.
33. Bertero, V. V., and Popov, E. P., "Seismic Behavior of Ductile Moment-Resisting Reinforced Concrete Frames," Reinforced Concrete Structures in Seismic Zones, SP-53, American Concrete Institute, Detroit, 1977, p. 247.
34. Proposed Changes Relative to Earthquake Resistant Design, City of Los Angeles, Department of Building and Safety, Los Angeles, 1976.
35. Recommended Lateral Force Requirements and Commentary, Structural Engineers Association of California, San Francisco, 1973.
36. Yamaguchi, I., et al., "An Experimental Study on Cyclic Behavior of R/C Short Columns," U.S.-Japan Seminar on Earthquake Engineering, University of California at Berkeley, Sept. 1973.
37. "A List of Experimental Results on Deformation Ability of Reinforced Concrete Columns under Large Deflections (No. 3)," Building Research Institute, Committee on R/C Structures, Japan Building Center, Tokyo, Japan, 1978.
38. Joint ASCE-ACI Committee 426, "The Shear Strength of Reinforced Concrete Members," Proceedings, ASCE, V. 99, ST6, June 1973.
39. Ramirez, H., "Effect of Axial Loads on the Behavior of Reinforced Concrete Short Columns under Cyclic Lateral Deformations," Ph.D. dissertation, The University of Texas at Austin, May 1979.
40. Jirsa, J. O., Maruyama, K., and Ramirez, H., "Development of Loading System and Initial Tests--Short Columns under Bidirectional Loading," CESRL Report No. 78-2, The University of Texas at Austin, September 1978.